AD-A164420

Naval Ocean Research and Develop

NSTL, Mississippi 39529   NORDA Report 83

Coastal Secchi Depth Atl

"Original contains color plates: All DTIC reproductions will be in black and white"

Rob A. Arnone
Branch
Prediction Division
Directorate

Foreword

Ocean optical properties significantly influenced performance of electro-optical systems presently being designed and constructed for the Defense Mapping Agency. The temporal and spatial distribution of these properties is highly variable, especially in coastal areas. Oceanographic atlases of these properties offer preliminary assessments of environmental constraints and focus future environmental research on more regional studies.

R. P. Onorati, Captain, USN
Commanding Officer, NORDA

Executive summary

A seasonal Secchi depth atlas has been developed for the world's coastlines. Optical data have been compiled from data gathered by the National Oceanographic Data Center and from open literature for water depths less than 500 meters. These data have been averaged by one-degree squares, sorted by season, and placed in a category of six classes of Secchi depth ranges. Four charts were used to cover the world at a scale of 1:12,233,000, and four seasons were selected to encompass 3-month intervals. Additionally, annual mean Secchi depths have been compiled in four charts. Secchi depth data were found for approximately 50% of the world's coastlines. In the areas where no optical data were available other oceanographic, meteorologic, and geomorphic data sources were used to estimate the expected Secchi depth ranges.

Global distribution of coastal Secchi depths indicates a high percentage of relatively clear waters. Less than 5% of the coastlines are shown to have less than 5-meter Secchi depth values. Little seasonal changes in a global scale in the percentage of each range were observed. The highest percentage of coastal waters has Secchi depth values between 15 and >25 meters.

Secchi depth values show high temporal and spatial variability in certain coastal regions, even though the amount of data was highly limited. This variability suggests that improved techniques of compiling coastal optical properties, such as through use of satellites, be examined both to aid in understanding historical ship data and to serve as an additional optical data source.

Acknowledgments

This program was funded by the Defense Mapping Agency Hydrographic/Topographic Center under program element 63701B/3201. Appreciation is extended to LCDR Vic Hultstrand, program coordinator at the Naval Ocean Research and Development Activity. Special appreciation is extended to Dr. F. Hilder for computer efforts and arduous compiling and plotting of data. Gratitude is extended to Dr. S. Tucker for consulting efforts. Additional appreciation is extended to the Naval Oceanographic Office for making data available. Thanks are extended to Mr. R. S. Oriol IV for technical assistance.

Contents

Illustrations

Tables

Coastal Secchi depth atlas

I. Introduction

Recent developments within the oceanographic community have improved data collection and handling procedures. These developments have shown that spatial and temporal variability of oceanographic parameters are much higher than previously surmised. Attempts to compile oceanographic data into an atlas format, such as for ocean temperature, salinity, and currents, have been somewhat successful. Ocean optical data has been quite restrictive, since major problems exist in which data techniques and lack of the basic optical relationships with physical or biochemical properties are not well understood. For these reasons the development of a seasonal optics atlas has not been feasible.

A comprehensive study of ocean optical properties was done by Frederick (1970) that was regional in extent and did not address the seasonal optical variability. Seventeen regions were studied, and statistical relationships were obtained between optical and other oceanographic properties. Another coastal turbidity study by Lepley (1968) was performed in which the water clarity of the world was classified based on photographs from the Gemini mission. The resolution in this study was extremely gross and did not describe the seasonality of coastal waters.

The coastal regions have an extremely high variability of oceanographic parameters, since these areas are responsive to local meteorological and coastal processes. Similarly, water optical properties have an extremely high variability in coastal areas because they respond to changes in biology, chemistry, and geological processes.

The necessity for a coastal optics data base arose from requirements of the Defense Mapping Agency (DMA), which is developing coastal hydrographic charting systems (Van Norden and Litts, 1979). These system capabilities are constrained by the water optical properties in which they operate. The seasonal distribution of the coastal optical properties provides a method by which planning operational surveys for coastal areas utilizing these charting systems can be effectively and efficiently achieved. Proper planning will increase the system performance and accuracy. The variability of the optical properties is also a strong indication of the biological, physical and geological processes occurring within a region, and provides an improved understanding of the oceanography when coupled with other parameters.

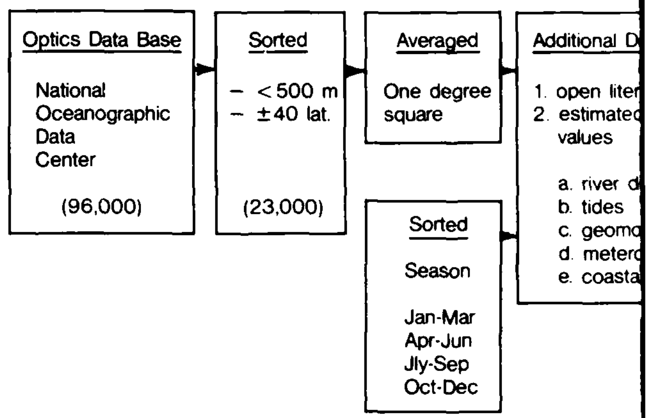

Figure 1. Flow chart for development

The establishment of an optics data base for global conditions required selection of an optical property in which numerous measurements have been made. Also, this property should be standardized such that various investigators' data can be jointly utilized. Although the Secchi depth measurement is not the most quantitative optical property, this measurement did meet the abovementioned criteria and was selected as the basis for this global coastal atlas.

The objective of this report is to quantify the variability of coastal optical properties by using historical measurements of coastal optical properties, or by inferring the optical properties from response to coastal/oceanographic processes and meteorological conditions.

The coverage area of this coastal atlas is limited to all coastlines from 40°N to 40°S, except for the United States coastal waters. Extensive optics literature for U.S. coastal waters is available (Arnone, 1982, and Van Norden and Litts, 1979).

II. Methods

Figure 1 represents the flow chart by which the coastal Secchi depth atlas was developed. The steps in this process will be discussed in some detail.

The basic data base from which the optical data was established was taken from the National Oceanographic Data Base (NODC).

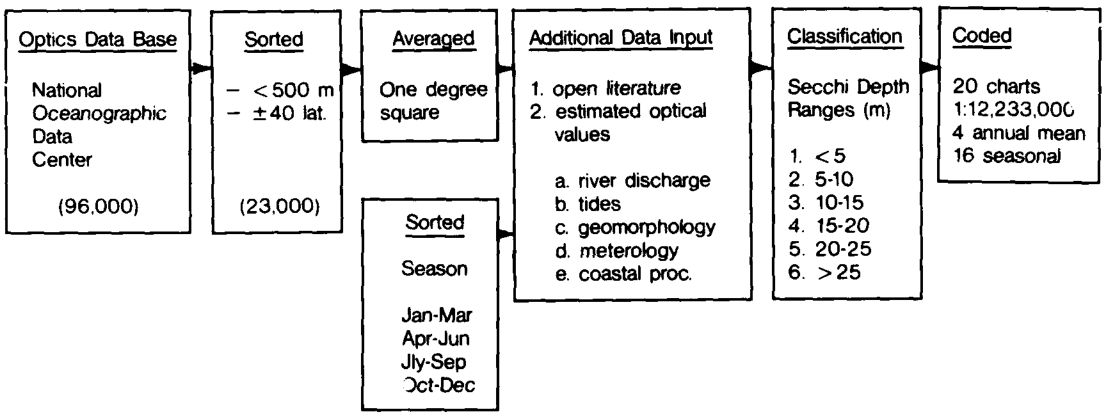

Figure 1. Flow chart for development of coastal Secchi depth atlas.

The establishment of an optics data base for global conditions required selection of an optical property in which numerous measurements have been made. Also, this property should be standardized such that various investigators' data can be jointly utilized. Although the Secchi depth measurement is not the most quantitative optical property, this measurement did meet the abovementioned criteria and was selected as the basis for this global coastal atlas.

The objective of this report is to quantify the variability of coastal optical properties by using historical measurements of coastal optical properties, or by inferring the optical properties from response to coastal/oceanographic processes and meteorological conditions.

The coverage area of this coastal atlas is limited to all coastlines from 40°N to 40°S, except for the United States coastal waters. Extensive optics literature for U.S. coastal waters is available (Arnone, 1982, and Van Norden and Litts, 1979).

II. Methods

Figure 1 represents the flow chart by which the coastal Secchi depth atlas was developed. The steps in this process will be discussed in some detail.

The basic data base from which the optical data was established was taken from the National Oceanographic Data Base (NODC). These estimated 96,000 Secchi depths for worldwide waters were screened for coastal values by eliminating all Secchi depths in waters greater than 500 m. The remaining 23,000 worldwide data points were used in this coastal atlas study. Selection of this depth figure was somewhat subjective in that by selection of data less than 100 m, the amount of available data was reduced considerably, and atlas development would be greatly impeded. It is recognized that waters at 500 m depth may have considerable different optical properties than those waters in shallow waters. This problem is inherent in atlas development and should be taken into consideration in examination of the final atlas.

These 23,000 data points were then sorted into one-degree squares such that the horizontal coastal variability could be averaged. For each one-degree square bordering a coastline or having water depth less than 500 m, the average Secchi depth was obtained. This has the effect of smoothing the large horizontal variation that could occur if values were obtained from various offshore distances. Examination of the variability of the data for each one-degree square suggests the estimate of the averaging process. However, the statistical analysis of this variance of the data for each is misleading if only a few data points exist within a one-degree square. The high variance could indicate extremely high horizontal variability or an insufficient number of data points.

Next, the values for each one-degree square were sorted into four seasons. The seasonal annual mean for each square was computed. The oceanographic ...
world has substantially diffe...
of several seasonal atlases ...
selected for the entire atla...

- January–March,
- April–June,
- July–September,
- October–December.

Regions that do not neces...
(e.g., monsoon season, Indi...
sideration upon examination...
other types of oceanographic...
utilized in compiling the ...
properties.

The seasonal optical data ...
classified into one of six S...
mechanism to permit rapid ...
and allowed for a color cod...
charts. The Secchi depth r...

Range Code	
1	
2	
3	
4	
5	
6	

These ranges were select...
ing the coastal optical wat...
compare with other optic...
schemes will be discussed ...

A series of four base char...
hydrographic chart number...
6010, 6011) were used to c...
The charts were at a scale ...
one-degree squares. They ...

Chart	Coverag...
1	North & Sou... Atlantic Oce...
2	Western Indi... African Coast...

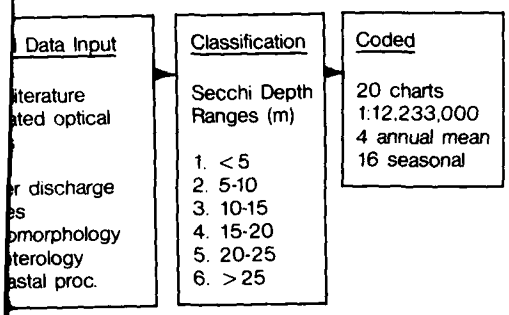

ent of coastal Secchi depth atlas.

These estimated 96,000 Secchi depths for worldwide waters were screened for coastal values by eliminating all Secchi depths in waters greater than 500 m. The remaining 23,000 worldwide data points were used in this coastal atlas study. Selection of this depth figure was somewhat subjective in that by selection of data less than 100 m, the amount of available data was reduced considerably, and atlas development would be greatly impeded. It is recognized that waters at 500 m depth may have considerable different optical properties than those waters in shallow waters. This problem is inherent in atlas development and should be taken into consideration in examination of the final atlas.

These 23,000 data points were then sorted into one-degree squares such that the horizontal coastal variability could be averaged. For each one-degree square bordering a coastline or having water depth less than 500 m, the average Secchi depth was obtained. This has the effect of smoothing the large horizontal variation that could occur if values were obtained from various offshore distances. Examination of the variability of the data for each one-degree square suggests the estimate of the averaging process. However, the statistical analysis of this variance of the data for each is misleading if only a few data points exist within a one-degree square. The high variance could indicate extremely high horizontal variability or an insufficient number of data points.

Next, the values for each one-degree square were sorted into four seasons. The seasonal annual mean for each square was computed. The oceanographic climate of various regions around the world has substantially different seasons. To avoid the development of several seasonal atlases for various regions, four seasons were selected for the entire atlas development:

- January–March,
- April–June,
- July–September,
- October–December.

Regions that do not necessarily reflect these oceanographic seasons (e.g., monsoon season, Indian Ocean) should be taken into consideration upon examination of the atlas. As will be described later, other types of oceanographic and meteorologic conditions were also utilized in compiling the season variability of coastal optical properties.

The seasonal optical data for each one-degree square were next classified into one of six Secchi depth ranges. This provided a mechanism to permit rapid screening of the data for regional trends and allowed for a color coded method of placing the data on the charts. The Secchi depth ranges follow:

Range Code	Range (m)	Chart Color
1	< 5	Brown
2	5–10	Yellow
3	10–15	Orange
4	15–20	Green
5	20–25	Blue
6	> 25	Purple

These ranges were selected to permit a rapid method of classifying the coastal optical waters. Examination of how these ranges compare with other optical properties and water classification schemes will be discussed later.

A series of four base charts obtained from DMA (compiled from hydrographic chart numbers 6004, 6005, 6006, 6007, 6008, 6009, 6010, 6011) were used to compile the worldwide optics data base. The charts were at a scale of 1:12,233,000 and were divided in one-degree squares. They are labeled in the following fashion:

Chart	Coverage Area	Longitude
1	North & South Americas Atlantic Ocean	5°E–95°W
2	Western Indian Ocean African Coasts	5°E–70°E

3	Western Pacific, Indonesia, Australia, Eastern Indian Ocean	70°E-165°E
4	East and Central Pacific	165°E-95°W

The coverage of each of these charts for the world is shown in Figure 2. Therefore, a total of 16 charts representing the four seasons on four charts of the world has been developed. In addition, the annual mean coastal Secchi depth values are represented on the four world charts, which resulted in a total of 20 charts represented in Plates 1-20.

The NODC data base, which provided the framework on which the atlas was developed, has insufficient Secchi depth data available for complete world coastal coverage. Large amounts of these data are concentrated in specific regions. For these reasons it was necessary to supplement the data base with optics data reported in open literature. These optics data were also limited, and in many cases, the data have to be converted to Secchi depth values. Several studies from the Naval Postgraduate School (Murdock, 1980) were also compiled within this atlas. For instances where contoured data was available at a resolution greater than the one-degree square, the data was used without loss of detail. The open literature on ocean optical properties is contained in several bibliographies (Arnone, 1982; Tucker, 1982; Hickman 1979), and the reader is directed to these regional studies if a more detailed requirement is necessary.

Results of the extensive open literature search still left a large gap with regard to the seasonal variation of coastal optics needed to complete the atlas. Based on additional sources of oceanographic, meteorological and coastal information, water optical properties were inferred. The data base was extended, first by examination of the Secchi depth values. For example, if a square was surrounded by a specific range of Secchi depths, then the same range was assigned to it. The color code was striped in this one-degree square rather than colored in solidly to signify that the data had been inferred.

An extension of this extrapolation procedure was utilized for several coastlines where no data was available. The assignment of the Secchi range was based on oceanographic/coastal processes, meteorologic conditions, geomorphic processes, and other local conditions; for example, proximity to major river mouths, major offshore currents, upwelling zones, etc. Several of the parameters that influence optical properties will be discussed in a following section.

A Soviet atlas (Isokov, 1953) of summer and winter water transparency was also consulted as a data source, although it does not contain the detail in the coastal area. The Soviet atlas appears more relevant to deeper oceanic waters, since some coastline areas were found to conflict with some regional Secchi depth data found in the data base.

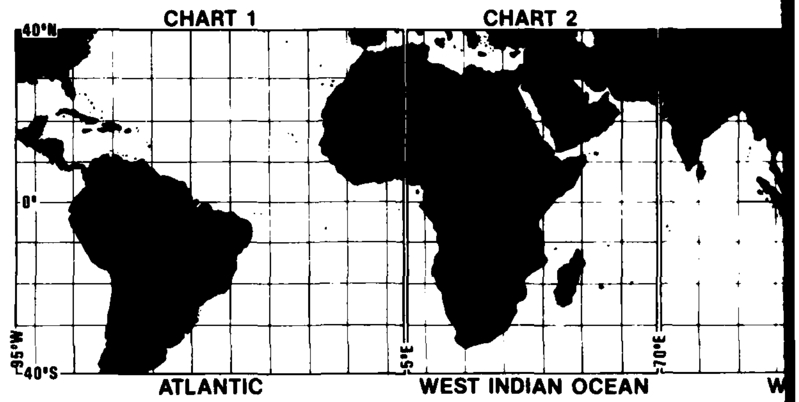

Figure 2. Geographical cover

Examination of the 20 color plates indicates that the extent of optical data immediately available is rapidly discerned for the worldwide coastlines by the solid colors shown in the plates. The striped values, which constitute at least 50% of the coastlines, indicate that no optics data was found and that other sources of information were used to determine the Secchi depth range. The actual techniques and methods for relating the oceanographic climate to waters optical parameters will be described in the following sections.

III. Difficulties and problems

Foremost in the problems encountered in generating the coastline atlas is the insufficient amount of data. The inference techniques implemented are limited, and actual in situ measurements are required to validate the procedures used.

In obtaining data in coastal regions, the spatial variability is difficult to characterize from ship-collected data. Averaging optical properties with a one-degree square leads to a bias toward the deeper water optical values. Measurements in shallow water are quite restrictive due to ship handling problems and navigational hazards within several miles from the coast. Collection of shallow water data is further compounded by political problems, especially in foreign areas. The optical ranges presented for each one-degree square will be slightly more turbid closer to the coast. It is extremely difficult to represent near-shore optical properties, since the local conditions (land/sea breeze, surf conditions, etc.) will strongly influence the optical climate.

The Secchi depth measurement is restrictive in clear water where the bottom can be seen. In areas where the bottom is readily visible (e.g., Bahamas, atolls) a Secchi range of 6 (>25 m; purple) was used on the plates. The use of the Secchi depth measurement

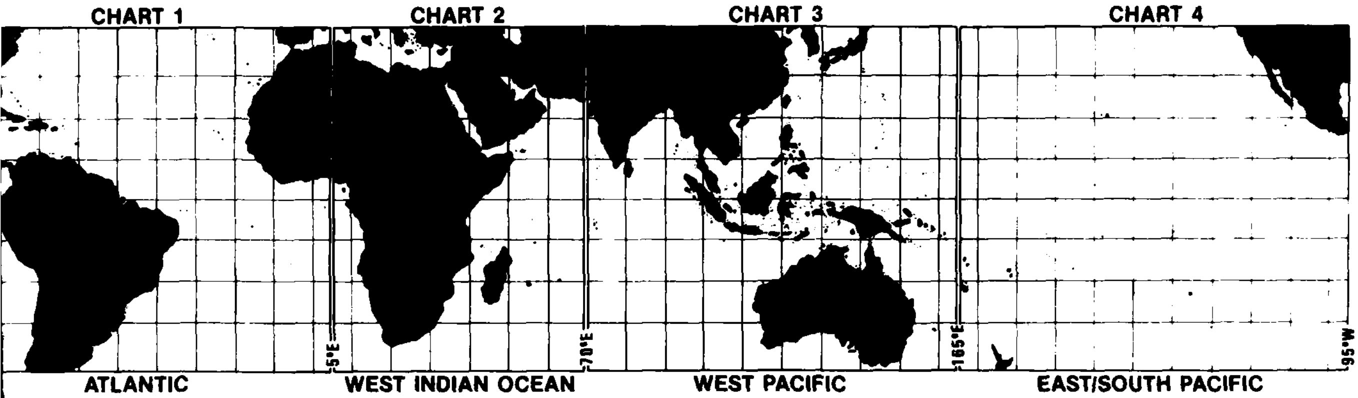

Figure 2. Geographical coverage for Charts 1-4.

amination of the 20 color plates indicates that the extent of al data immediately available is rapidly discerned for the lwide coastlines by the solid colors shown in the plates. The d values, which constitute at least 50% of the coastlines, in- that no optics data was found and that other sources of in- ation were used to determine the Secchi depth range. The techniques and methods for relating the oceanographic climate ters optical parameters will be described in the following ns.

Difficulties and problems

emost in the problems encountered in generating the coastline s the insufficient amount of data. The inference techniques nented are limited, and actual in situ measurements are re- to validate the procedures used.

btaining data in coastal regions, the spatial variability is dif- to characterize from ship-collected data. Averaging optical ties with a one-degree square leads to a bias toward the deeper optical values. Measurements in shallow water are quite tive due to ship handling problems and navigational hazards several miles from the coast. Collection of shallow water further compounded by political problems, especially in areas. The optical ranges presented for each one-degree will be slightly more turbid closer to the coast. It is ex- y difficult to represent near-shore optical properties, since al conditions (land/sea breeze, surf conditions, etc.) will strong- ence the optical climate.

Secchi depth measurement is restrictive in clear water where tom can be seen. In areas where the bottom is readily visi- ., Bahamas, atolls) a Secchi range of 6 (>25 m; purple) ed on the plates. The use of the Secchi depth measurement has this distinctive problem and suggests utilization of another optical property for future work.

IV. Relationship of Secchi depths to water optical parameters

The Secchi depth is a rough measure of the water transparency in which a circular white disk, 43-237 cm in diameter, is lowered in the water and the depth at which it disappears from sight is observed. This measurement was first introduced in the 1865 cruise of the *Immaculate Concezione* in the Mediterranean (Cialdi and Secchi, 1968). Since then there have been attempts to standardize the procedures, although no consistent method is presently being used. Certain procedures indicate that the measurement should be done on the sun side of the ship, while others indicate the ship shadow side. The measurement is affected by both the solar elevation and the sea surface height (Hojerslev, 1974). The Secchi depth measurement is, to a certain extent, independent of the spectral characteristic of water because the human eye selects the optimum wavelength for maximum transparency when making the measurement. Different water masses have specific inherent characteristics by which a specific visible wavelength has maximum transmission. In clear ocean waters this wavelength occurs around 495 nanometers (nm) (blue-green), while in coastal waters a spectral shift toward 550 nm (brown) occurs (Fig. 3). The wavelength dependence of a water masses' maximum transmission coefficients is important for optical classifications (Jerlov, 1976). Similarly, this spectral dependence is characteristic of the biochemical properties.

Figure 4 indicates the range of Secchi depths for other types of optical parameters. Notice that the coastal water mass for harbors and estuaries has Secchi values of 1-3 m, which corresponds

to diffuse attenu tion coefficient is is dependent on of measurement

$k = -d [ln (E$

where E = irra

Therefore, k is logarithm of the tion coefficient downwelling radi of change for u (Austin and Petz wavelength dep

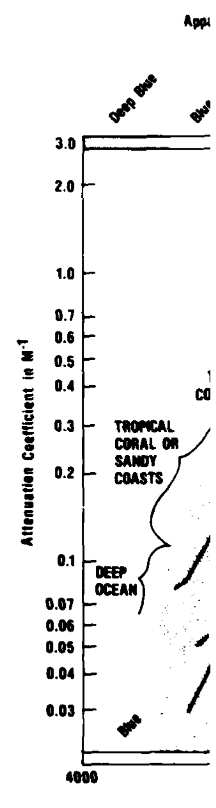

Figure 3. Spectral various water typ

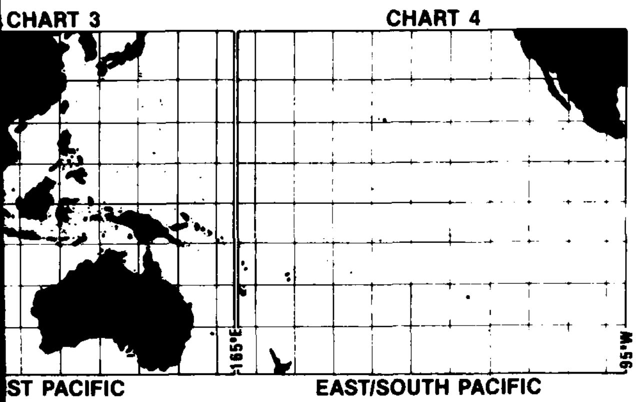

e for Charts 1-4.

s this distinctive problem and suggests utilization of another op-
al property for future work.

V. Relationship of Secchi depths to ater optical parameters

The Secchi depth is a rough measure of the water transparency which a circular white disk, 43-237 cm in diameter, is lowered the water and the depth at which it disappears from sight is served. This measurement was first introduced in the 1865 cruise the *Immaculate Concezione* in the Mediterranean (Cialdi and cchi, 1968). Since then there have been attempts to standardize e procedures, although no consistent method is presently being ed. Certain procedures indicate that the measurement should be ne on the sun side of the ship, while others indicate the ship adow side. The measurement is affected by both the solar eleva-n and the sea surface height (Hojerslev, 1974). The Secchi depth easurement is, to a certain extent, independent of the spectral aracteristic of water because the human eye selects the optimum velength for maximum transparency when making the measure-nt. Different water masses have specific inherent characteristics which a specific visible wavelength has maximum transmission. clear ocean waters this wavelength occurs around 495 nanometers n) (blue-green), while in coastal waters a spectral shift toward) nm (brown) occurs (Fig. 3). The wavelength dependence of vater masses' maximum transmission coefficients is important optical classifications (Jerlov, 1976). Similarly, this spectral endence is characteristic of the biochemical properties.

Figure 4 indicates the range of Secchi depths for other types optical parameters. Notice that the coastal water mass for har-s and estuaries has Secchi values of 1-3 m, which corresponds to diffuse attenuation coefficient values of 2-1. The diffuse attenuation coefficient is an apparent optical property in that its magnitude is dependent on the radiance distribution that exists at the point of measurement. The diffuse attenuation coefficient is defined as

$$k = -d\,[\ln (E_Z)]\,dZ, \qquad (1)$$

where E = irradiance at depth, Z.

Therefore, k is a measure of the rate of change (slope) of the logarithm of the irradiance or radiance depth profile. The attenuation coefficient is typically a measure of the rate of change for downwelling radiance, k_d into the water column, although the rate of change for upwelling radiance, k_u, can also be determined (Austin and Petzold, 1980). This attenuation coefficient is very much wavelength dependent as is shown in Figure 4.

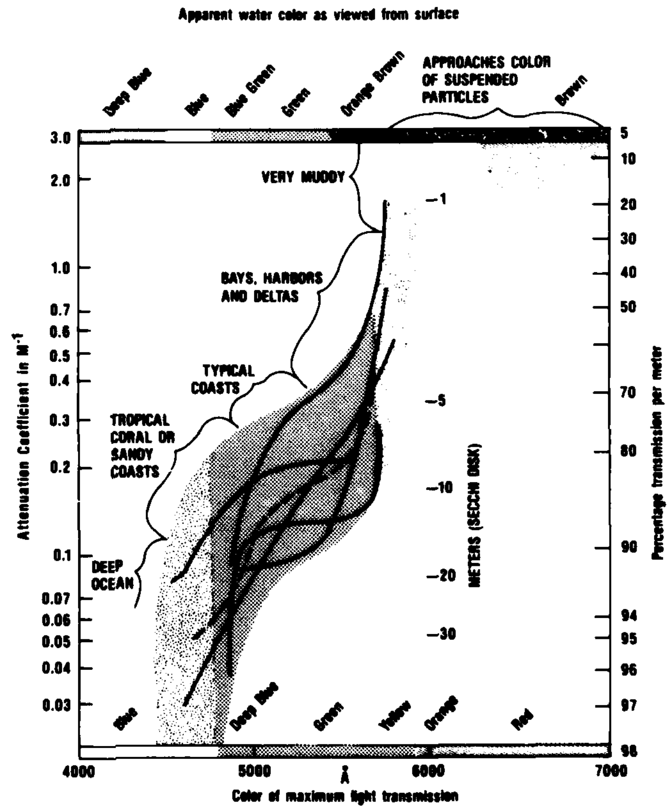

Figure 3. Spectral distribution of the attenuation coefficient for various water types.

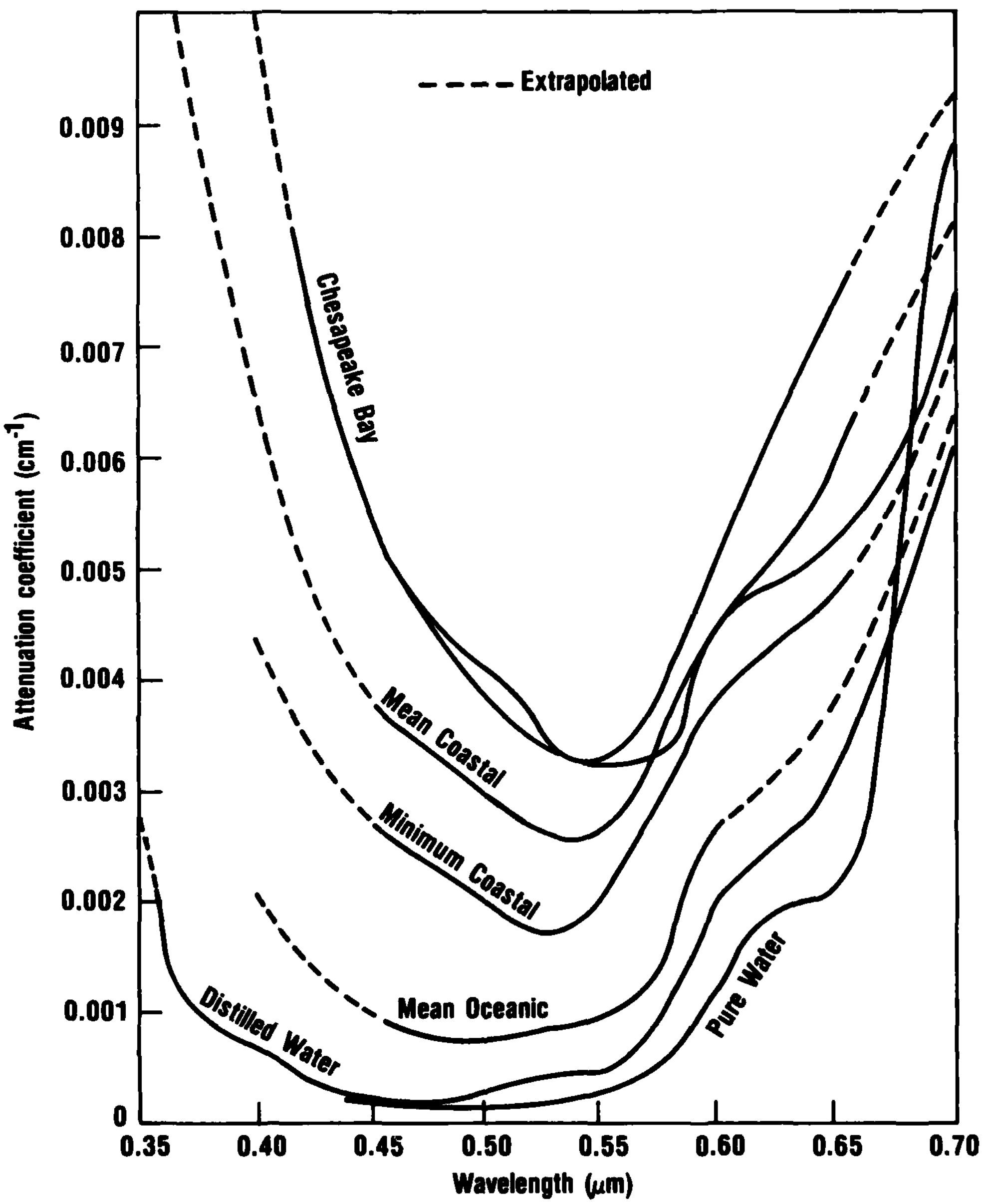

Attenuation coefficients vs. wavelength (μm)

Figure 4. Spectral relationships of water optical properties and water color for various water types (Lepley, 1968).

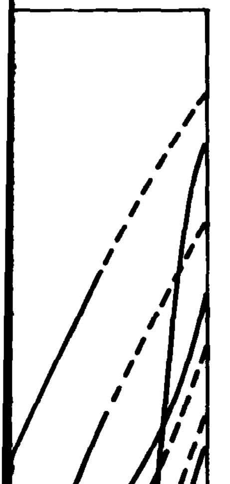

s water types (Lepley, 1968).

Shannon (1975) has established an empirical relationship between the average diffuse attenuation coefficient and Secchi depth.

$$\bar{k} = 1.15\ Z_s + 0.03\ [m^{-1}]\ , \tag{2}$$

where Z_s = Secchi depth.

$\bar{k}$ = average diffuse attenuation coefficient.

Additional relationships by other investigators can be found in Van Norden and Litts (1979).

The beam attenuation coefficient is an inherent, spectrally dependent optical property that characterizes the attenuation due to scattering and absorption in a collimated beam of monochromatic light across a fixed pathlength of homogeneous water. The measurement is a point measurement within the water column that, through a continuous depth profile, is used to describe vertical inhomogeneity of the water properties. The measurement obtains the percent transmission of the water column, which is then computed to beam attenuation coefficient by

$$C_\lambda = -\frac{1}{R}\ ln\left(\frac{T_\lambda}{100}\right), \tag{3}$$

where C = beam attenuation coefficient at wavelength, λ,
R = pathlength,
T = percent transmission.

Shannon (1975) has suggested a relationship between C and $\bar{k}$, as follows:

$$\bar{k} = 0.2\ C + 0.04\ (m^{-1})\ .$$

The optical properties of coastal waters and deep ocean waters are significantly different as a result of the biological and chemical processes that occur in each of these water types. The optical properties in deep ocean waters are influenced by the absorption characteristics of the phytoplankton population. In coastal areas high concentrations of suspended sediment have significant scattering and absorption influence on optical properties. Because of these two types of influence the correlation of water optic properties with the biochemical distribution becomes extremely complex (Arnone, 1983)

Gordon and Wounters (1978) have suggested that the use of the Secchi depth measurement provides significant information on the absorption and scattering coefficient of water when combined with additional measurements of k or scattering coefficients of the particles, *bp*. Other studies in coastal waters have attempted to relate Secchi depth measurements to suspended sediment concentrations. It was found that this inverse relationship was strongly dependent on the size distributions of the suspended sediments. Manheim and

Mead (1970) indicated that th
relationship:

$$Z_s = \frac{A d \varrho}{w}$$

where d = mean diameter,
ϱ = density,
w = weight of suspend
A = constant.

Other studies have related the
nephelometric turbidity units (

V. Environmental ir Secchi depth

Several factors that have a di
Secchi depth values in coastal w
tors were used to estimate the Se
squares for various regions of th
available. As mentioned, the inf
ner are color striped in the on

A. Phytoplankton

Chlorophyll, which is the pign
sible for photosynthesis, is pre
organisms called phytoplank
phytoplankton acidify chloroph
components, chlorophyll a and
been termed phytoplankton pign
absorption and scattering proper
radiance absorption from this p
nm (Fig. 5), and some spectral
ferent species are noted. Howe
about these wavelengths is beli
tion of the pigment.

There are vertical, seasonal,
plankton abundance. The vertica
by the depth of the euphotic
occur. This depth may range fr
shore areas to about 150 m in cl
tions in phytoplankton abunda
duction occur as a consequenc
temperature, mixing rate of th
Si, Fe, Mn, Mo) and herbivore
ble within 24 hours, provided a

:stablished an empirical relationship between :enuation coefficient and Secchi depth.

$$3\ [m^{-1}] , \quad (2)$$

epth.

diffuse attenuation coefficient.

's by other investigators can be found in Van 79).

›n coefficient is an inherent, spectrally depend- ıat characterizes the attenuation due to scat- in a collimated beam of monochromatic light ıgth of homogeneous water. The measure- rement within the water column that, through ›file, is used to describe vertical inhomogeneity :ies. The measurement obtains the percent ater column, which is then computed to beam ıt by

$$\frac{\lambda}{0}\Big) . \quad (3)$$

ttenuation coefficient at wavelength, λ, gth,

transmission.

suggested a relationship between C and $\bar{k}$, as

$$(m^{-1}) .$$

ties of coastal waters and deep ocean waters rent as a result of the biological and chemical n each of these water types. The optical prop- ı waters are influenced by the absorption phytoplankton population. In coastal areas of suspended sediment have significant scat- ı influence on optical properties. Because of fluence the correlation of water optic proper- ıical distribution becomes extremely complex

ıters (1978) have suggested that the use of surement provides significant information on :attering coefficient of water when combined ırements of k or scattering coefficients of the ıdies in coastal waters have attempted to relate ments to suspended sediment concentrations. ı inverse relationship was strongly dependent ›ns of the suspended sediments. Manheim and Mead (1970) indicated that the Secchi depth had the following relationship:

$$Z_s = \frac{Ad\varrho}{w} \quad (4)$$

where d = mean diameter,
ϱ = density,
w = weight of suspended particles,
A = constant.

Other studies have related the Secchi depths in coastal waters to nephelometric turbidity units (NTU) (Arnone, 1983).

V. Environmental influence on coastal Secchi depth

Several factors that have a direct influence on the variability of Secchi depth values in coastal waters will be discussed. These factors were used to estimate the Secchi depth values in the one-degree squares for various regions of the atlas where Secchi data was not available. As mentioned, the inferred values obtained in this manner are color striped in the one-degree squares in the plates.

A. Phytoplankton

Chlorophyll, which is the pigment present in living plants responsible for photosynthesis, is present in sea water in microscopic organisms called phytoplankton. Zooplankton feeding on phytoplankton acidify chlorophyll a to phaeopigments. These two components, chlorophyll a and phaeopigments of sea water, have been termed *phytoplankton pigment concentration* and have similar absorption and scattering properties in the visible spectrum. Strong radiance absorption from this pigment is observed at 440 and 665 nm (Fig. 5), and some spectral dependencies resulting from different species are noted. However, the intensity of the absorption about these wavelengths is believed to be related to the concentration of the pigment.

There are vertical, seasonal, and regional variations in phytoplankton abundance. The vertical distribution is influenced primarily by the depth of the euphotic zone in which photosynthesis can occur. This depth may range from less than a meter in turbid nearshore areas to about 150 m in clear oceanic waters. Seasonal oscillations in phytoplankton abundance, species composition and production occur as a consequence of a complex interacting of light, temperature, mixing rate of the watermass, plant nutrients (N, P, Si, Fe, Mn, Mo) and herbivore abundance. Growth rates can double within 24 hours, provided adequate conditions prevail. Limiting

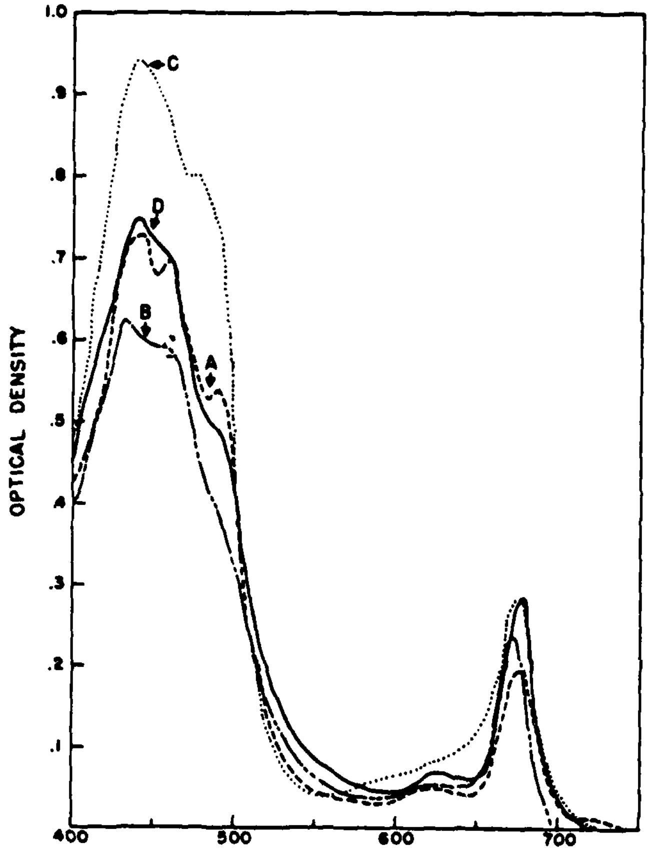

Figure 5. Absorption spectra of extracts of plankton algae: (A) a diatom, Cyclotella sp.; (B) a dinoflagellate, Amphidinium sp.; (C) a green flagellate, Chlamydomonas; (D) a natural population sampled from Woods Hole waters (from Yentsch, 1960).

factors of phytoplankton growth are inadequate illumination, excessive vertical mixing, nutrient limitation by extraction of Si and Fe through growth, and excessive grazing of zooplankton.

Regional variations in phytoplankton abundance, species distribution, and production also result from environmental conditions. Phytoplankton growth is stimulated in areas where two water masses diverge (equatorial Pacific and Norwegian Sea) or where upwelling of cool, nutrient-rich water reaches the surface from displacement of offshore winds (west coast of Africa, Central and South America).

The optical properties that result from phytoplankton are a product of both the absorption characteristics of the concentration and the scattering characteristics of the size distribution of the species. Various theoretical optical models have been constructed to examine the optical properties of phytoplankton (Morel and Bricand, 1980; Yentsch, 1960). The results indicate that backscattering is weak but is strongly influenced by absorption, and that specific absorption (per unit of pigment concentration in the water) varies with cell size as well as intracellular pigment concentration.

Morel and Prieur (1977) have classified seawaters according to the constituents responsible for absorption and scattering. The influence of phytoplankton and their covarying detrital products is compared to inorganic and organic suspended particulates. Case 1 waters were classified as those whose optical properties are derived from the response of phytoplankton and its detrital products. Case 2 waters are classified as those whose optical properties result from inorganic and/or organic sediments arising from resuspended sediments, terrigeneous particles, dissolved organic matter, and phytoplankton and associated detrital products.

Case 1 waters usually are associated with deep ocean water areas, although there are regions where Case 1 waters are present in coastal areas. Regional upwelling areas bordering coastal areas will contain Case 1 waters, which mix with inner-shelf, coastal-type Case 2 waters. Because of the strong relationship between the phytoplankton and optical properties, the term bio-optical properties has been associated with Case 1 waters.

Case 2 waters show high scattering from the interaction with the high concentrations of suspended particles as compared to Case 1 waters. Phytoplankton concentrations can be quite high in Case 2 waters, but they do not covary with the optical properties. Numerous cases have shown that Case 2 waters generated in coastal regions have been carried far offshore into the deeper oceanic waters. The spectral classification of the water optical properties results from the combined complex interaction of absorption, resulting from the phytoplankton, and scattering from the various size distributions of the particles. This combined interaction results in the ocean color. The strong absorption characteristics in the blue spectrum resulting from phytoplankton tend to result in greenish coloration of the water body. This water color is contrasted to a brown color resulting from increased scattering from suspended sediments. Methods of classifying water masses have been based on the spectral optical properties (ocean color), which distinctly define the interrelationships of the absorption and scattering properties of the water mass constituents.

B. Proximity to river discharge

A major influence on water optical variability in coastal areas is the proximity to river discharge. The increased concentrations of suspended sediments and dissolved organic material resulting from river discharge have significant effects on scattering and ab-

ieoretical optical models have been constructed to ex- optical properties of phytoplankton. (Morel and Bricand, itsch, 1960). The results indicate that backscattering is is strongly influenced by absorption, and that specific (per unit of pigment concentration in the water) varies size as well as intracellular pigment concentration.
nd Prieur (1977) have classified seawaters according to uents responsible for absorption and scattering. The in- phytoplankton and their covarying detrital products is to inorganic and organic suspended particulates. Case ere classified as those whose optical properties are derived esponse of phytoplankton and its detrital products. Case re classified as those whose optical properties result from and/or organic sediments arising from resuspended terrigeneous particles, dissolved organic matter, and kton and associated detrital products.
vaters usually are associated with deep ocean water areas, iere are regions where Case 1 waters are present in coastal ional upwelling areas bordering coastal areas will con- 1 waters, which mix with inner-shelf, coastal-type Case Because of the strong relationship between the kton and optical properties, the term bio-optical proper- een associated with Case 1 waters.
waters show high scattering from the interaction with oncentrations of suspended particles as compared to Case Phytoplankton concentrations can be quite high in Case but they do not covary with the optical properties. cases have shown that Case 2 waters generated in coastal ve been carried far offshore into the deeper oceanic waters. ral classification of the water optical properties results combined complex interaction of absorption, resulting phytoplankton, and scattering from the various size ns of the particles. This combined interaction results in color. The strong absorption characteristics in the blue resulting from phytoplankton tend to result in greenish of the water body. This water color is contrasted to a or resulting from increased scattering from suspended Methods of classifying water masses have been based ectral optical properties (ocean color), which distinctly interrelationships of the absorption and scattering prop- he water mass constituents.

mity to river discharge

influence on water optical variability in coastal areas imity to river discharge. The increased concentrations ed sediments and dissolved organic material resulting discharge have significant effects on scattering and absorption of coastal optical properties. These properties are indirectly the result of the drainage basin of the river.

The drainage basin's size, type of terrain, and composition of the soil ultimately influence the water optical properties. A large drainage basin in a low-lying, clayey soil usually will have river waters that contain a high concentration of suspended sediments with a small size distribution and slow-settling velocities. Thus, at the river discharge point the optical environment will be significantly influenced by turbid water conditions for a large surrounding area. The slow dissipation of the discharge plume will be influenced by local circulation patterns that could affect coastal areas along an entire coastal region. Higher energy drainage basins (e.g., Colorado River), typical in mountainous (tectonic) regions, contain larger-sized particles in suspension. The discharge of these type rivers is more localized at the river mouth, since these particles will settle out of solution rapidly. Drainage basins in low-lying, organically rich environments emit high concentrations of dissolved organic material to the coastal environment. Heavy rains during flood seasons flush the swamp of decaying organic material and produce large concentrations of humic and tannic acid in the river waters (referred to as a yellow substance or dissolved organic matter). The tea-colored Suwannee River, which drains Georgia's Okefenokee swamp, is an example. Upon entering the coastal environment this material is diluted with sea waters and responds to the local circulation patterns. Thus, the dynamic turbulence mixing that occurs at the river mouth determines the influence of the distribution of yellow substance in the overall coastal optical environment. Dissolved organic material is responsible for strong absorption of radiation especially in the shorter wavelengths.

In coastal areas where a significantly large discharge of suspended sediment is introduced into the environment, the optical properties show a covarying response. Instances where this occurs result in suspended sediment concentrations greater than 100 mg/l. In these instances the phytoplankton growth response is inhibited by the reduced light levels that result from the suspended sediment load. Thus, the optical properties are dominated by the response of the suspended sediment concentration. Coastal areas where these conditions arise are located at major river mouths. Table 1 lists the 21 major rivers of the world and their corresponding sediment discharge rates.

Figure 6 illustrates the annual discharge rates for various regions of the world (Milliman and Meade, 1983). The significance of this figure in regard to coastal properties is that it indicates regions where suspended sediments from river emission are important. Through correlation of this figure with local coastal currents the distribution of the sediment pattern in the near shore can be established. This figure should be contrasted to results of the Secchi values shown in the plates. The optical values in proximity to the river mouths are observed to be reduced.

Table 1. Quality
discharges to the

River
1. Ganges/Brahma
2. Yellow (Hwang)
3. Amazon
4. Yangtze
5. Irrawaddy
6. Magdalena
7. Mississippi
8. Orinoco
9. Hungho (Red)
10. Mekong
11. Indus
12. MacKenzie
13. Godavari
14. La Plata
15. Haiho
16. Purari
17. Zhu Jiang (Pearl)
18. Copper
19. Danube
20. Choshui
21. Yukon

The coastal optic directly influenced b The seasonal discha available on a limit

C. Tides

The importance o erties arises primari caused by tidal curr local regions where by coastline conditi these areas, high tid velocity to resuspen resuspension is depe tion, composition, d ditional information where the suspende that they remain in sediment concentrati tide. Constant tidal tremely turbid wate the global range in to determine the eff properties from this

of coastal optical properties. These properties are indirectly ılt of the drainage basin of the river.
lrainage basin's size, type of terrain, and composition of ultimately influence the water optical properties. A large basin in a low-lying, clayey soil usually will have river hat contain a high concentration of suspended sediments small size distribution and slow-settling velocities. Thus, river discharge point the optical environment will be ıntly influenced by turbid water conditions for a large sur- g area. The slow dissipation of the discharge plume will enced by local circulation patterns that could affect coastal ong an entire coastal region. Higher energy drainage basins olorado River), typical in mountainous (tectonic) regions, larger-sized particles in suspension. The discharge of these ers is more localized at the river mouth, since these par- ill settle out of solution rapidly. Drainage basins in low- rganically rich environments emit high concentrations of d organic material to the coastal environment. Heavy rains lood seasons flush the swamp of decaying organic material duce large concentrations of humic and tannic acid in the ters (referred to as a yellow substance or dissolved organic The tea-colored Suwannee River, which drains Georgia's okee swamp, is an example. Upon entering the coastal en- ent this material is diluted with sea waters and responds cal circulation patterns. Thus, the dynamic turbulence mix- occurs at the river mouth determines the influence of the tion of yellow substance in the overall coastal optical en- ent. Dissolved organic material is responsible for strong ab- ı of radiation especially in the shorter wavelengths.
ıstal areas where a significantly large discharge of suspend- nent is introduced into the environment, the optical prop- ow a covarying response. Instances where this occurs result nded sediment concentrations greater than 100 mg/l. In stances the phytoplankton growth response is inhibited by ıced light levels that result from the suspended sediment ıus, the optical properties are dominated by the response ıspended sediment concentration. Coastal areas where these ns arise are located at major river mouths. Table 1 lists najor rivers of the world and their corresponding sediment ge rates.
e 6 illustrates the annual discharge rates for various regions orld (Milliman and Meade, 1983). The significance of this n regard to coastal properties is that it indicates regions uspended sediments from river emission are important. h correlation of this figure with local coastal currents the tion of the sediment pattern in the near shore can be ed. This figure should be contrasted to results of the Secchi hown in the plates. The optical values in proximity to the ouths are observed to be reduced.

Table 1. Quality of data base for 21 largest river-sediment discharges to the ocean (Milliman and Meade, 1983).

River	Average Sediment Discharge (10^6 1/yr)	Adequacy of Data Base
1. Ganges/Brahmaputra	1670	Inadequate
2. Yellow (Hwang)	1080	Good
3. Amazon	900	Inadequate
4. Yangtze	478	Good
5. Irrawaddy	285	Inadequate(?)
6. Magdalena	220	Inadequate
7. Mississippi	210	Good
8. Orinoco	210	Sufficient
9. Hungho (Red)	160	Inadequate
10. Mekong	160	Sufficient
11. Indus	100	Sufficient
12. MacKenzie	100	Poor to Fair
13. Godavari	96	Inadequate
14. La Plata	92	Inadequate to Sufficient
15. Haiho	81	Good
16. Purari	80	Inadequate
17. Zhu Jiang (Pearl)	69	Sufficent to Good
18. Copper	70	Sufficient
19. Danube	67	Good
20. Choshui	66	Sufficient
21. Yukon	60	Sufficient

The coastal optical conditions resulting from river discharge are directly influenced by the seasonal run-off patterns of the river basin. The seasonal discharge of suspended sediments of major rivers is available on a limited basis.

C. Tides

The importance of tidal influence on coastal water optical properties arises primarily from the resuspension of bottom material caused by tidal currents. This influence is extremely important in local regions where significantly high tidal ranges are restricted by coastline conditions (i.e., Bay of Fundy, English Channel). In these areas, high tidal currents are capable of reaching the critical velocity to resuspend bottom material. The critical velocity for resuspension is dependent on the bottom type (i.e., size distribution, composition, density, shear strength, porosity, etc.). For additional information see Miller et al. (1977). In coastal conditions where the suspended particles have slow settling velocities, such that they remain in suspension during slack tide, the suspended sediment concentration remains quite high during all stages of the tide. Constant tidal reversals in coastal regions can result in extremely turbid water conditions at all times. Figure 7 illustrates the global range in tides in coastal areas. Although it is difficult to determine the effect that these ranges have on coastal optical properties from this figure alone, by correlating these tidal ranges

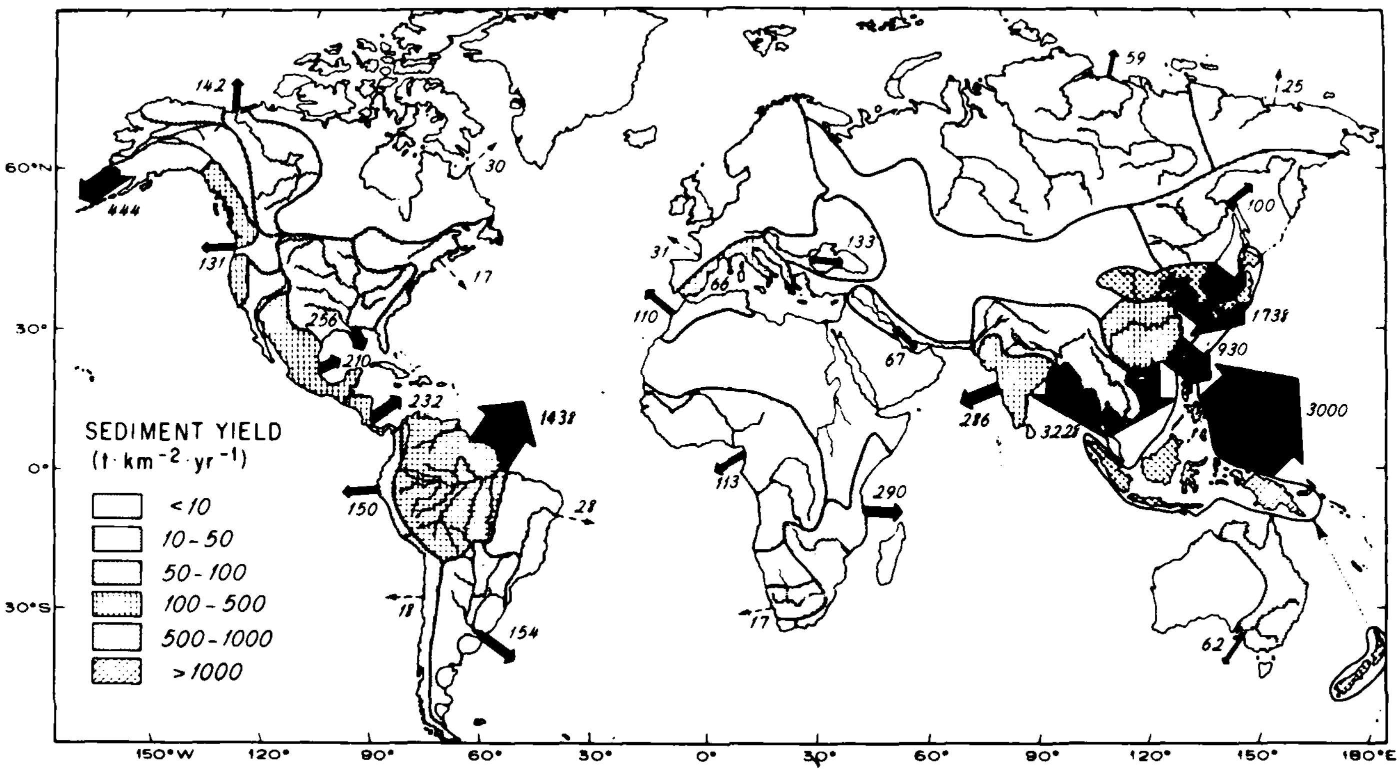

Figure 6. Annual discharge of suspended sediment from various drainage basins of the world; width of arrows corresponds to relative discharge. Numbers refer to average annual input in millions of tons. Direction of arrows does not indicate direction of sediment movement. The sediment yields and major rivers of the various basins also are shown; open patterns indicate essentially no discharge to the ocean (Milliman and Mead, 1983).

with local geomorphology, bathymetry and bottom type, an estimate of the tidal influence on optical conditions can be realized. Areas with high tidal ranges are expected to have more turbid coastal properties than for small tidal ranges.

D. Offshore currents

The distribution of coastal optical properties can be influenced by offshore currents. Figure 8 illustrates the major ocean currents in the oceans. The westward boundary currents (Gulf Stream, Kuroshio) are significantly strong and can have significant influence on the near-shore circulation and distribution of optical properties. The influence of ocean currents in coastal areas is more pronounced if the continental shelf is narrow and the clearer ocean waters are able to extend closer to the coast. The direction of the offshore currents provides an indication of the transport direction of coastal water masses. The discharge of the Amazon River is transported by the effects of the Guiana current to the northwest; thus, the coastal optical properties are significantly different than to the southeast of the Amazon delta. Similarly, coastal optical properties can be estimated along the west African coast at the convergence of the Canary current and the Benguela current. Increased water turbidity is expected, as resulting from transport of nutrient-rich coastal water and consequent bloom of phytoplankton.

The seasonal variation in ocean currents should be noted to also create seasonal changes in the distribution of coastal optical values. The effect of the monsoons has significant effects on the east African coastal current (Somali current). During the winter months this current flows south, whereas the current is shown to flow north during the monsoon. The influence on coastal water mass transport has not been adequately researched although the seasonal variability of coastal optics is evident.

Most ocean current waters are characterized by clear water optical properties having low phytoplankton concentrations (i.e., Gulf Stream, Loop Current). However, at the current boundaries where

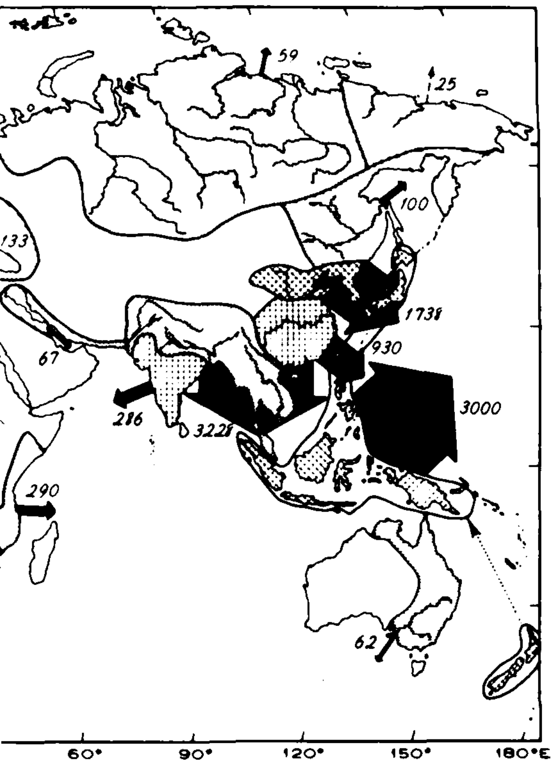

f the world; width of arrows corresponds to relative of arrows does not indicate direction of sediment)wn; open patterns indicate essentially no discharge

oastal optical properties are significantly different than ieast of the Amazon delta. Similarly, coastal optical propbe estimated along the west African coast at the con- the Canary current and the Benguela current. Increased dity is expected, as resulting from transport of nutrient-l water and consequent bloom of phytoplankton.

onal variation in ocean currents should be noted to also onal changes in the distribution of coastal optical values. of the monsoons has significant effects on the east African rent (Somali current). During the winter months this ws south, whereas the current is shown to flow north monsoon. The influence on coastal water mass transport n adequately researched although the seasonal variability optics is evident.

ean current waters are characterized by clear water opties having low phytoplankton concentrations (i.e., Gulf op Current). However, at the current boundaries where ocean fronts occur, numerous chemical, biological, and physical processes produce increased water turbidity. The ocean frontal zones are an extremely complex current shear area in which instabilities in the flow give rise to spin-off rings. The movements of spin-off rings and ocean frontal areas are presently under investigation, as is their physical and biological effect on coastal optics waters.

From a biochemical point of view, frontal areas can be viewed as giant chemical reactors fueled by components supplied via water mass transport, with the resultant chemical reactions biologically radiated by photosynthesis, respiration, and microbial degradation. Chemical, biological, and physical processes are being studied to characterize the spatial and temporal variability of the frontal regime in regard to optical properties. Fronts are recognized on large-scale ocean fronts and on a small scale as coastal fronts. Similar response of the optical properties is expected.

E. Meteorology

Local meteorology has a significant influence on the local coastal waters. Specific regions have certain types of local meteorology that directly influence the land/water boundary conditions. For example, the typical land/sea breeze pattern typical of summer low-latitude areas influences the coastal optical properties. The afternoon thundershowers, which result from this climatic pattern, produce freshwater runoff and increased wave conditions that ultimately increase the water turbidity. For this regime, early morning conditions are perhaps the best t at a minimum and to settle.

Frontal passages passage of cold fro and heavy rains (de results in turbulent sion of bottom sedi water turbidity will The time required to clear depends on generated by tides. elapse with extreme clarity returns to n Bahamas) can beco front or a severe st water conditions ca The passage of front high-pressure area Although these co tics, it can require clarity improves.

As indicated, the different for specific compiled into four

Figure 7. Tidal range along the coasts of the w

its occur, numerous chemical, biological, and physical roduce increased water turbidity. The ocean frontal zones emely complex current shear area in which instabilities give rise to spin-off rings. The movements of spin-off ocean frontal areas are presently under investigation, as ysical and biological effect on coastal optics waters. biochemical point of view, frontal areas can be viewed emical reactors fueled by components supplied via water port, with the resultant chemical reactions biologically photosynthesis, respiration, and microbial degradation. biological, and physical processes are being studied to e the spatial and temporal variability of the frontal regime o optical properties. Fronts are recognized on large-scale ts and on a small scale as coastal fronts. Similar response ical properties is expected.

orology

eteorology has a significant influence on the local coastal ecific regions have certain types of local meteorology that fluence the land/water boundary conditions. For exam- ical land/sea breeze pattern typical of summer low-latitude nces the coastal optical properties. The afternoon thunder- which result from this climatic pattern, produce fresh- ff and increased wave conditions that ultimately increase turbidity. For this regime, early morning conditions are perhaps the best for clear water conditions, since the winds are at a minimum and the suspended coastal particulates have had time to settle.

Frontal passages are often common in many coastal areas. The passage of cold frontal systems usually has associated strong winds and heavy rains (dependent on the severity of the front). This passage results in turbulent mixing of the upper water column and resuspension of bottom sediment material in the near-shore areas. Resulting water turbidity will be severely increased in these localized areas. The time required for the particulates to settle out and the waters to clear depends on the particle size and density, and the turbulence generated by tides, etc. It is common for a period of 3–4 days to elapse with extremely calm sea and wind conditions before the water clarity returns to normal conditions. Clear water conditions (i.e., Bahamas) can become extremely turbid with the passage of a cold front or a severe storm within several hours. The resulting turbid water conditions can persist for 5 days before clear waters return. The passage of fronts in many instances is followed by a cold, stable, high-pressure area in which the winds are somewhat reduced. Although these conditions appear excellent for coastal water optics, it can require several days of this condition before the water clarity improves.

As indicated, the coastal oceanographic climate is significantly different for specific regions. Although the present atlas has been compiled into four seasons (winter, spring, summer, fall), certain

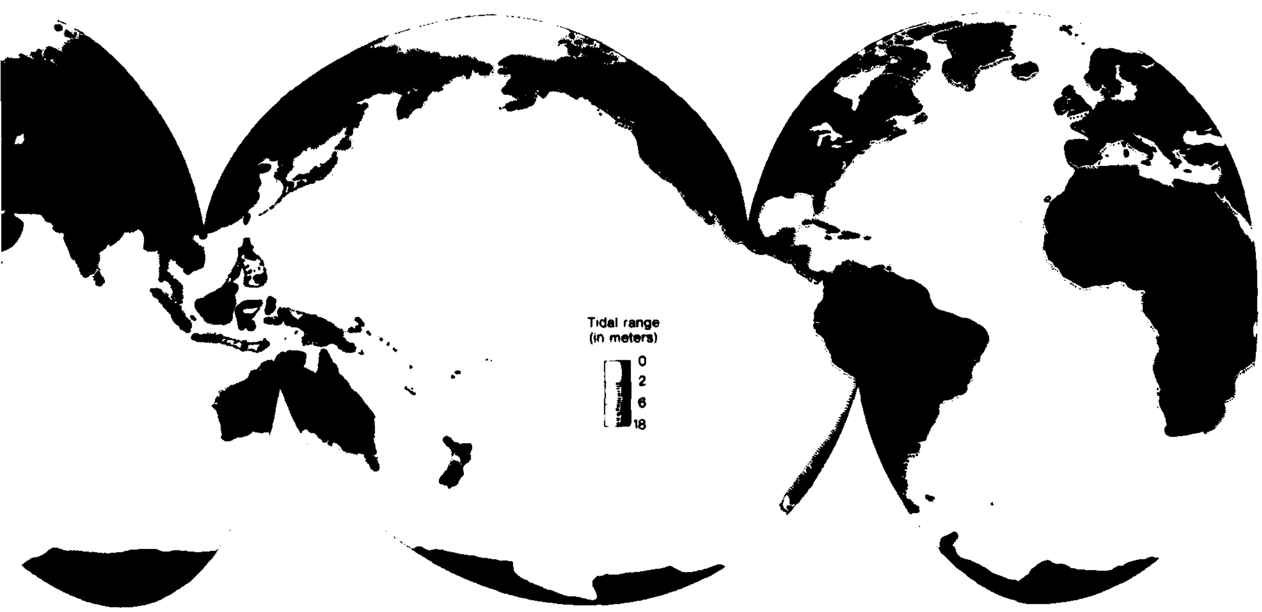

Figure 7. Tidal range along the coasts of the world.

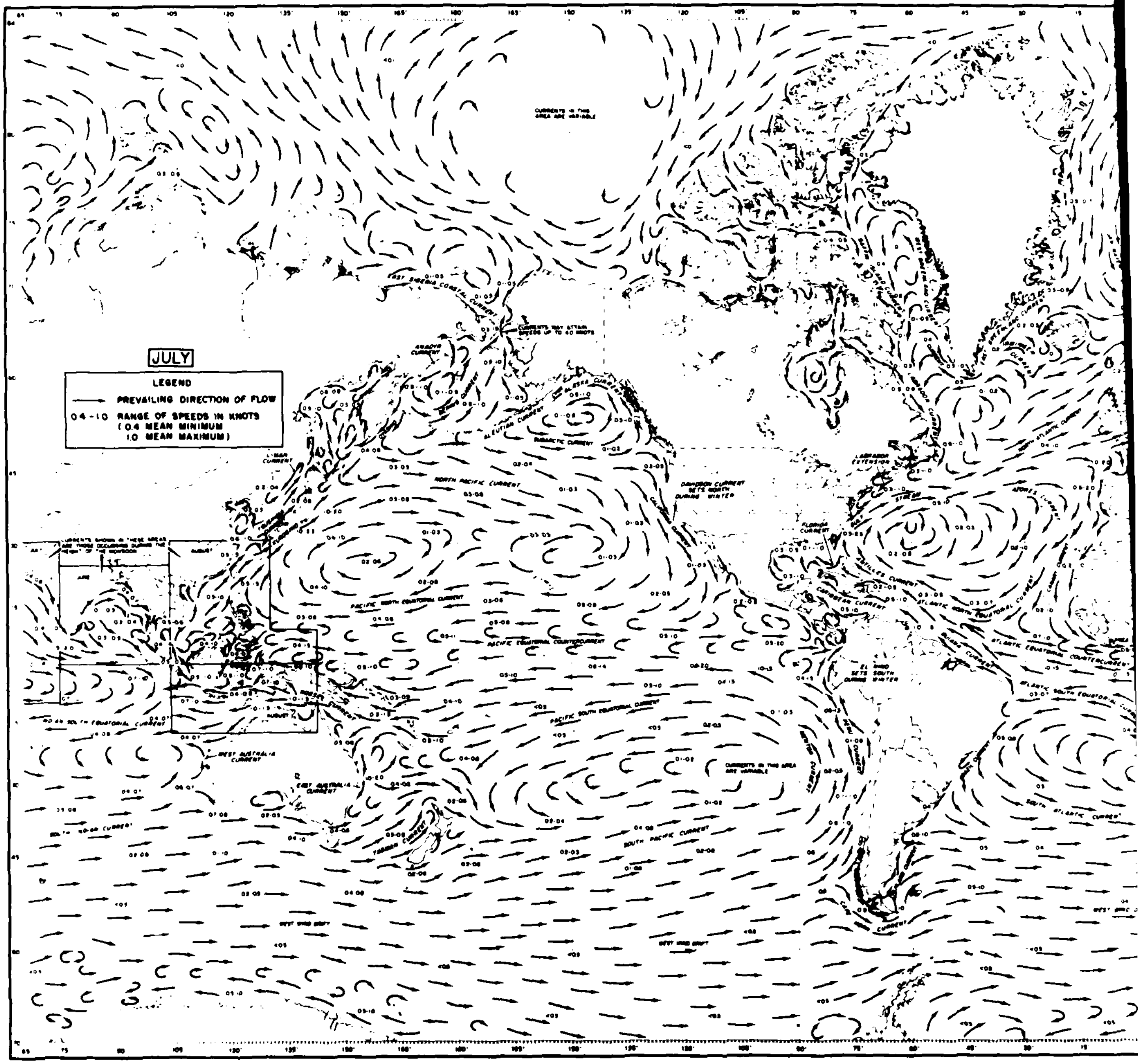

Figure 8. World ocean currents for July (Bialek, 1966).

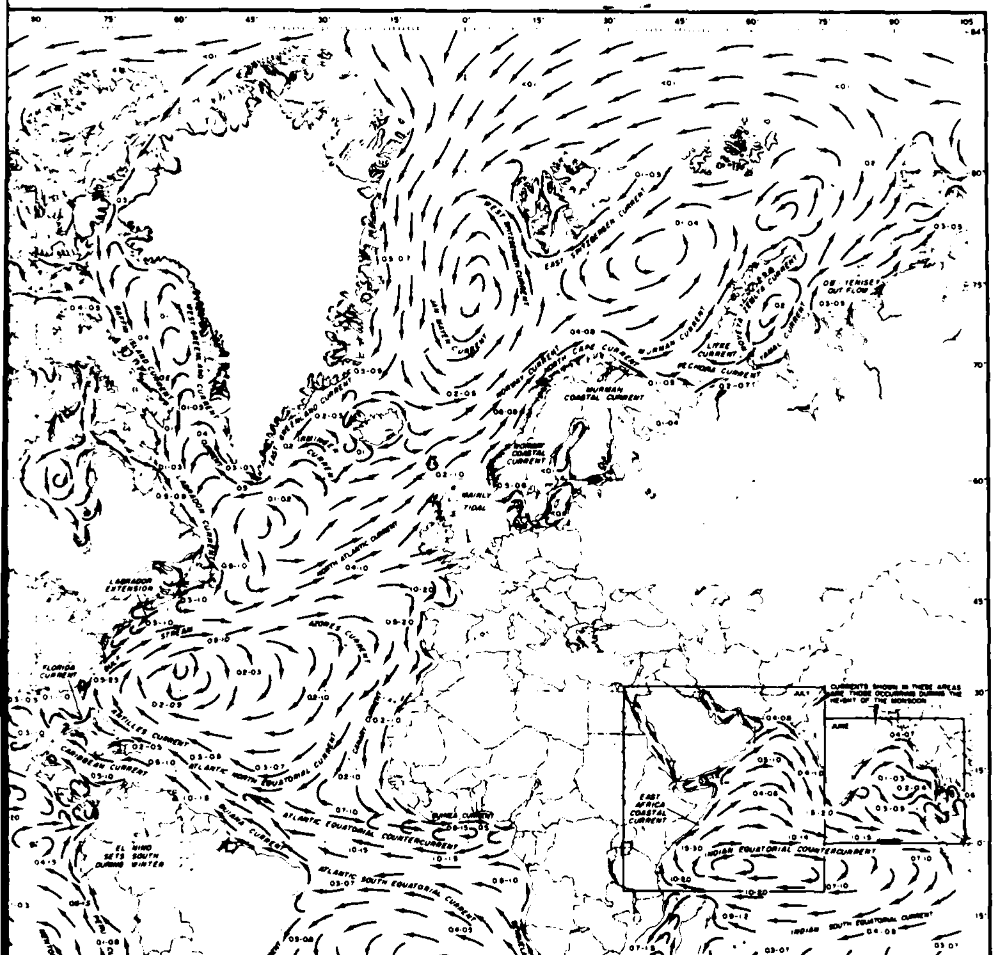

rrents for July (Bialek, 1966).

regions have significantly different seasons. which occurs in the Indian Ocean, has fou northeast monsoon (Dec–Mar), the interperio mer monsoon (Jun–Sep), and the fall interper the monthly progression of the wind and r thern Indian Ocean. The strong onshore w and July period result in high wave condi clarity is reduced. This is compounded by h months. The offshore wind patterns along result in decreased coastal fetch and decrea winter months are, therefore, most probable in this region.

F. Coastal geomorphology

The basic geologic coastal landforms int tical properties. The classification of the coa the soil composition, geomorphic condition tectonic activity. For a chart of coastal landfo In many instances the general coastal classi as an influence on the coastal optical prop proceeding coastline that is being developed l of clay will most likely have large concentra ticles within the water column. Their slow bined with the high sediment input to the turbid coastal waters.

VI. Results

The results of the color-coded atlas are illu The annual mean for Chart 1 is illustrated 1–4. This sequence is followed for Charts 2 one-degree squares are clearly observed alor the areas where ranges were estimated, the in by the appropriate color code. The annu 1, 6, 11, 16) contain the most data, as show of solid one-degree squares. The seasonal c less data available, and additional Secchi required.

The spatial variability characterized by t the rapidly changing coastal optics. Notice t (Chart 3, Plate 11) is quite turbid and th nautical miles (NM) to the northeast, wate Similar high spatial variability is observed n This high variability is perhaps more st estimated, since the data has been averaged c and overall seasons. This procedure should quency variability. The existing high variabi data are required to determine whether tl variability is more prevalent.

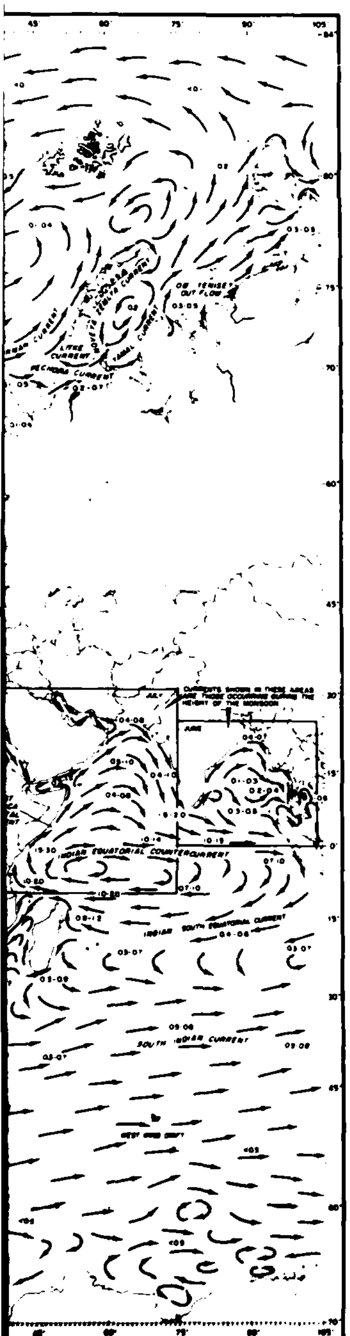

regions have significantly different seasons. The monsoon season, which occurs in the Indian Ocean, has four distinct seasons: the northeast monsoon (Dec–Mar), the interperiod (Apr–May), the summer monsoon (Jun–Sep), and the fall interperiod. Figure 9 illustrates the monthly progression of the wind and rain pattern in the northern Indian Ocean. The strong onshore winds during the June and July period result in high wave conditions, and the coastal clarity is reduced. This is compounded by heavy rains during these months. The offshore wind patterns along the west Indian coast result in decreased coastal fetch and decreased coastal waves. The winter months are, therefore, most probable for clear coastal waters in this region.

F. Coastal geomorphology

The basic geologic coastal landforms influence the coastal optical properties. The classification of the coastline is dependent on the soil composition, geomorphic conditions, beach stability, and tectonic activity. For a chart of coastal landforms, see McGill (1958). In many instances the general coastal classification can be utilized as an influence on the coastal optical properties. For example, a proceeding coastline that is being developed by sedimentary deposits of clay will most likely have large concentrations of fine-sized particles within the water column. Their slow-settling velocity, combined with the high sediment input to the coastal area, results in turbid coastal waters.

VI. Results

The results of the color-coded atlas are illustrated in Plates 1–20. The annual mean for Chart 1 is illustrated, followed by Seasons 1–4. This sequence is followed for Charts 2, 3, and 4. The blocky one-degree squares are clearly observed along the coastal areas. In the areas where ranges were estimated, the area has been striped in by the appropriate color code. The annual mean charts (Plates 1, 6, 11, 16) contain the most data, as shown by the large amount of solid one-degree squares. The seasonal charts have sufficiently less data available, and additional Secchi depth estimates were required.

The spatial variability characterized by these figures illustrates the rapidly changing coastal optics. Notice that the Malacca Strait (Chart 3, Plate 11) is quite turbid and that approximately 200 nautical miles (NM) to the northeast, waters are extremely clear. Similar high spatial variability is observed near the Gulf of Tonkin. This high variability is perhaps more striking than might be estimated, since the data has been averaged over one-degree squares and overall seasons. This procedure should filter out the high frequency variability. The existing high variability suggests that more data are required to determine whether the temporal or spatial variability is more prevalent.

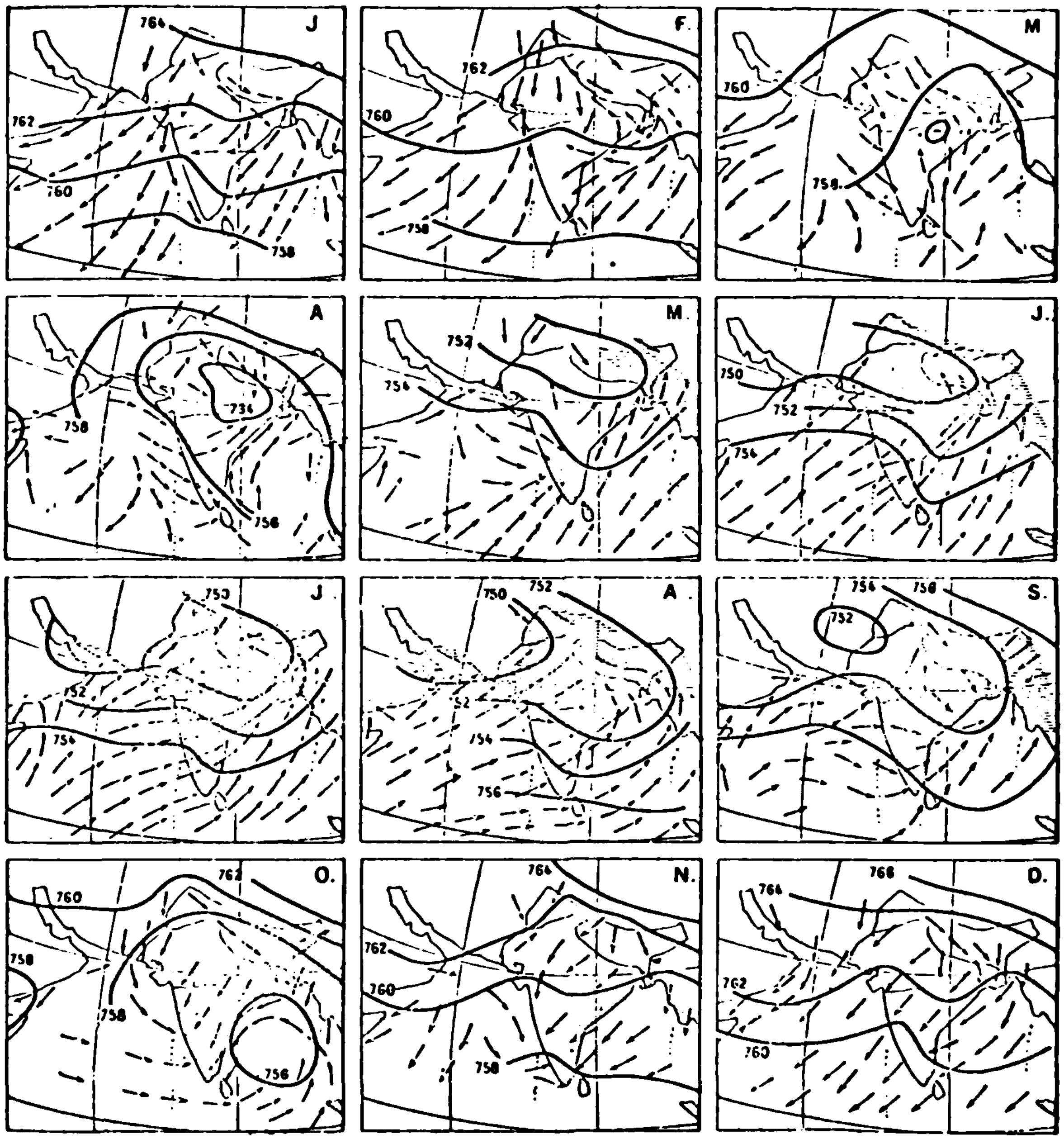

Figure 9. Annual evolution of the wind and pressure systems over the northern Indian Ocean from January to December. Rainfall areas are shaded (from de Martonne, 1950). (750 mm = 1000 mb; 760 mm = 1013 mb)

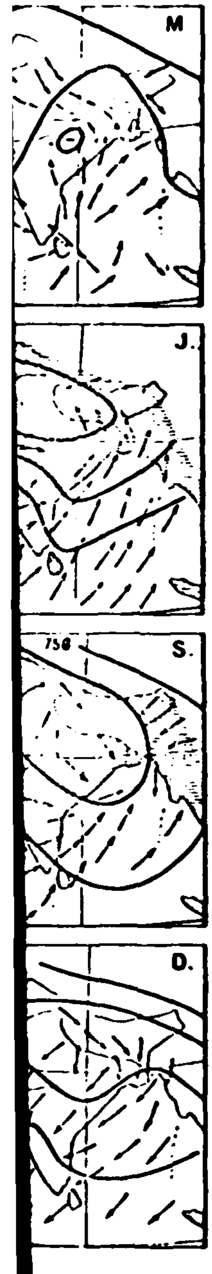

ary to December. Rainfall

The positions of the equatorial oceanic and coastal currents are observed to affect the coastal optical properties in such areas as the west African and west South American coasts. Discharge of major rivers is also observed to control the seasonal coastal turbidity along long coastlines.

To characterize the general water turbidity ranges for global coverage and to estimate the seasonal trends, the number of one-degree squares for each Secchi depth range for each chart was counted to establish the seasonal variability for the coastlines.

The results of this analysis are illustrated in Figure 10 and tabulated in Tables 2-6. It should be noted that the four charts have unequal numbers of one-degree squares bordering coastlines. The percentage of coastline (water depths less than 500 m) for each chart follows: Chart 1—25%; Chart 2—19%; Chart 3—45%; Chart 4—13%.

Figure 10a illustrates coastal coverage for each season for Chart 1 for each Secchi depth range. Chart 1 contains mostly the waters bordering the Atlantic Ocean. Range-1 (<5 m) is observed to have a slightly higher percentage in October-March than in the other months. The variability in this percentage can be attributed to the seasonal outflow of the Amazon River, whose discharge affects a large coastal area along northern South America. Although this percentage range is quite small ($\sim 6\%$), it is slightly higher than for the global average, as will be shown below. Range-2 shows a seasonal distribution similar to that for range-1. Range-4 is observed to contain the highest percentage of this chart, with a mean percentage of 31%. Ranges-5 and -6 do not indicate high seasonal variability. The percentage of very clear waters (range-6) is 21%, which is quite high compared to all continental coastal areas covered by this chart.

Figure 10b illustrates the percentage estin
chart covers the western Indian Ocean, so
and Red Sea areas. A significant change is
sion with the previous chart in that the p
water is reduced to approximately 1%. Th
observed to occur in the July-September peri
water comprises about 39%. Elevated coas
in the October-December period, most like
ly flow of the Somali current along the Af
of the monsoon.

Figure 10c illustrates percentage estimates
includes the largest coastal borders in the wo
high percentage of range-1 waters is found
The seasonal distribution indicates that the J
has the highest percentage of clear water
distribution is observed for range-2 waters. R
show very little seasonal variability. A rela
distribution is observed between ranges-5

Figure 10d illustrates percentage estimates
Pacific in Chart 4. This area of coastal co
numerous atolls, yet it represents only 13
coastlines. The percentage of turbid range-
siderably lower in this area, and range-6 wat
of the coastal water in this area.

Figure 10e illustrates the global coastal p
a composite of all four charts. The season
coastal areas indicates that the July-Septem
clearer water conditions than for the other t
is attributed to the influence of the monsoo
indicated on charts 2 and 3 estimates whe
tions were observed during the October-M

the equatorial oceanic and coastal currents are the coastal optical properties in such areas as nd west South American coasts. Discharge of o observed to control the seasonal coastal tur- coastlines.

the general water turbidity ranges for global timate the seasonal trends, the number of one- each Secchi depth range for each chart was h the seasonal variability for the coastlines.

this analysis are illustrated in Figure 10 and s 2-6. It should be noted that the four charts bers of one-degree squares bordering coastlines. coastline (water depths less than 500 m) for each 1 – 25%; Chart 2—19%; Chart 3—45%; Chart

ates coastal coverage for each season for Chart epth range. Chart 1 contains mostly the waters ntic Ocean. Range-1 (< 5 m) is observed to er percentage in October-March than in the variability in this percentage can be attributed low of the Amazon River, whose discharge af- area along northern South America. Although ge is quite small (~ 6%), it is slightly higher verage, as will be shown below. Range-2 shows n similar to that for range-1. Range-4 is observ- ighest percentage of this chart, with a mean Ranges-5 and -6 do not indicate high seasonal centage of very clear waters (range-6) is 21%, compared to all continental coastal areas covered

Figure 10b illustrates the percentage estimates for Chart 2. This chart covers the western Indian Ocean, southern African coast, and Red Sea areas. A significant change is observed by comparision with the previous chart in that the percentages of range-1 water is reduced to approximately 1%. The clear water range is observed to occur in the July-September period, where the range-6 water comprises about 39%. Elevated coastal turbidity is shown in the October-December period, most likely because of southerly flow of the Somali current along the African coast as a result of the monsoon.

Figure 10c illustrates percentage estimates for Chart 3. This chart includes the largest coastal borders in the world (45%). A relatively high percentage of range-1 waters is found along the coasts (5%). The seasonal distribution indicates that the July-September period has the highest percentage of clear waters. A similar seasonal distribution is observed for range-2 waters. Ranges-3 and -4 waters show very little seasonal variability. A relatively similar seasonal distribution is observed between ranges-5 and -6.

Figure 10d illustrates percentage estimates for the East and South Pacific in Chart 4. This area of coastal coverage is composed of numerous atolls, yet it represents only 13% of the total world coastlines. The percentage of turbid range-1 or -2 waters is considerably lower in this area, and range-6 water occupies about 66% of the coastal water in this area.

Figure 10e illustrates the global coastal percentage taken from a composite of all four charts. The seasonal distribution for the coastal areas indicates that the July-September period has slightly clearer water conditions than for the other times. This seasonality is attributed to the influence of the monsoon seasons, which were indicated on charts 2 and 3 estimates where more turbid conditions were observed during the October-March period.

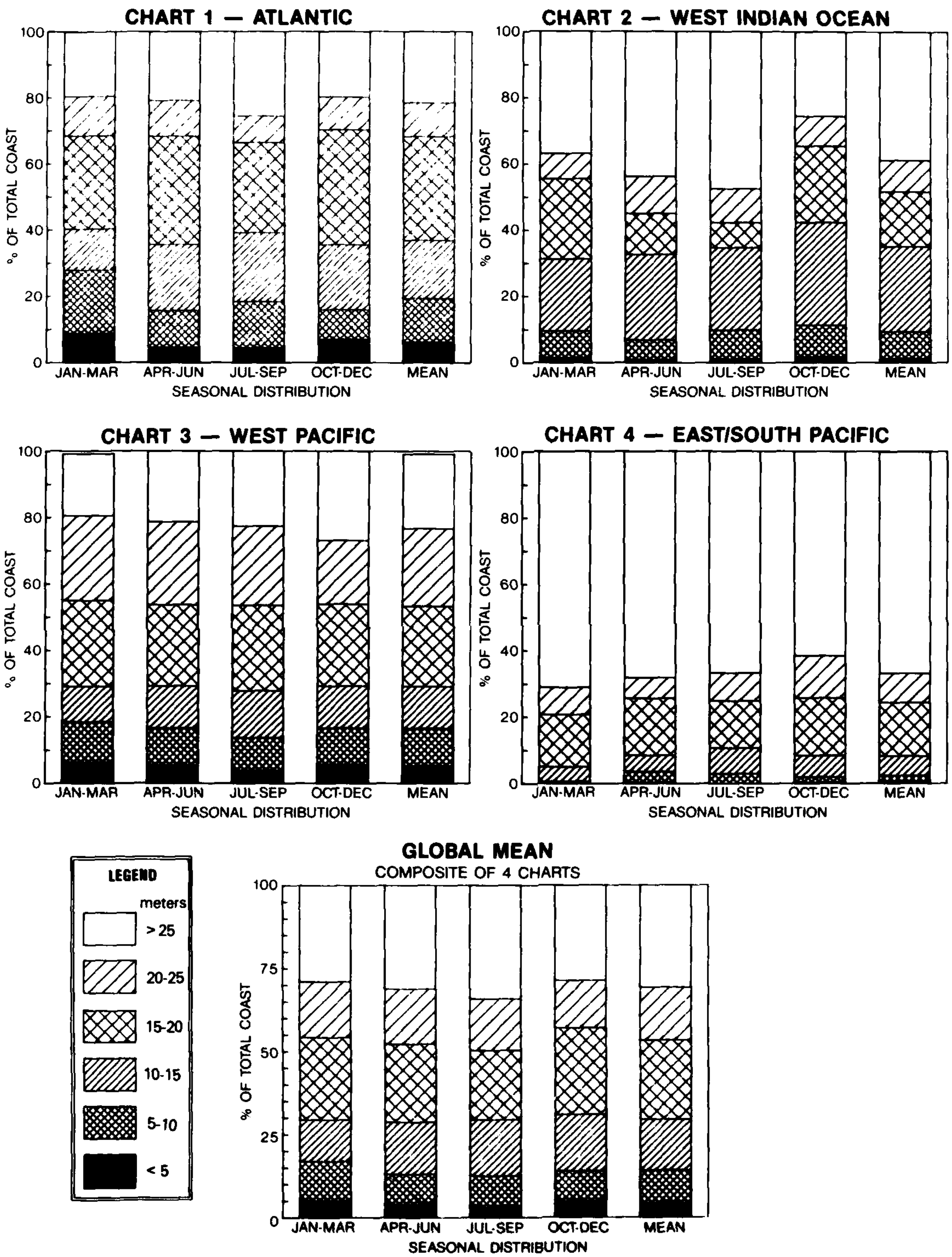

Figure 10. Seasonal and annual distribution of the percentage of Secchi depth ranges.

Table 2. Chart 1—Percentage of one-degree squares.

Secchi Depth Range	Season 1	2	3	4	Annual Mean
1	8.70	4.63	4.53	6.96	6.17
2	19.18	11.10	13.90	9.03	13.16
3	12.43	19.94	20.78	19.55	17.46
4	28.24	32.72	27.18	34.66	31.25
5	11.90	10.81	7.96	9.92	10.23
6	19.53	20.78	25.62	19.85	21.79
Total # of squares 2560					

Table 3. Chart 2—Percentage of one-degree squares.

Secchi Depth Range	Season 1	2	3	4	Annual Mean
1	1.35	0.79	1.11	1.71	1.23
2	8.14	5.97	8.69	9.62	8.09
3	21.70	25.70	24.77	31.00	25.65
4	24.22	12.35	7.58	23.07	16.57
5	7.56	11.15	10.17	8.97	9.47
6	37.01	44.02	47.70	25.64	38.97
Total # of squares 2027					

Table 4. Chart 3—Percentage of one-degree squares.

Secchi Depth Range	Season 1	2	3	4	Annual Mean
1	6.15	5.43	3.84	5.60	5.25
2	13.15	11.09	9.80	10.95	11.23
3	10.67	12.65	14.22	12.63	12.56
4	25.88	24.52	25.65	24.67	24.16
5	25.53	24.98	23.94	19.23	23.44
6	18.62	21.33	22.55	26.92	22.35
Total # of squares 4880					

Table 5. Chart 4—Percentage of one-degree squares.

Secchi Depth Range	Season 1	2	3	4	Annual Mean
1	0.00	0.27	0.00	0.32	0.14
2	0.06	3.25	2.90	1.62	2.19
3	4.40	4.87	7.65	6.51	5.92
4	15.71	7.07	14.24	17.26	16.10
5	8.20	6.23	8.44	12.70	8.78
6	71.10	68.29	66.75	61.56	66.83
Total # of squares 1366					

Table 6. Global coverage—Percentage of on

Secchi Depth Range	Season 1	2	3
1	4.98	3.76	2.94
2	11.91	9.19	9.59
3	12.50	15.73	16.88
4	24.80	23.46	20.94
5	16.78	16.64	15.48
6	29.01	31.19	34.16
Total # of squares 10,833			

VII. Summary and conclusio

A seasonal Secchi depth atlas of global conditio
has been compiled on 20 charts from a limited an
data. Six ranges of values have been assigned to
are 60 NM square and less than 500 m deep.
base illustrates a high coastal spatial and temporal
able mechanisms for the variability are suggested.
modeling the optical variability with coastal proc
ditional investigation and high-resolution data.

The global distribution of coastal Secchi depths
percentage of relatively clear waters. Less than 5%
are shown to have less than 5 m Secchi depth valu
changes in the percentage of each range were obse
percentage of coastal waters occurred in ranges-
-6 (>25 m).

Insufficient spatial and temporal data in coast
sidered the most significant problem with atlas c
provements of the data base require that synopt
spatial coverage be considered. Since field progra
cost intensive, the applications of visible remote
should be investigated for data collection. Only
the spatial and temporal variability of the coastal
be established for modeling purposes.

Application of remote sensing technology for
tical data base has significant advantages in addit
temporal coverage. Presently, a regional study
Zone Color Scanner aboard the Nimbus 7 satelli
an optical data base is nearing completion, and th
encouraging.

—Percentage of one-degree squares.

	Season			Annual
	2	3	4	Mean
70	4 63	4.53	6.96	6.17
18	11.10	13.90	9.03	13.16
43	19.94	20.78	19.55	17.46
24	32.72	27.18	34.66	31.25
90	10.81	7.96	9.92	10.23
53	20.78	25.62	19.85	21.79
0				

—Percentage of one-degree squares.

	Season			Annual
	2	3	4	Mean
35	0.79	1.11	1.71	1.23
14	5.97	8.69	9.62	8.09
70	25.70	24.77	31.00	25.65
22	12.35	7.58	23.07	16.57
56	11.15	10.17	8.97	9.47
01	44.02	47.70	25.64	38.97
7				

—Percentage of one-degree squares.

	Season			Annual
	2	3	4	Mean
15	5.43	3.84	5.60	5.25
15	11.09	9.80	10.95	11.23
67	12.65	14.22	12.63	12.56
88	24.52	25.65	24.67	24.16
53	24.98	23.94	19.23	23.44
62	21.33	22.55	26.92	22.35
0				

—Percentage of one-degree squares.

	Season			Annual
	2	3	4	Mean
00	0.27	0.00	0.32	0.14
06	3.25	2.90	1.62	2.19
40	4.87	7.65	6.51	5.92
71	7.07	14.24	17.26	16.10
20	6.23	8.44	12.70	8.78
10	68.29	66.75	61.56	66.83
6				

Table 6. Global coverage—Percentage of one-degree squares.

Secchi Depth Range	Season 1	2	3	4	Annual Mean
1	4.98	3.76	2.94	4.66	4.07
2	11.91	9.19	9.59	9.17	9.96
3	12.50	15.73	16.88	16.97	15.33
4	24.80	23.46	20.94	26.14	23.85
5	16.78	16.64	15.48	14.32	15.86
6	29.01	31.19	34.16	28.72	30.92
Total # of squares 10,833					

VII. Summary and conclusions

A seasonal Secchi depth atlas of global conditions ($\pm 40^\circ$ latitude) has been compiled on 20 charts from a limited amount of available data. Six ranges of values have been assigned to coastal areas that are 60 NM square and less than 500 m deep. This limited data base illustrates a high coastal spatial and temporal variability Probable mechanisms for the variability are suggested, although detailed modeling the optical variability with coastal processes requires additional investigation and high-resolution data.

The global distribution of coastal Secchi depths indicates a high percentage of relatively clear waters. Less than 5% of the coastlines are shown to have less than 5 m Secchi depth values. Little seasonal changes in the percentage of each range were observed. The highest percentage of coastal waters occurred in ranges-4 (15-20 m) and -6 (>25 m).

Insufficient spatial and temporal data in coastal areas was considered the most significant problem with atlas development. Improvements of the data base require that synoptic and improved spatial coverage be considered. Since field programs are man and cost intensive, the applications of visible remote sensing systems should be investigated for data collection. Only in this way can the spatial and temporal variability of the coastal optical properties be established for modeling purposes.

Application of remote sensing technology for generating an optical data base has significant advantages in addition to providing temporal coverage. Presently, a regional study using the Coastal Zone Color Scanner aboard the Nimbus 7 satellite for computing an optical data base is nearing completion, and the results are very encouraging.

VIII. References

Arnone, R. A. (1982). *Annotated Bibliography of Water Optical Properties of Ocean Waters.* Naval Ocean Research and Development Activity, NSTL, Mississippi, NORDA Technical Note 115.

Arnone, R. A. (1983). *Water Optics of Mississippi Sound.* Naval Ocean Research and Development Activity, NSTL, Mississippi, NORDA Report 63.

Austin, R. W. and T. J. Petzold (1980). The Determination of the Diffuse Attenuation Coefficient of Sea Water Using the Coastal Zone Color Scanner. *Oceanography from Space*, J. F. R. Gower (ed.), Plenum Publishing Corporation, p. 239.

Bialek, E. L. (1966). *Handbook of Oceanographic Tables.* U.S. Naval Oceanographic Office, NSTL, Mississippi, Special Publication 68.

Cialdi, A. and P. A. Secchi (1968). On the Transparency of the Sea. Translated by A. Collier, *Limnology and Oceanography* 13 (3), pp. 391-394.

De Martonne, H. R. (1950). *Encyclopedia of Oceanography.* R. W. Fairbridge (ed.), 1966.

Fairbridge, R. W. (ed.) (1966). *Encyclopedia of Oceanography.* Reinhold Publishing Corporation, New York.

Frederick, M. A. (1970). *An Atlas of Secchi Disc Transparency Measurements and Forel-Ule Color Codes for the Oceans of the World.* M.S. Thesis, Naval Postgraduate School, Monterey, California, 188 pp.

Gordon, H. R. and A. W. Wounters (1978). Some Relationships Between Secchi Depth and Inherent Optical Properties of Natural Waters. *Applied Optics*, v. 17, n. 21.

Hickman, G. D. (1979). *Flourescence and Ocean Color of the World's Oceans Annotated Bibliography.* Applied Science Technology, Inc., Rept. No. AST-R-040979, 1011 Arlington Blvd., Arlington, Virginia 22209.

Hojerslev, N. K. (1974). *Daylight Measurements for Photosynthetic Studies in the Western Mediterranean.* Univ. Copenhagen Inst., Physics Oceanogr., Report 26, May.

Isakov, I. S. (1953). Ministry of the Navy of the USSR. *Morskai*, Atlas 2.

Jerlov, N. G. (1976). *Optical Oceanography.* Elsevier Publishing Company.

Lepley, L. K. (1968). Coastal Water Clarity from Space Photographs. *Photogrammetric Engineering*, pp. 667-674, July.

Manheim, R. T., R. H. Mead, and G. C. Bond (1970). Suspended Matter in Surface Waters of the Atlantic Continental Margin from Cape Cod to the Florida Keys. *Science*, v. 167, pp. 371-376.

McGill, J. T. (1958). *Coastal Landforms of the World.* American Geographical Society, prepared under contract NONR-233(06), NR 388-013 between the Geography Branch, ONR and University of California.

Miller, M. C., I. N. McCave, and P. D. Komar (1977). Threshold of Sediment Motion Under Unidirectional Currents. *Sedimentology* v. 24, pp. 507-527.

Milliman, J. D. and R. H. Meade (1983). World-Wide Delivery of River Sediments to the Oceans. *The Journal of Geology*, v. 91, n. 1, pp. 1-21.

Morel, A. and A. Bricand (1980). Theoretical Results Concerning the Optics of Phytoplankton with Special Reference to Remote Sensing Applications. *Oceanography from Space*, J. R. Gower (ed.), Plenum Press, New York.

Morel and Prieur (1977). Analysis of Variations in Ocean Color. *Limnology and Oceanography*, v. 22, pp. 709-722.

Murdock, J. H. (1980). *The Transparency of Southeast Asian and Indonesian Waters.* M.S. Thesis, U.S. Naval Postgraduate School, Monterey, California.

Shannon, J. G. (1975). Correlation of Beam and Diffuse Attenuation Coefficients Measured in Selected Ocean Waters. Proceedings of the Society of Photo-Optical Instrumentation Engineers, *Ocean Optics*, v. 64, pp. 3-11.

Tucker, S. P. (1980). *A Bibliography of Optical Oceanography.* Naval Postgraduate School, Oceanography Dept., Monterey, California (unpublished).

Tucker, S. P. (1979). *Hydrooptics in the Soviet Union: A Bibliography.* Naval Postgraduate School, Oceanography Dept., Monterey, California (unpublished).

Van Norden, M. F. and S. E. Litts, (1979). *The Transparency of Selected U.S. Coastal Waters with Applications to Laser Bathymetry.* M.S. Thesis U.S. Navy Postgraduate School, Monterey, California.

Yentsch, C. S. (1960). The Influence of Phytoplankton Pigments in the Color of Sea Water. *Deep-Sea Res.*, v. 7, pp. 1-9.

968). Coastal Water Clarity from Space
rammetric Engineering, pp. 667–674, July.
. H. Mead, and G. C. Bond (1970). Suspend-
Waters of the Atlantic Continental Margin
Florida Keys. *Science*, v. 167, pp. 371–376.
). *Coastal Landforms of the World*. American
, prepared under contract NONR-233(06),
n the Geography Branch, ONR and Univer-

McCave, and P. D. Komar (1977). Threshold
Inder Unidirectional Currents. *Sedimentology*

d R. H. Meade (1983). World-Wide Delivery
the Oceans. *The Journal of Geology*, v. 91,

Bricand (1980). Theoretical Results Concern-
toplankton with Special Reference to Remote
Oceanography from Space, J. R. Gower (ed.),
York.
(1977). Analysis of Variations in Ocean Col-
Oceanography, v. 22, pp. 709–722.
980). *The Transparency of Southeast Asian*
ers. M.S. Thesis, U.S. Naval Postgraduate
alifornia.
75). Correlation of Beam and Diffuse Attenua-
sured in Selected Ocean Waters. Proceedings
o-Optical Instrumentation Engineers, *Ocean*
11.
). *A Bibliography of Optical Oceanography*.
hool, Oceanography Dept., Monterey, Califor-

79). *Hydrooptics in the Soviet Union: A*
Postgraduate School, Oceanography Dept.,
(unpublished).
and S. E. Litts, (1979). *The Transparency*
astal Waters with Applications to Laser
Thesis U.S. Navy Postgraduate School,

0). The Influence of Phytoplankton Pigments
Water. *Deep-Sea Res.*, v. 7, pp. 1–9.

UNCLASSIFIED
SECURITY CLASSIFICATION OF THIS PAGE

REPORT DOCUMENTATION PAGE

1a REPORT SECURITY CLASSIFICATION Unclassified	1b RESTRICTIVE MARKINGS None
2a SECURITY CLASSIFICATION AUTHORITY	3 DISTRIBUTION AVAILABILITY OF REPORT Approved for public release. unlimited.
2b DECLASSIFICATION DOWNGRADING SCHEDULE	
4 PERFORMING ORGANIZATION REPORT NUMBER(S) NORDA Report 83	5 MONITORING ORGANIZATION REPORT NUMBE NORDA Report 83
6 NAME OF PERFORMING ORGANIZATION Naval Ocean Research and Development Activity	7a NAME OF MONITORING ORGANIZATION Naval Ocean Research and D
6c ADDRESS (City, State, and ZIP Code) Ocean Science Directorate NSTL, Mississippi 39529-5004	7b ADDRESS (City, State and ZIP Code) Ocean Science Directorate NSTL, Mississippi 39529-50
8a NAME OF FUNDING SPONSORING ORGANIZATION Defense Mapping Agency — 8b OFFICE SYMBOL (If applicable)	9 PROCUREMENT INSTRUMENT IDENTIFICATION
8c ADDRESS (City, State, and ZIP Code) Washington, D.C. 20350	10 SOURCE OF FUNDING NOS PROGRAM ELEMENT NO: 63701B — PROJECT NO

11 TITLE (Include Security Classification)
Coastal Secchi Depth Atlas

12 PERSONAL AUTHOR(S)
Robert A. Arnone

13a TYPE OF REPORT	13b TIME COVERED	14 DATE OF REPORT (Yr, Mo, Day)
Final	From ____ To ____	July 1985

16 SUPPLEMENTARY NOTATION

17 COSATI CODES			18 SUBJECT TERMS (Continue on reverse if necessary and identify by block numb
FIELD	GROUP	SUB GR	Secchi depth, ocean data, spatial variability

19 ABSTRACT (Continue on reverse if necessary and identify by block number)

A seasonal Secchi depth atlas has been developed for the world's coastlines. Optica
compiled from data gathered by the National Oceanographic Data Center and from open li
depths less than 500 meters. These data have been averaged by one-degree squares, s
and placed in a category of six classes of Secchi depth ranges. Four charts were used to
at a scale of 1:12,233,000, and four seasons were selected to encompass 3-month inter
annual mean Secchi depths have been compiled in four charts. Secchi depth data were f
imately 50% of the world's coastlines. In the areas where no optical data were available othe
meteorologic, and geomorphic data sources were used to estimate the expected Secc

20 DISTRIBUTION AVAILABILITY OF ABSTRACT UNCLASSIFIED UNLIMITED — SAME AS RPT ■ — DTIC USERS	21 ABSTRACT SECURITY CLASSIFICATION Unclassified
22a NAME OF RESPONSIBLE INDIVIDUAL R. A. Arnone	22b TELEPHONE NUMBER (Include Area Code) (601) 688-5268

DD FORM 1473, 83 APR — EDITION OF 1 JAN 73 IS OBSOLETE

SECURITY (

CLASSIFIED
IRITY CLASSIFICATION OF THIS PAGE

REPORT DOCUMENTATION PAGE

REPORT SECURITY CLASSIFICATION: Unclassified	1b RESTRICTIVE MARKINGS: None
SECURITY CLASSIFICATION AUTHORITY	3 DISTRIBUTION/AVAILABILITY OF REPORT: Approved for public release; distribution is unlimited.
DECLASSIFICATION DOWNGRADING SCHEDULE	
PERFORMING ORGANIZATION REPORT NUMBER(S): NORDA Report 83	5 MONITORING ORGANIZATION REPORT NUMBER(S): NORDA Report 83
NAME OF PERFORMING ORGANIZATION: Naval Ocean Research and Development Activity	7a NAME OF MONITORING ORGANIZATION: Naval Ocean Research and Development Activity
ADDRESS (City, State, and ZIP Code): Ocean Science Directorate, NSTL, Mississippi 39529-5004	7b ADDRESS (City, State, and ZIP Code): Ocean Science Directorate, NSTL, Mississippi 39529-5004
NAME OF FUNDING SPONSORING ORGANIZATION: Defense Mapping Agency; 8b OFFICE SYMBOL (If applicable)	9 PROCUREMENT INSTRUMENT IDENTIFICATION NUMBER
ADDRESS (City, State, and ZIP Code): Washington, D.C. 20350	10 SOURCE OF FUNDING NOS: PROGRAM ELEMENT NO 63701B; PROJECT NO; TASK NO; WORK UNIT NO
TITLE (Include Security Classification): Coastal Secchi Depth Atlas	
PERSONAL AUTHOR(S): Robert A. Arnone	
a TYPE OF REPORT: Final; 13b TIME COVERED: From To	14 DATE OF REPORT (Yr., Mo., Day): July 1985; 15 PAGE COUNT: 30
SUPPLEMENTARY NOTATION	
COSATI CODES: FIELD, GROUP, SUB GR	18 SUBJECT TERMS (Continue on reverse if necessary and identify by block number): Secchi depth, ocean data, spatial variability

ABSTRACT (Continue on reverse if necessary and identify by block number)

A seasonal Secchi depth atlas has been developed for the world's coastlines. Optical data have been compiled from data gathered by the National Oceanographic Data Center and from open literature for water depths less than 500 meters. These data have been averaged by one-degree squares, sorted by season, and placed in a category of six classes of Secchi depth ranges. Four charts were used to cover the world at a scale of 1:12,233,000, and four seasons were selected to encompass 3-month intervals. Additionally, annual mean Secchi depths have been compiled in four charts. Secchi depth data were found for approximately 50% of the world's coastlines. In the areas where no optical data were available other oceanographic, meteorologic, and geomorphic data sources were used to estimate the expected Secchi depth ranges.

DISTRIBUTION/AVAILABILITY OF ABSTRACT: ICLASSIFIED UNLIMITED; SAME AS RPT ■; DTIC USERS	21 ABSTRACT SECURITY CLASSIFICATION: Unclassified
a NAME OF RESPONSIBLE INDIVIDUAL: R. A. Arnone	22b TELEPHONE NUMBER (Include Area Code): (601) 688-5268; 22c OFFICE SYMBOL: Code 321

FORM 1473, 83 APR   EDITION OF 1 JAN 73 IS OBSOLETE   UNCLASSIFIED
SECURITY CLASSIFICATION OF THIS PAGE

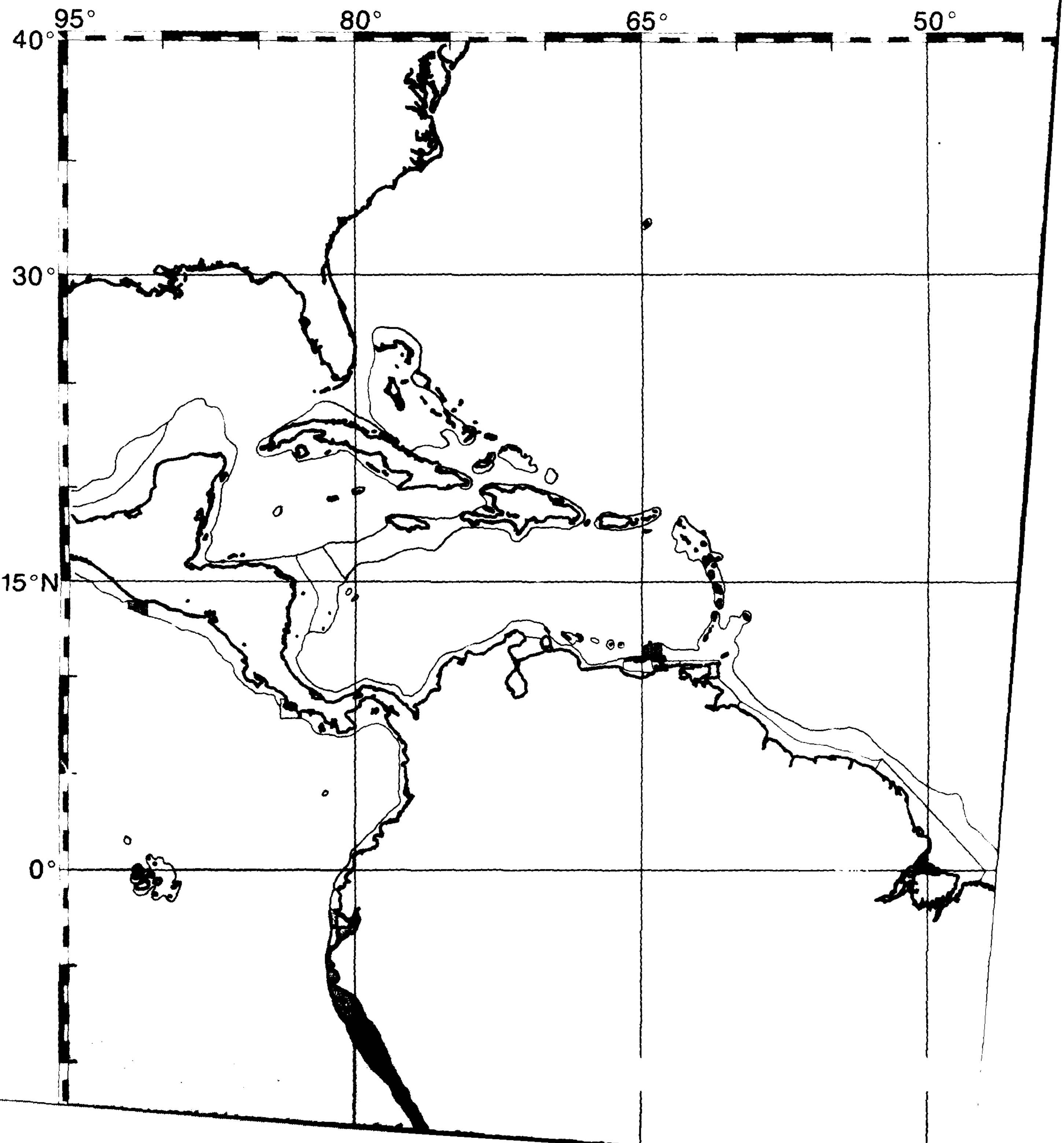
95°
80°
65°
50°
40°
30°
15°N
0°

2

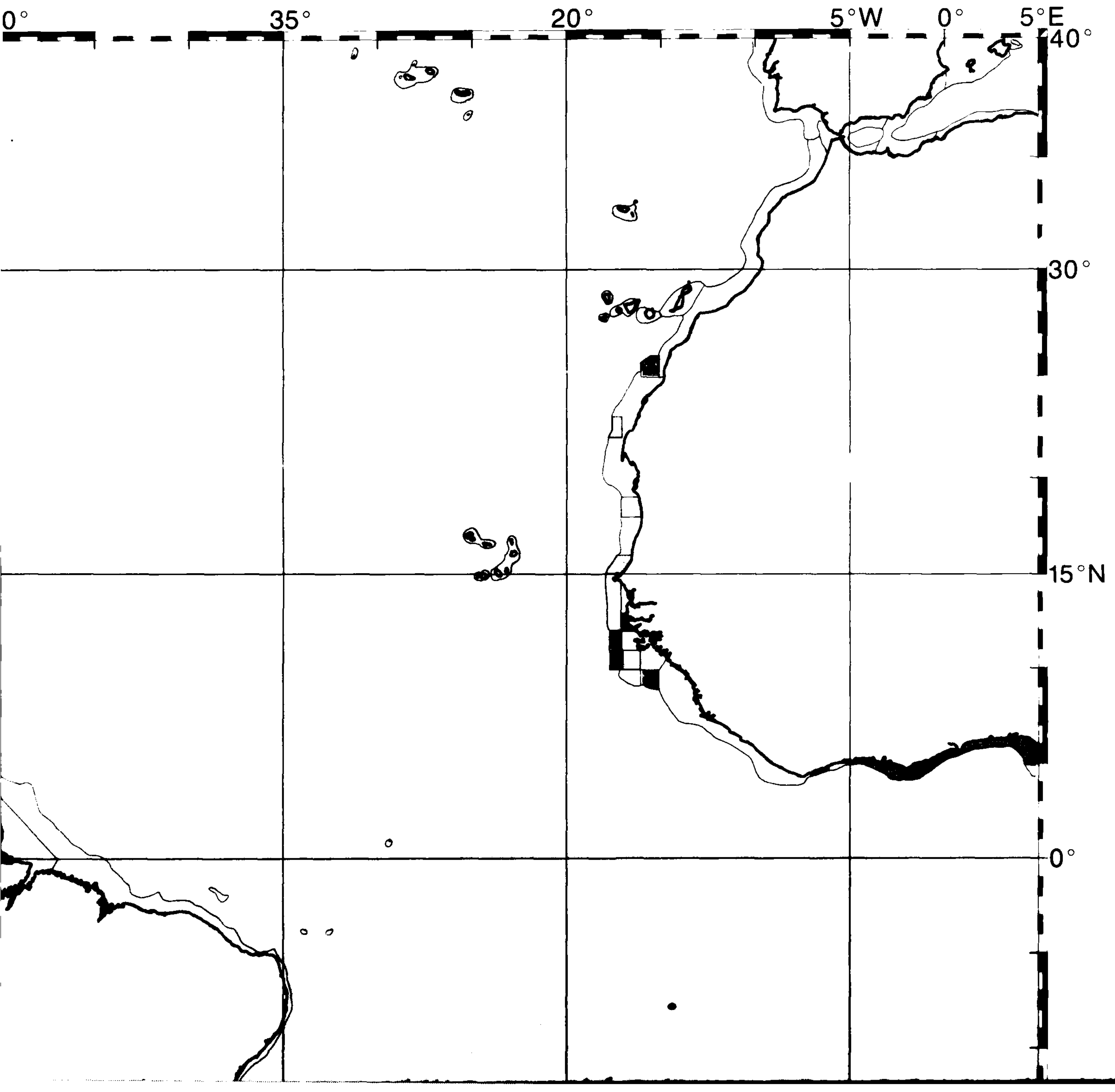

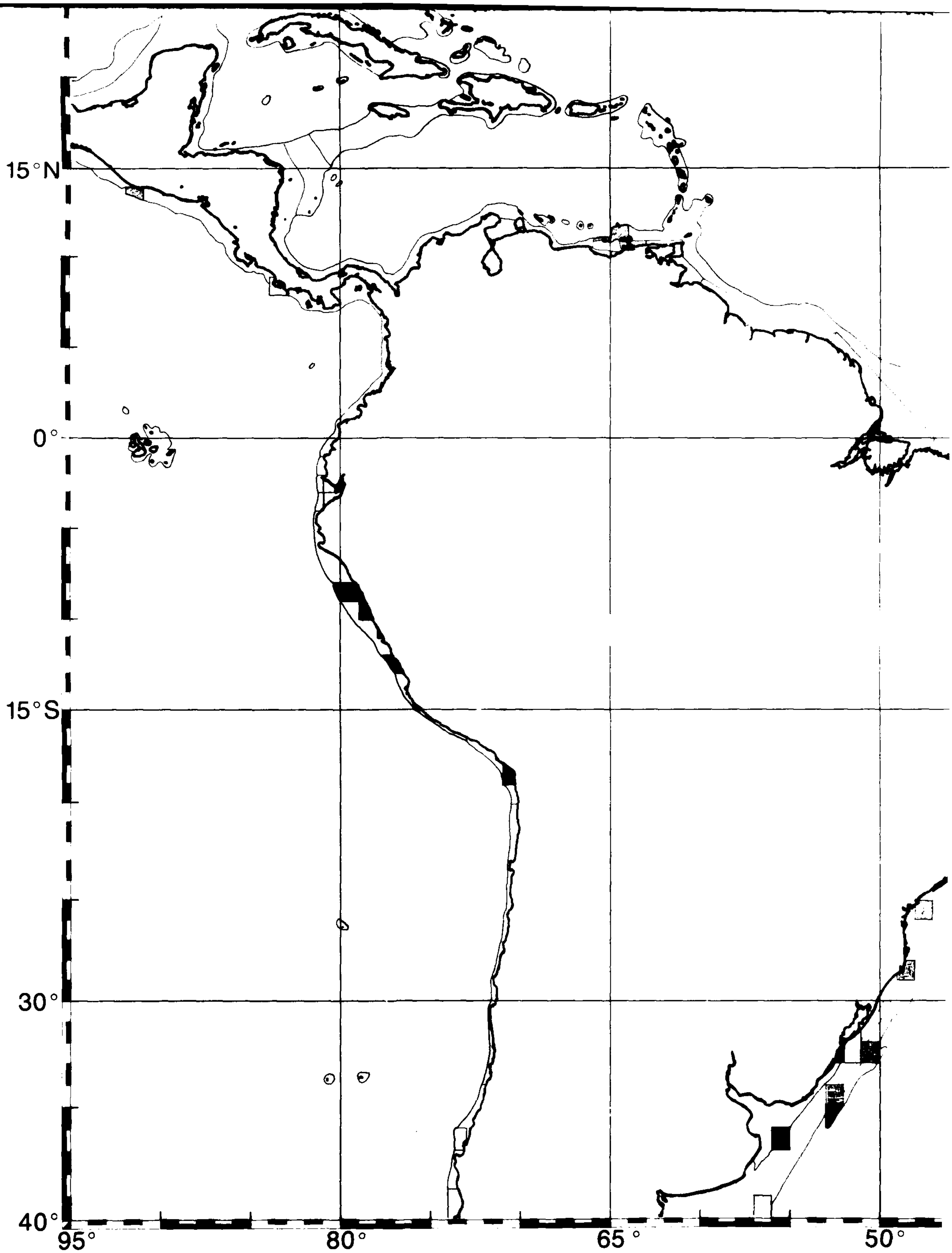

PLATE I JANUARY—MARCH

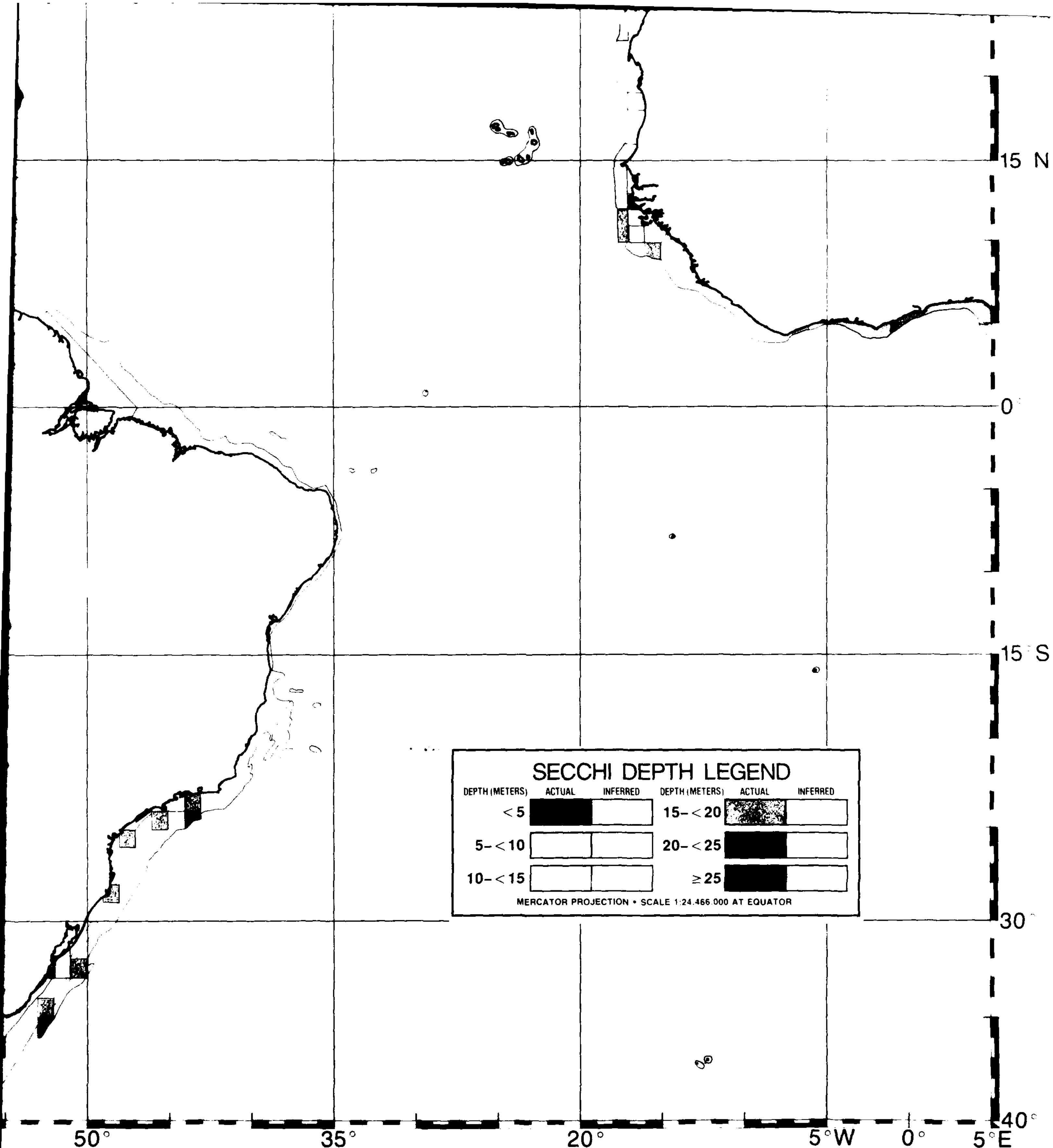

Compiled by: R.A. Arnone, F.A. Hilder, S.P. Tucker
Prepared for the Defense Mapping Agency by
the Naval Ocean Research and Development Activity
Remote Sensing Branch, NSTL, Mississippi

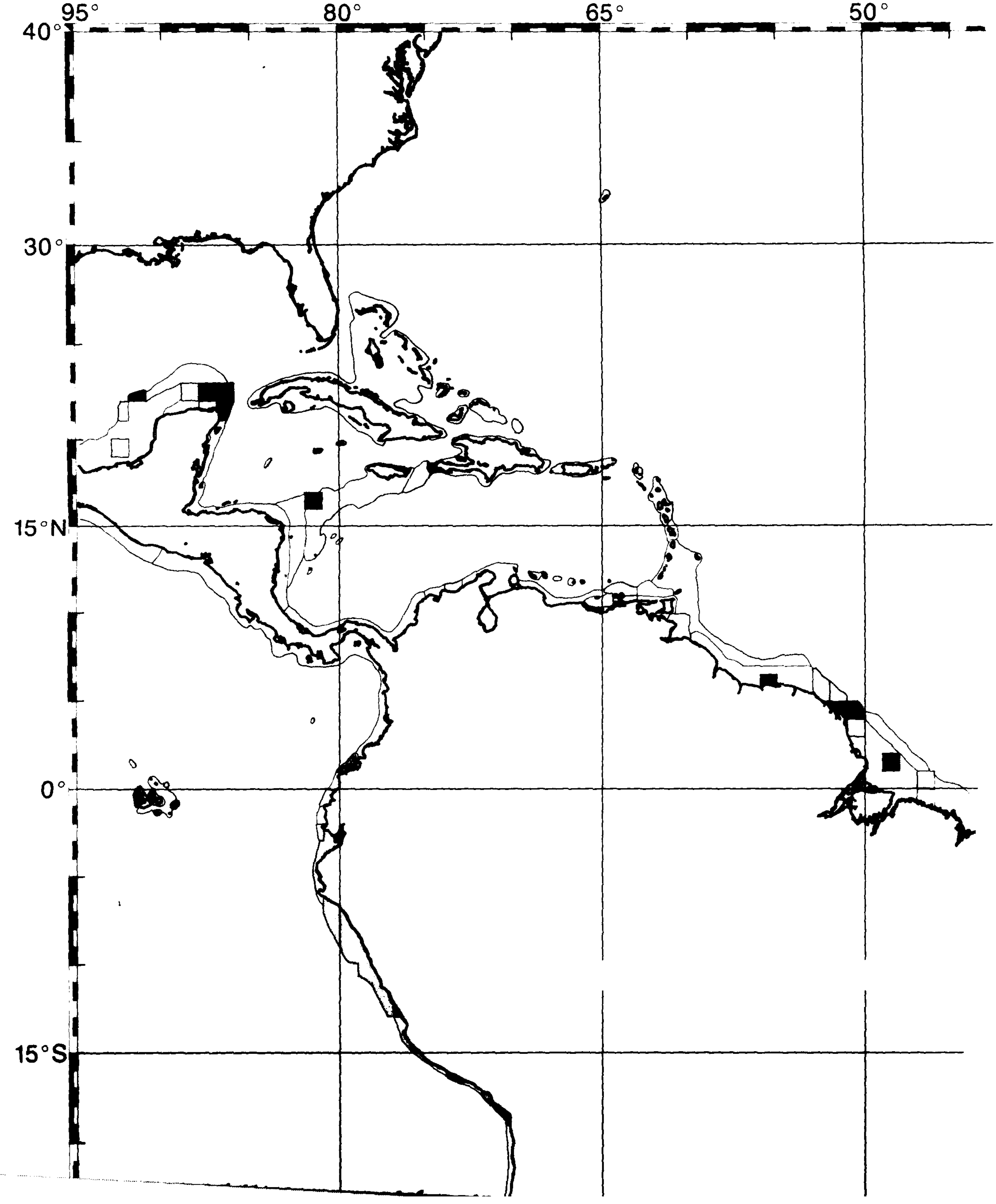
95°
80°
65°
50°
40°
30°
15°N
0°
15°S

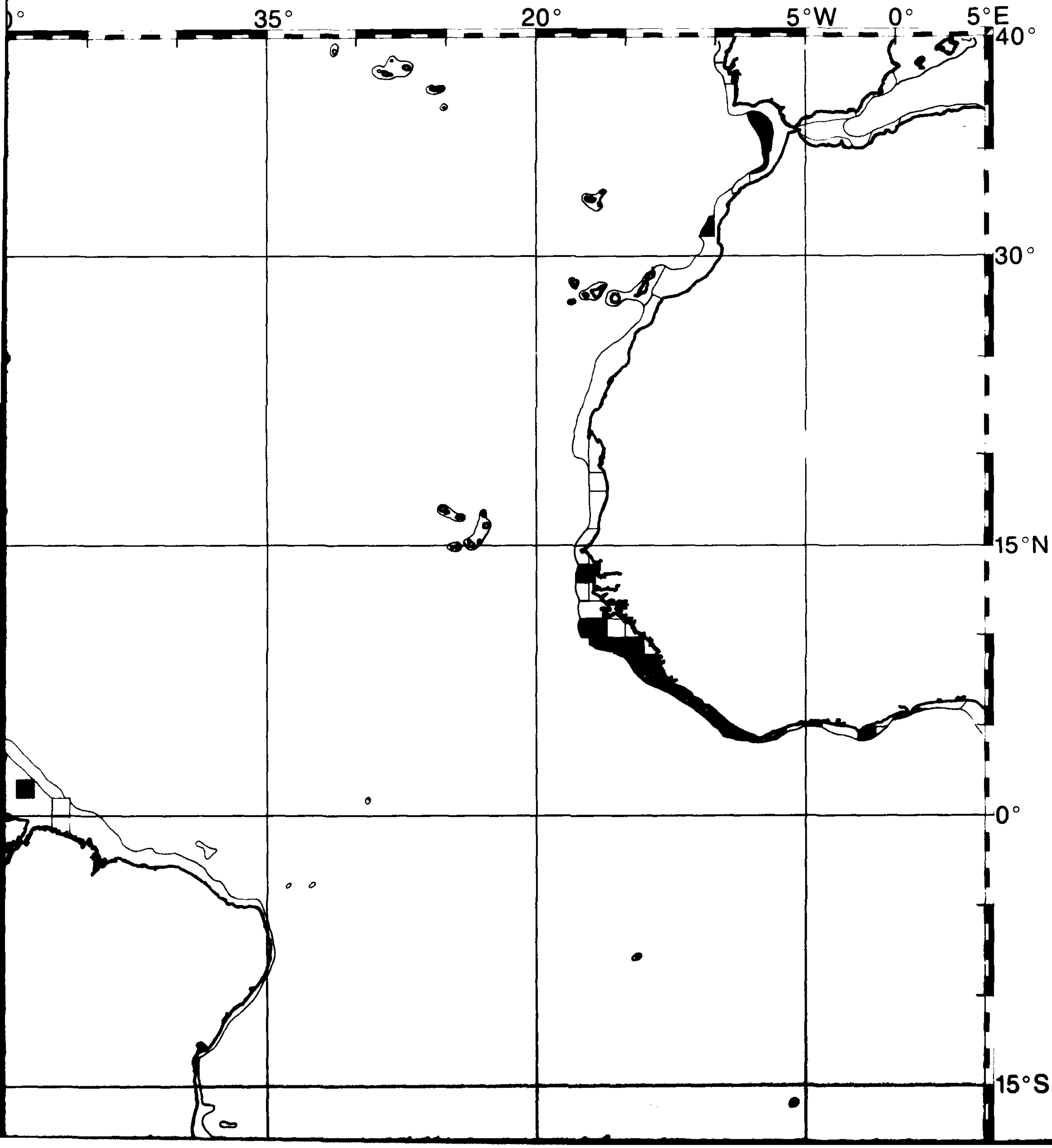

35°
20°
5°W
0°
5°E
40°
30°
15°N
0°
15°S

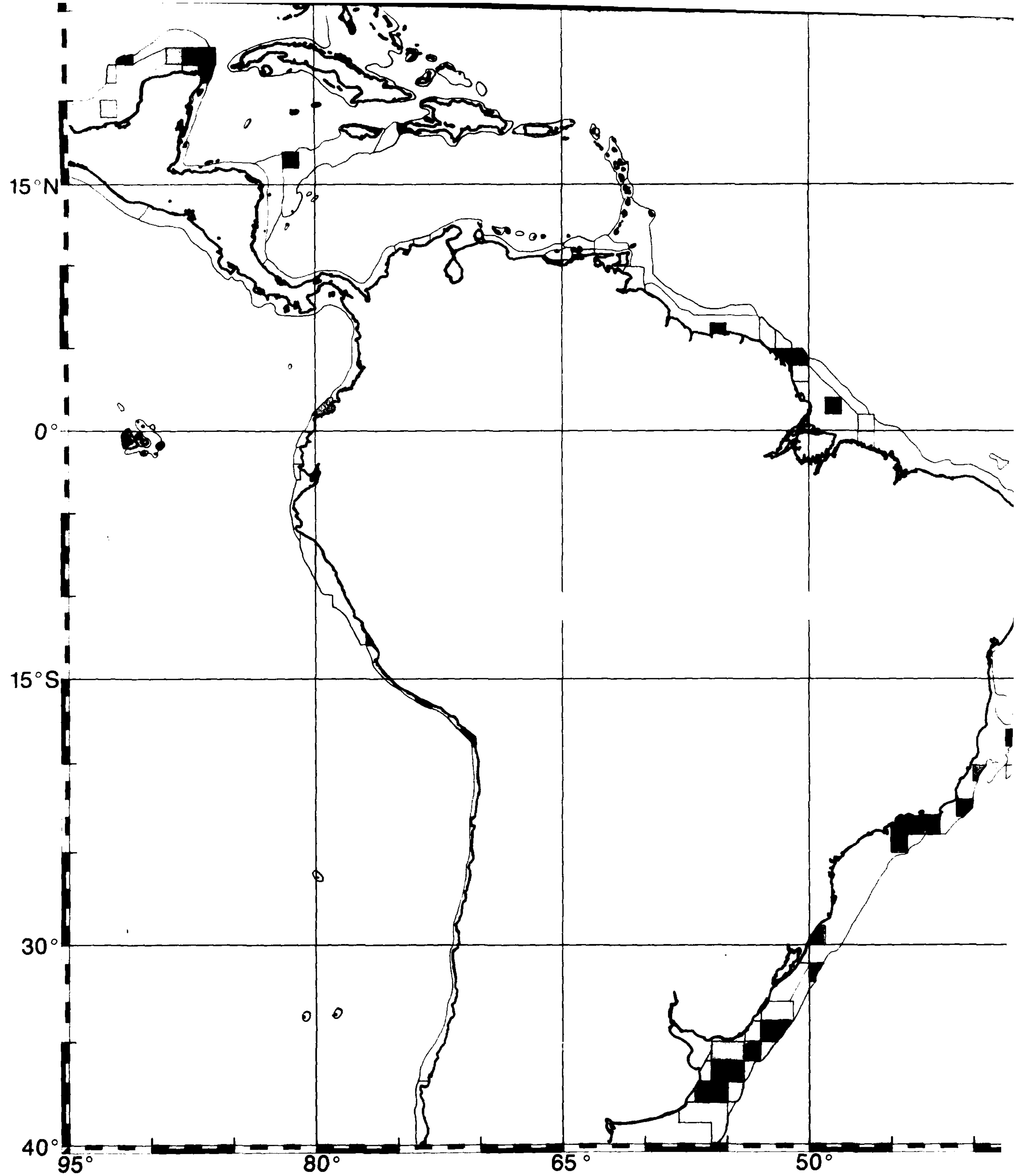

PLATE II APRIL—JUNE

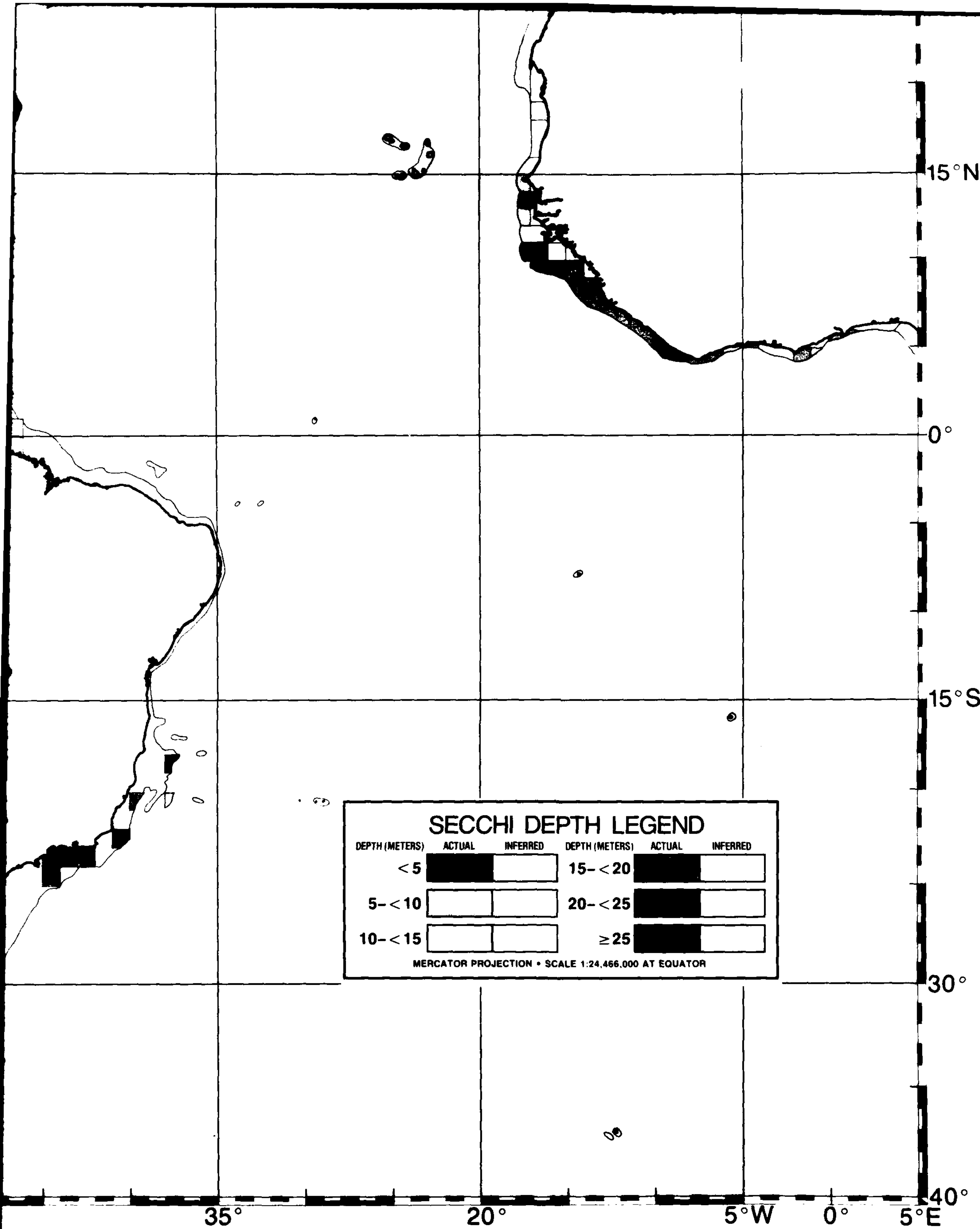

Compiled by: R.A. Arnone, F.A. Hilder, S.P. Tucker

Prepared for the Defense Mapping Agency by
the Naval Ocean Research and Development Activity
Remote Sensing Branch, NSTL, Mississippi

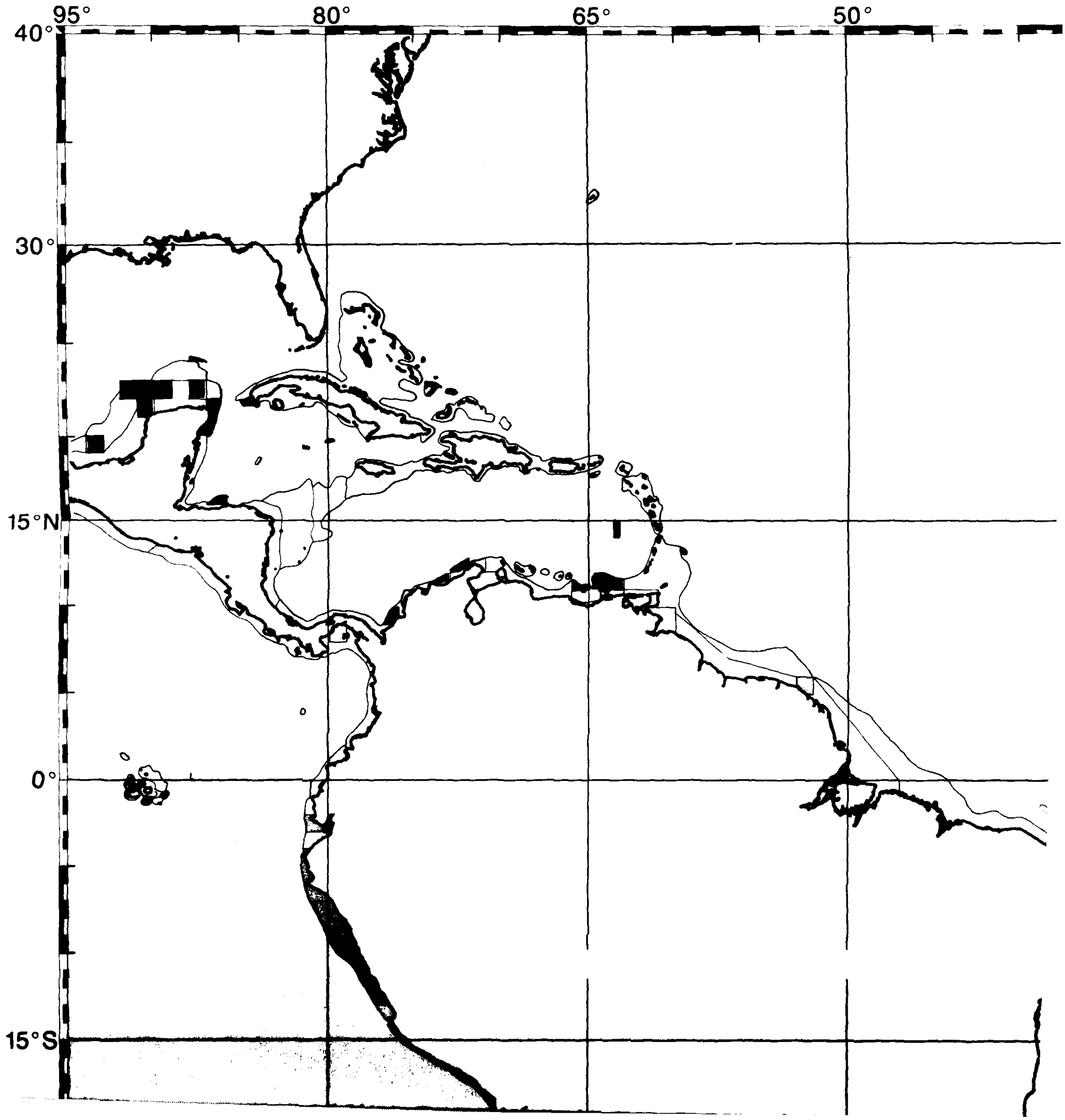
95°
80°
65°
50°
40°
30°
15°N
0°
15°S

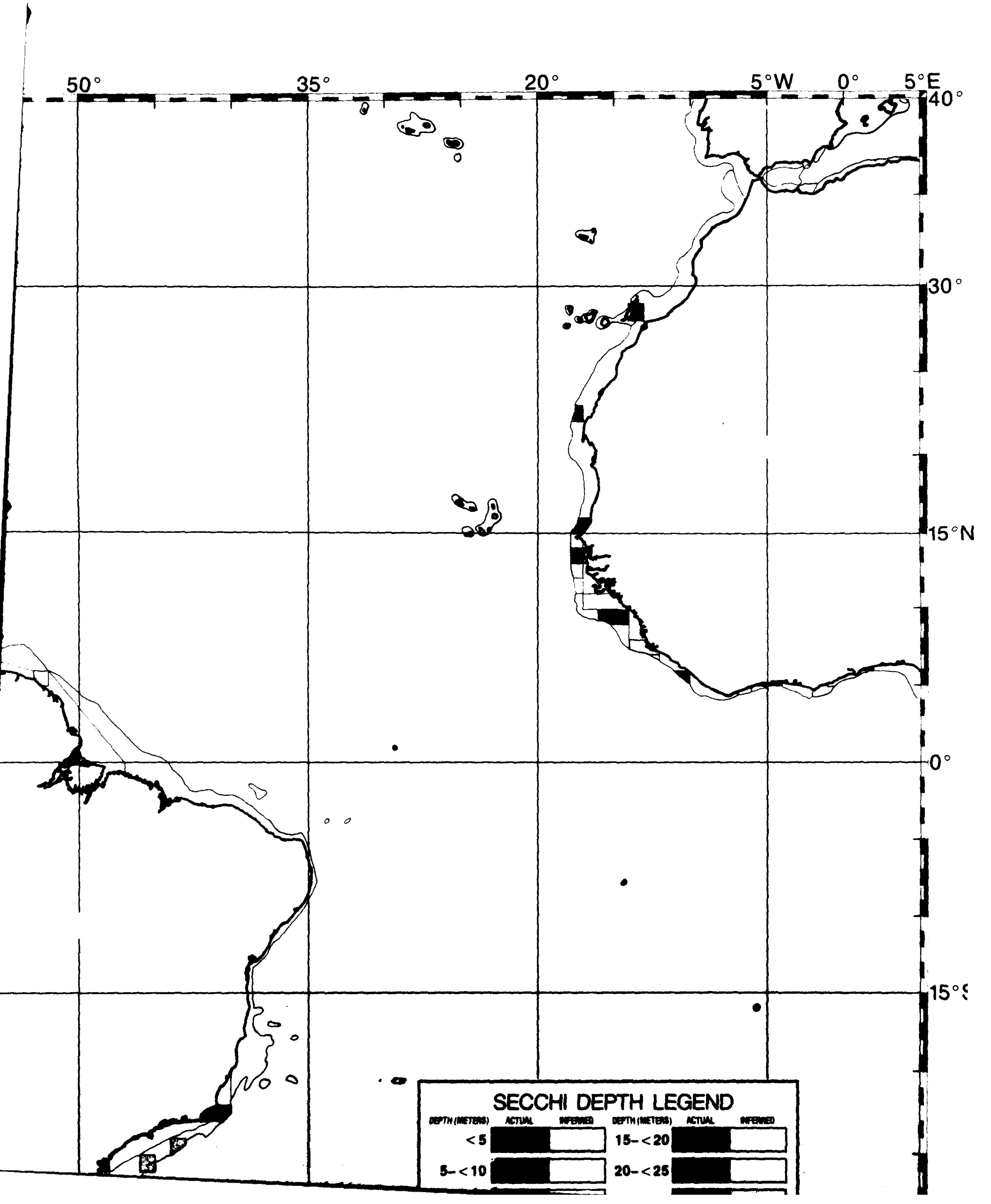

50°
35°
20°
5°W
0°
5°E
40°
30°
15°N
0°
15°S
SECCHI DEPTH LEGEND
DEPTH (METERS)
ACTUAL
INFERRED
DEPTH (METERS)
ACTUAL
INFERRED
< 5
15– < 20
5– < 10
20– < 25

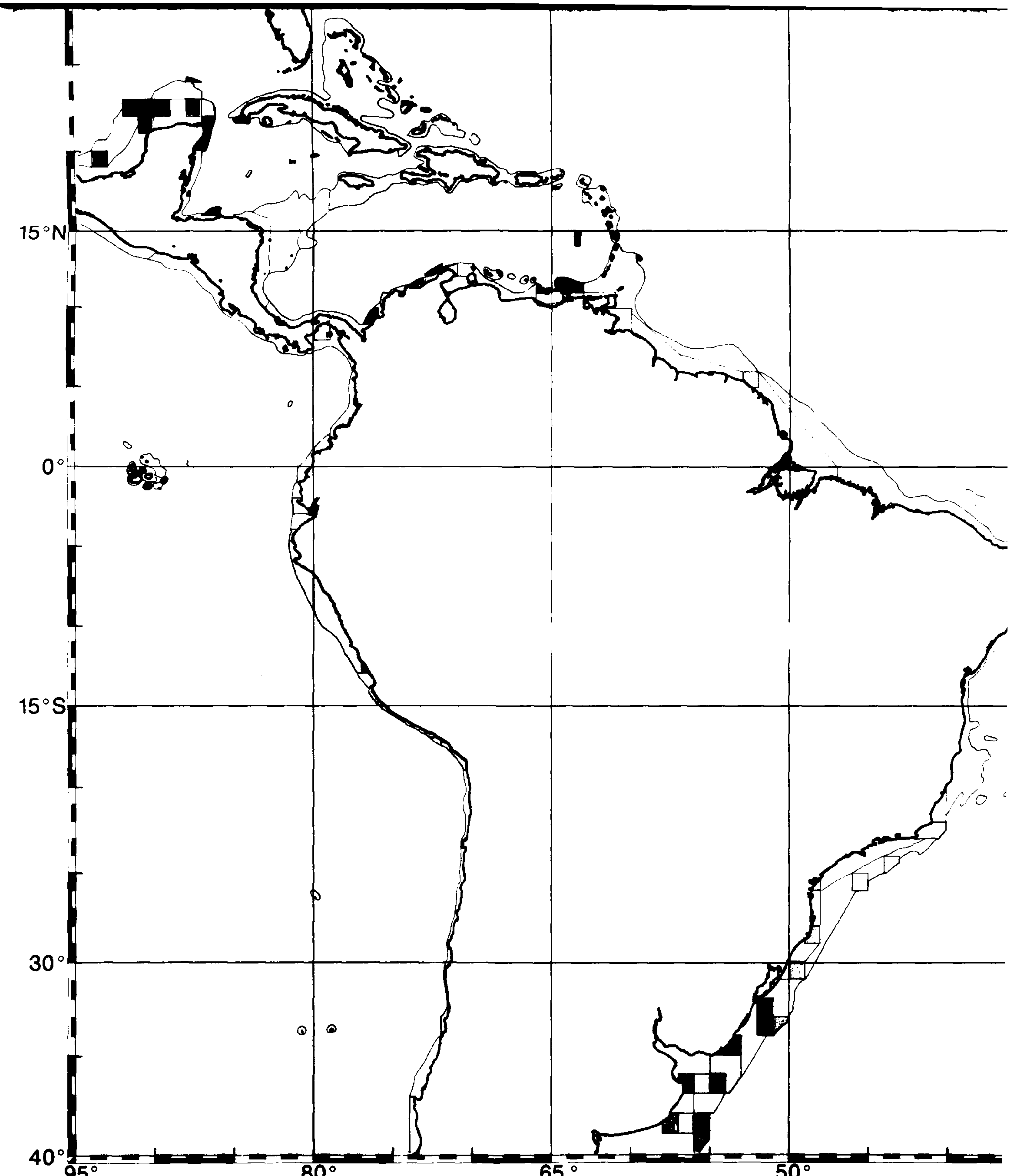

PLATE III JULY—SEPTEMBER

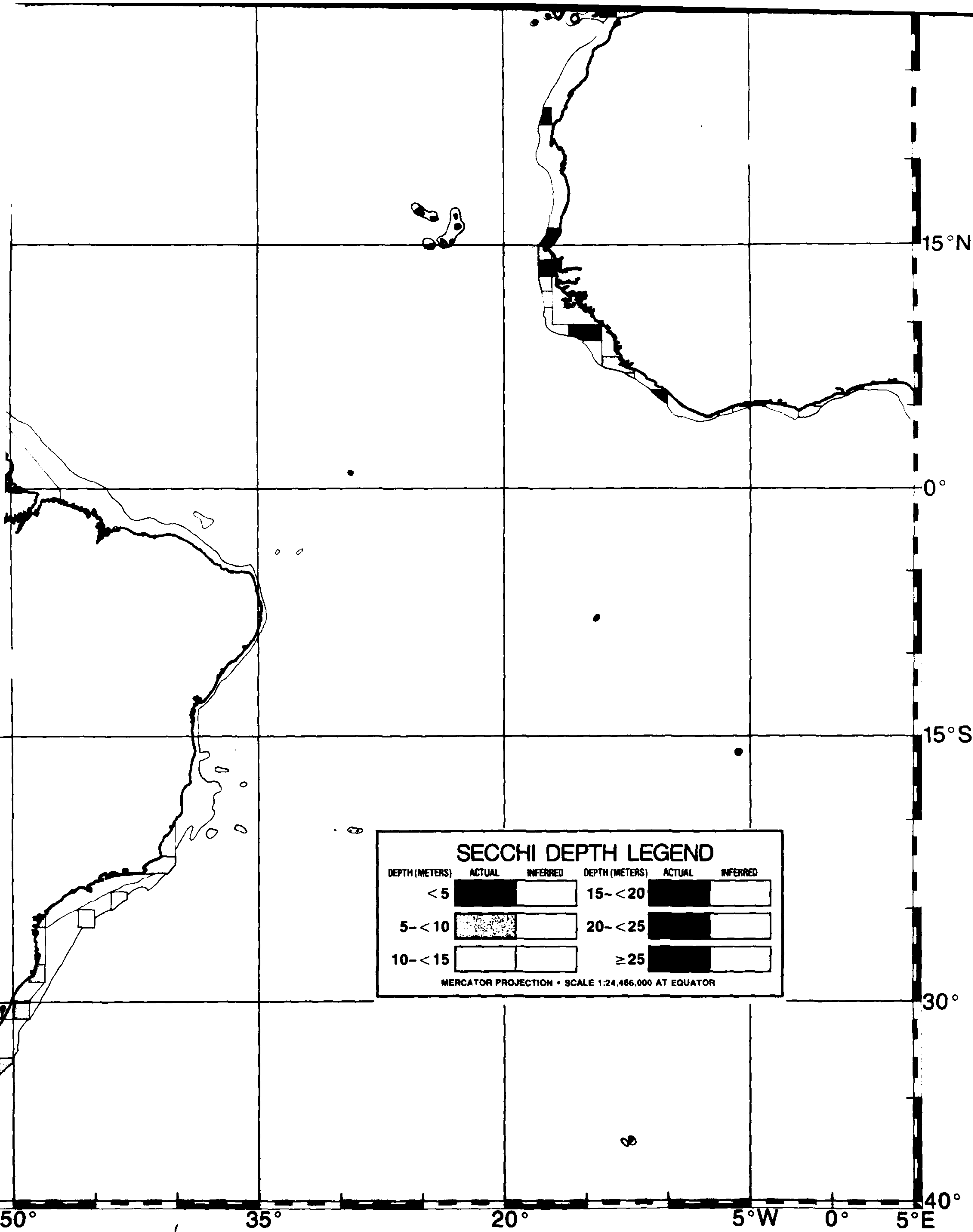

Compiled by: R.A. Arnone, F.A. Hilder, S.P. Tucker

Prepared for the Defense Mapping Agency by
the Naval Ocean Research and Development Activity
Remote Sensing Branch, NSTL, Mississippi

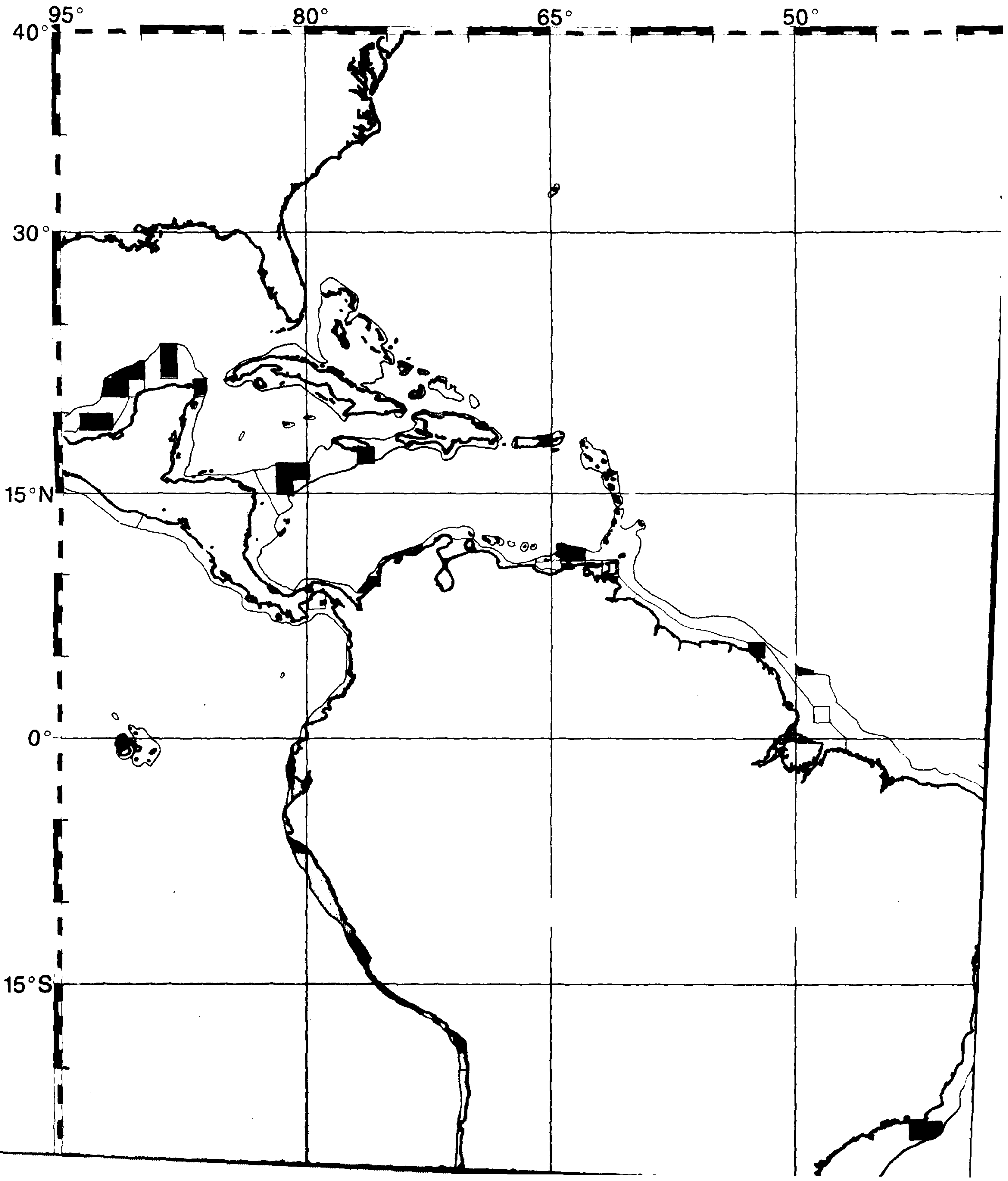

95°
80°
65°
50°
40°
30°
15°N
0°
15°S

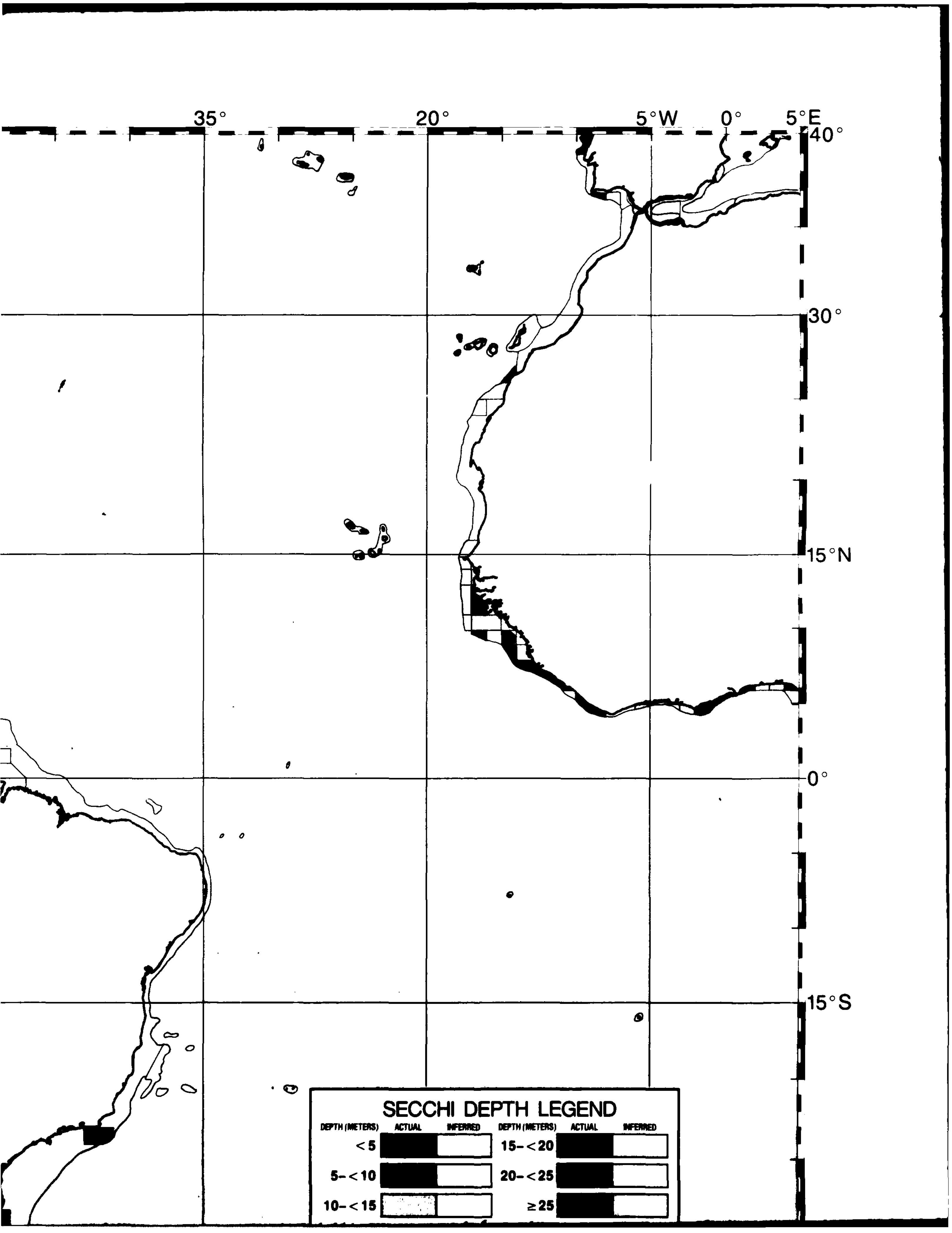
35°
20°
5°W
0°
5°E
40°
30°
15°N
0°
15°S
SECCHI DEPTH LEGEND
DEPTH (METERS)
ACTUAL
INFERRED
< 5
5 - < 10
10 - < 15
15 - < 20
20 - < 25
≥ 25

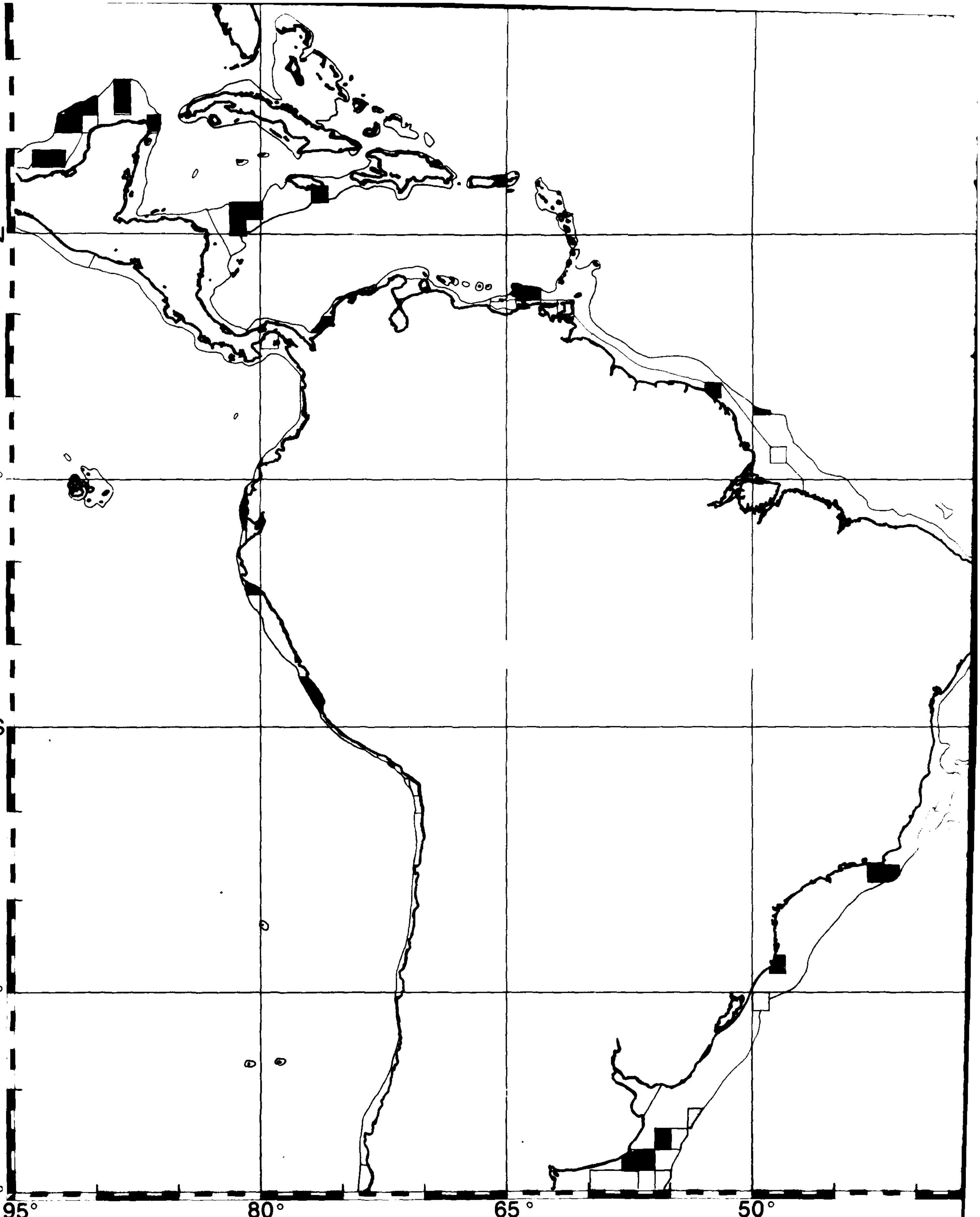

PLATE IV OCTOBER—DECEMBER

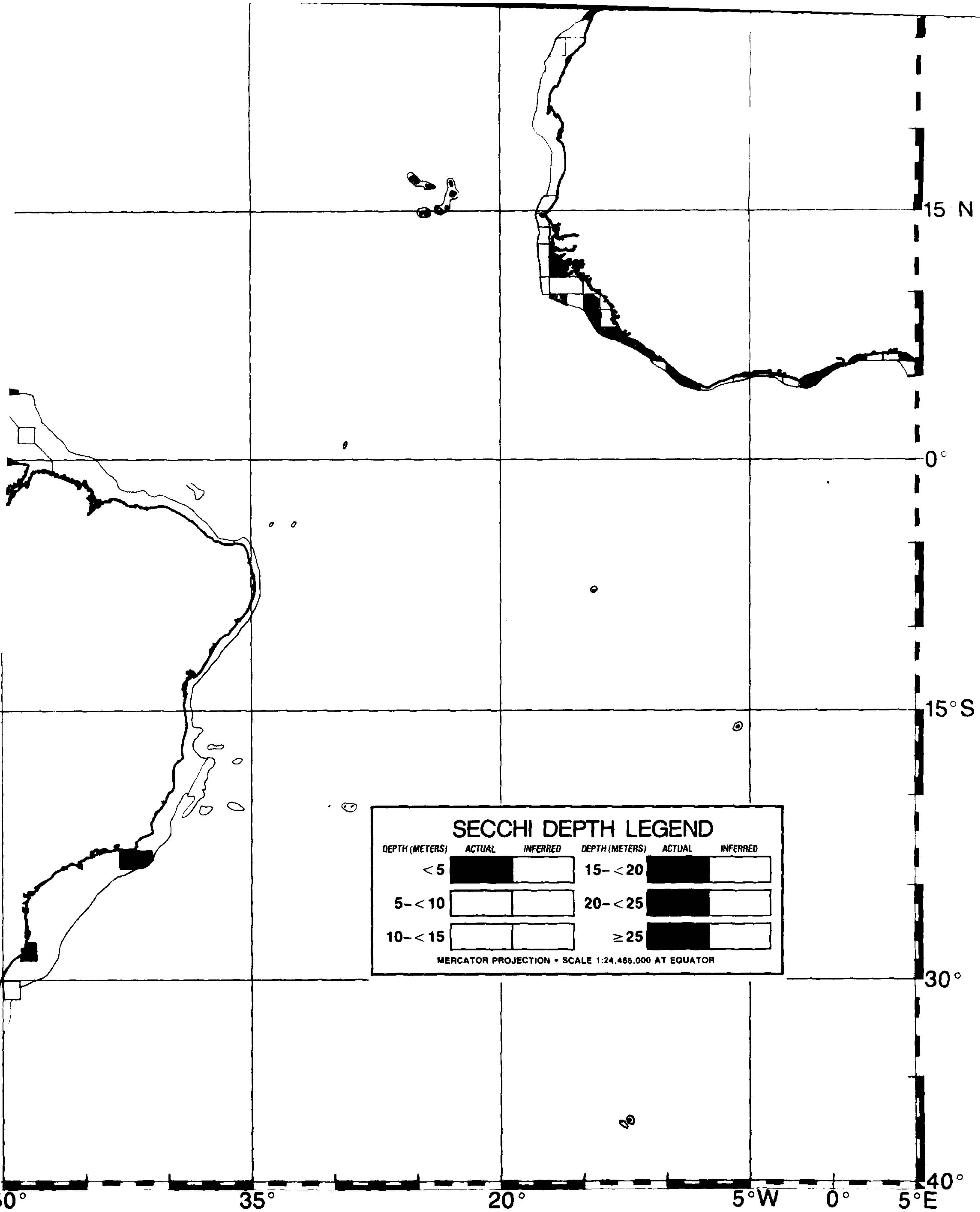

Compiled by: R.A. Arnone, F.A. Hilder, S.P. Tucker
Prepared for the Defense Mapping Agency by
the Naval Ocean Research and Development Activity
Remote Sensing Branch, NSTL, Mississippi

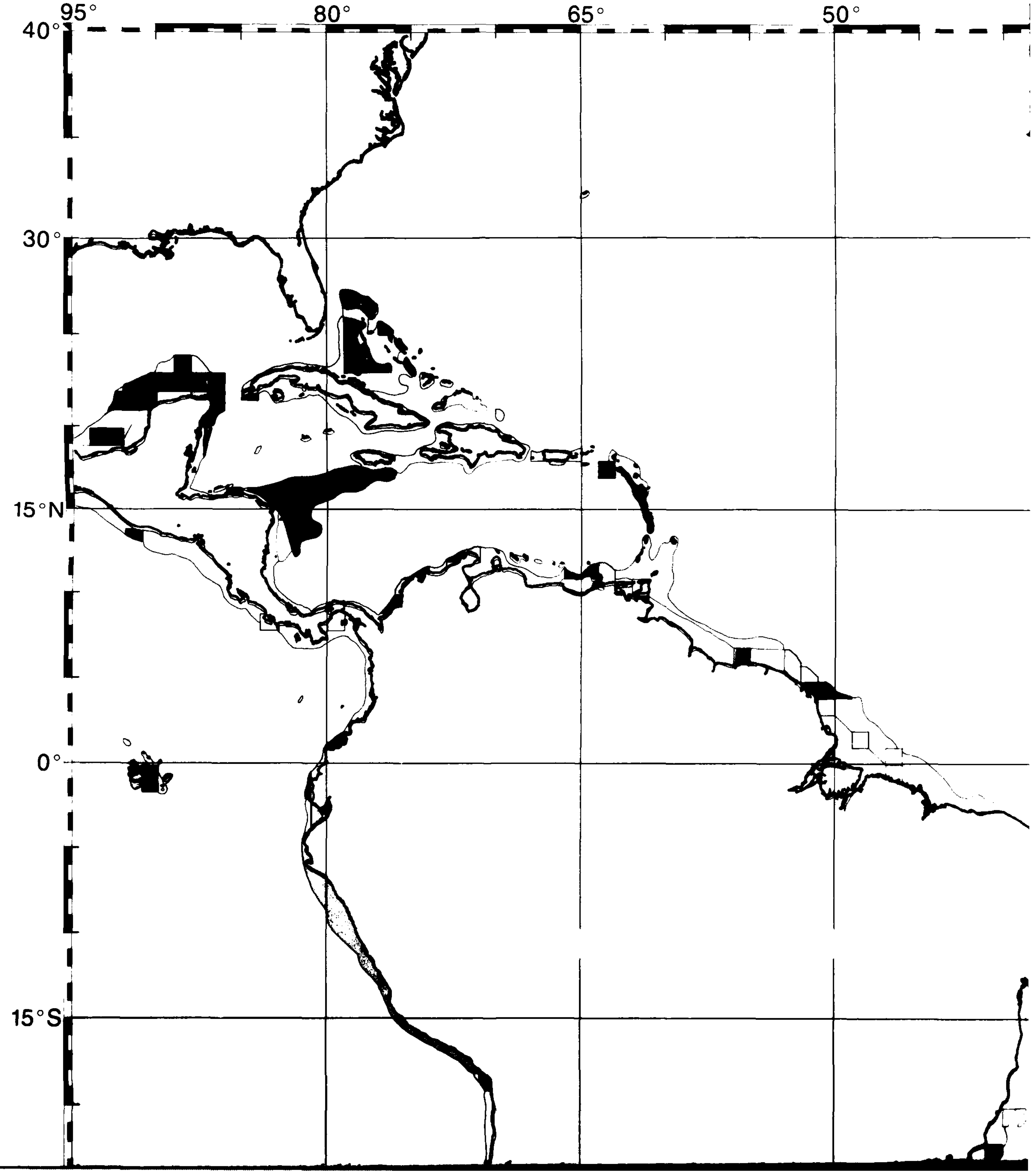
95°
80°
65°
50°
40°
30°
15°N
0°
15°S

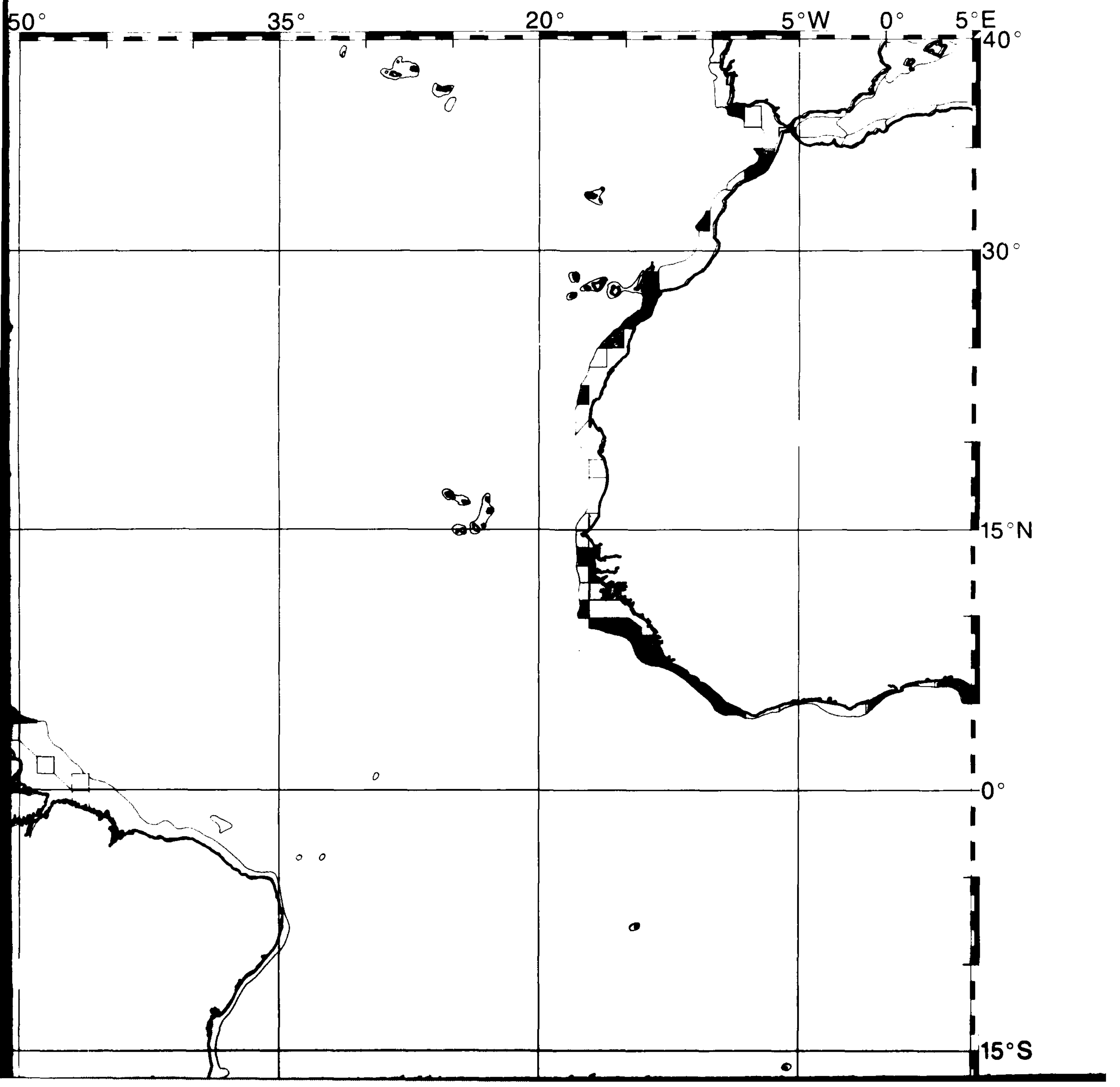
50°
35°
20°
5°W
0°
5°E
40°
30°
15°N
0°
15°S

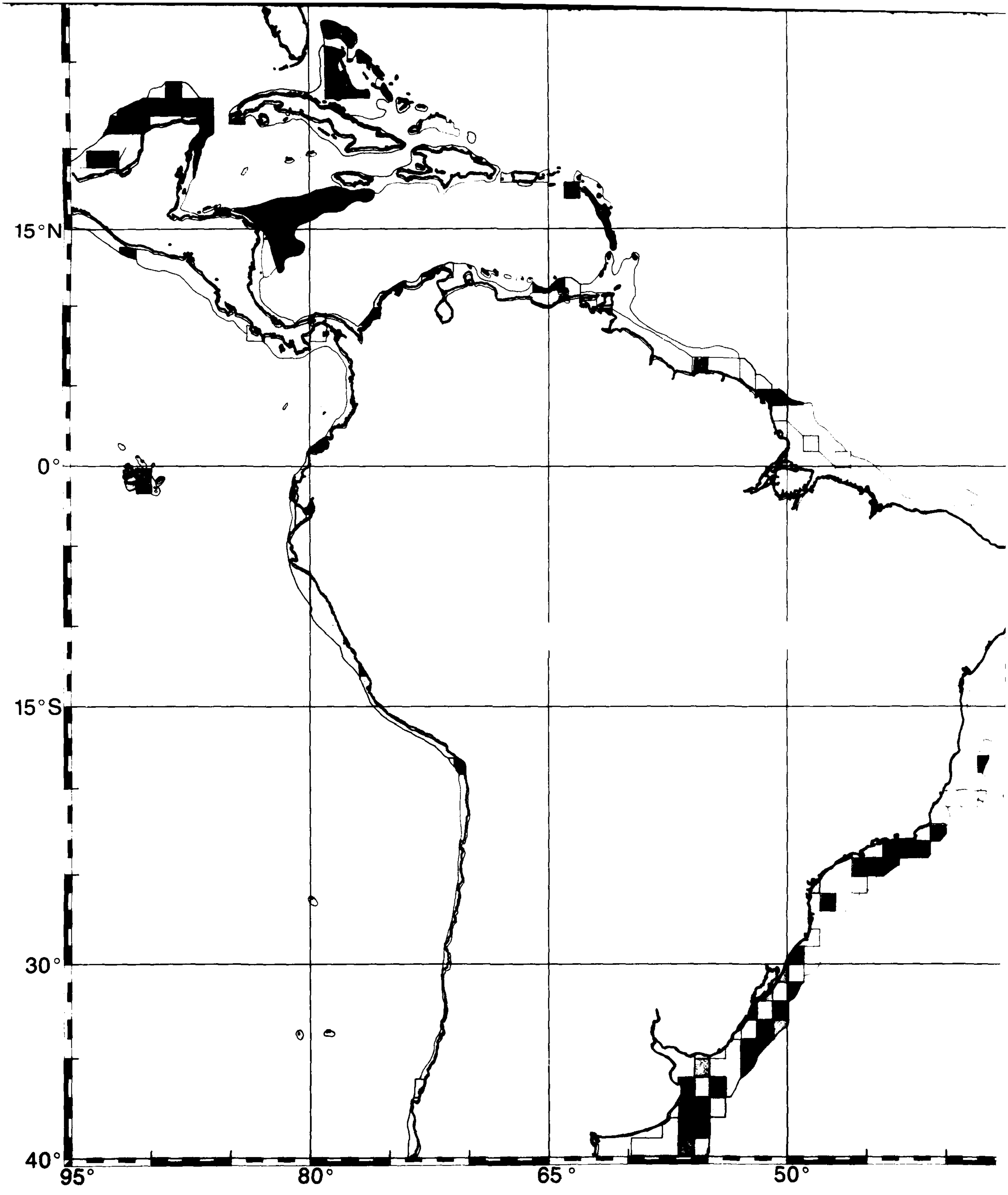

PLATE V ANNUAL MEAN

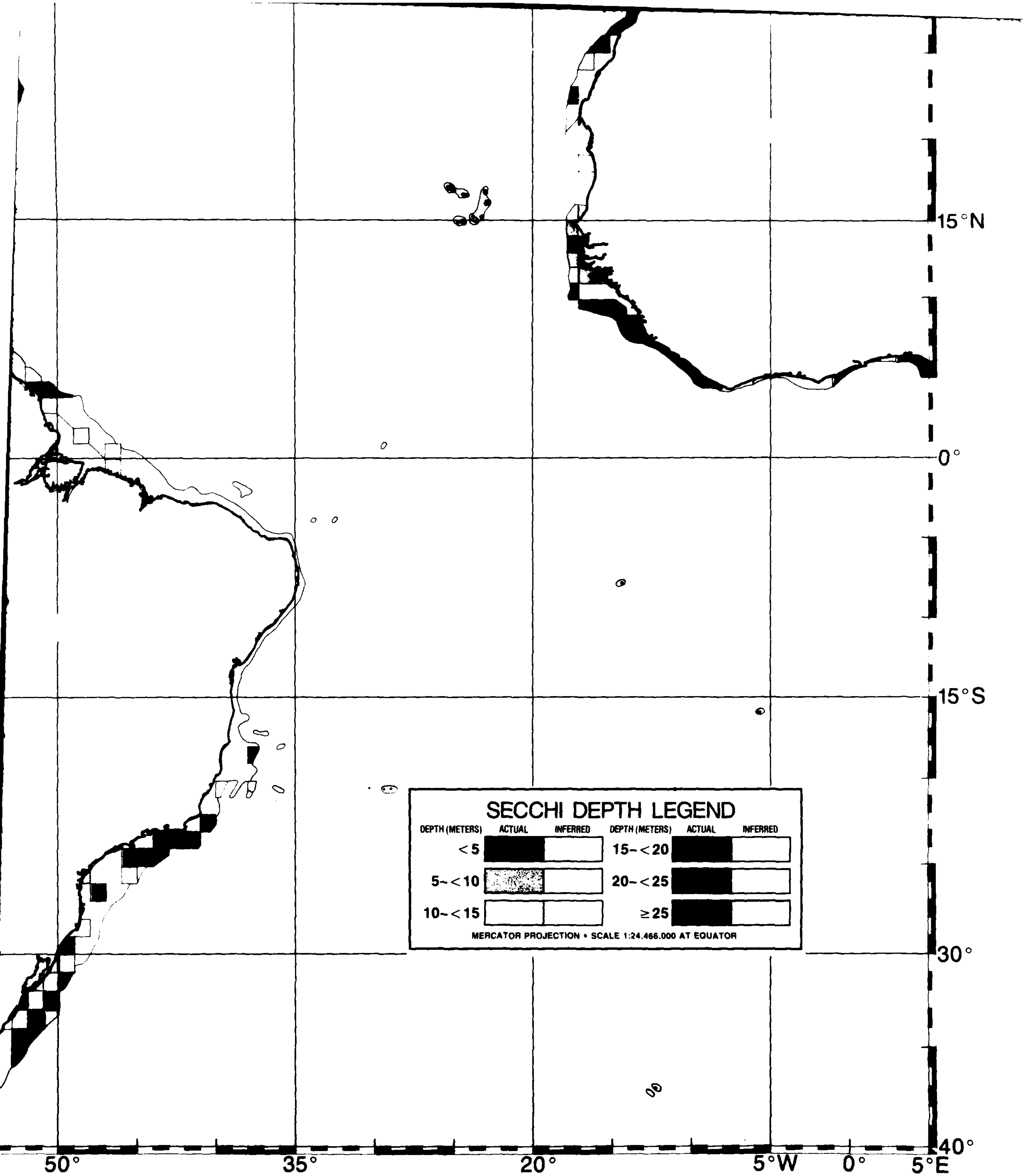

Compiled by: R.A. Arnone, F.A. Hilder, S.P. Tucker
Prepared for the Defense Mapping Agency by
the Naval Ocean Research and Development Activity
Remote Sensing Branch, NSTL, Mississippi

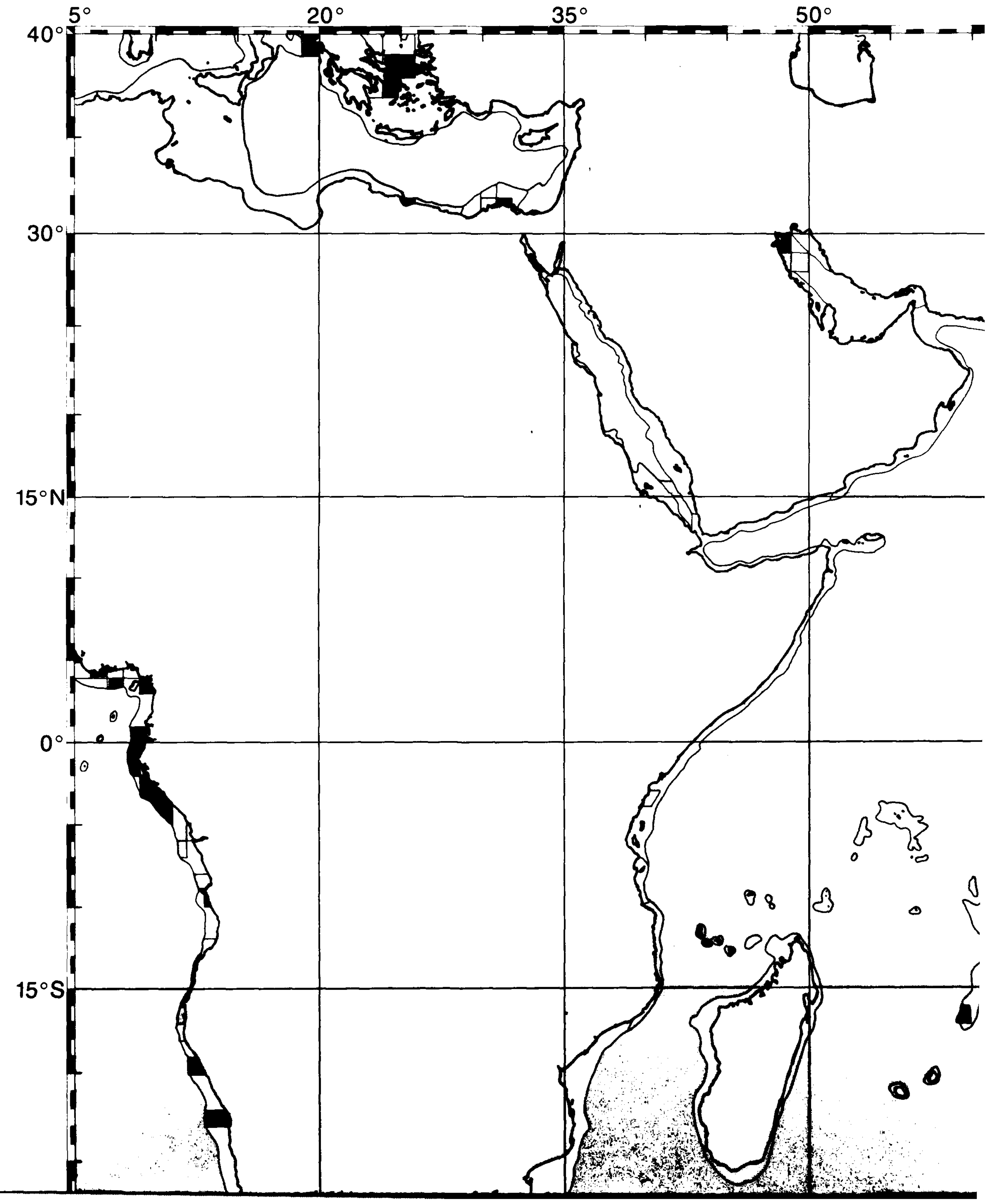
5°
20°
35°
50°
40°
30°
15°N
0°
15°S

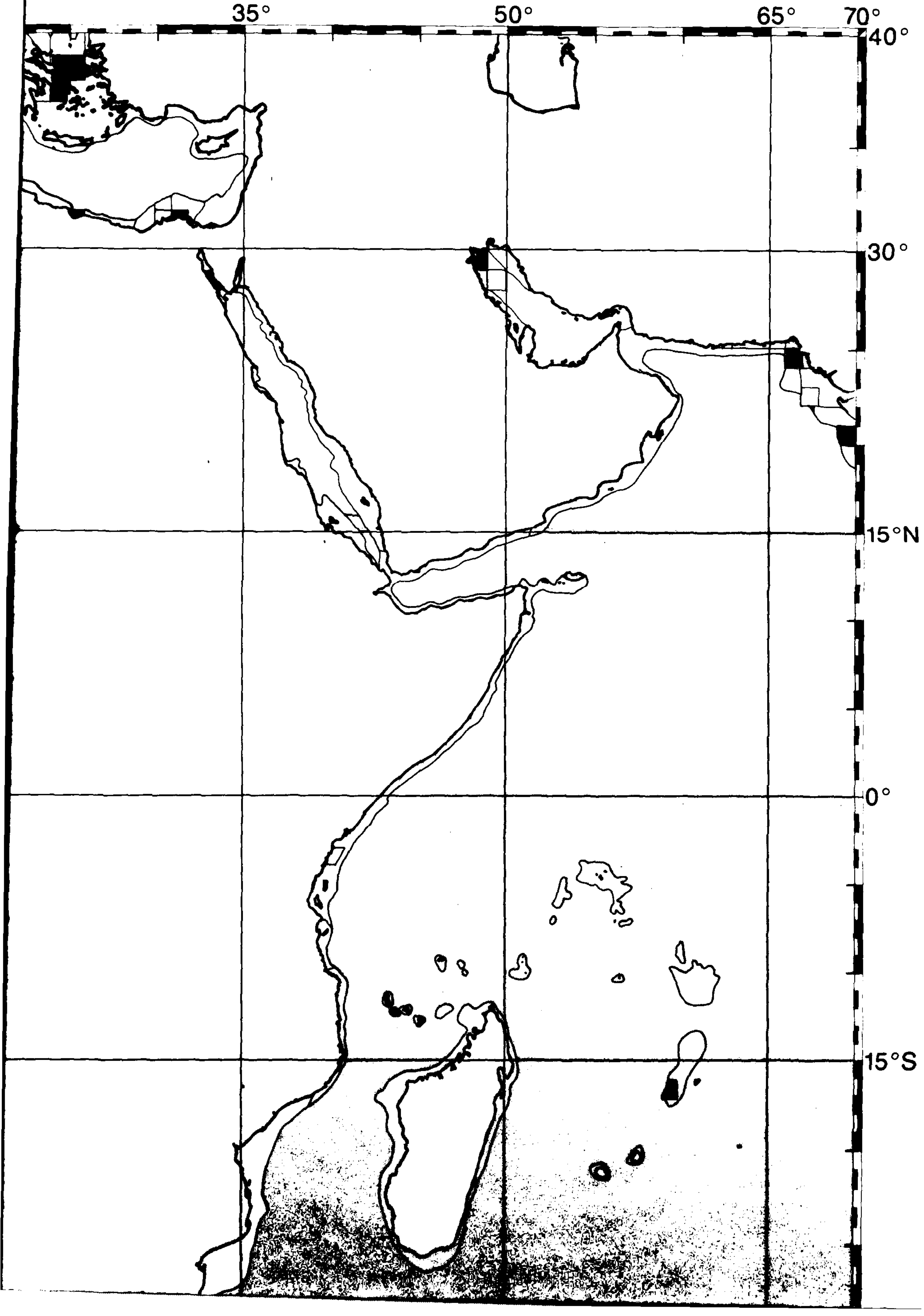
35°
50°
65°
70°
40°
30°
15°N
0°
15°S

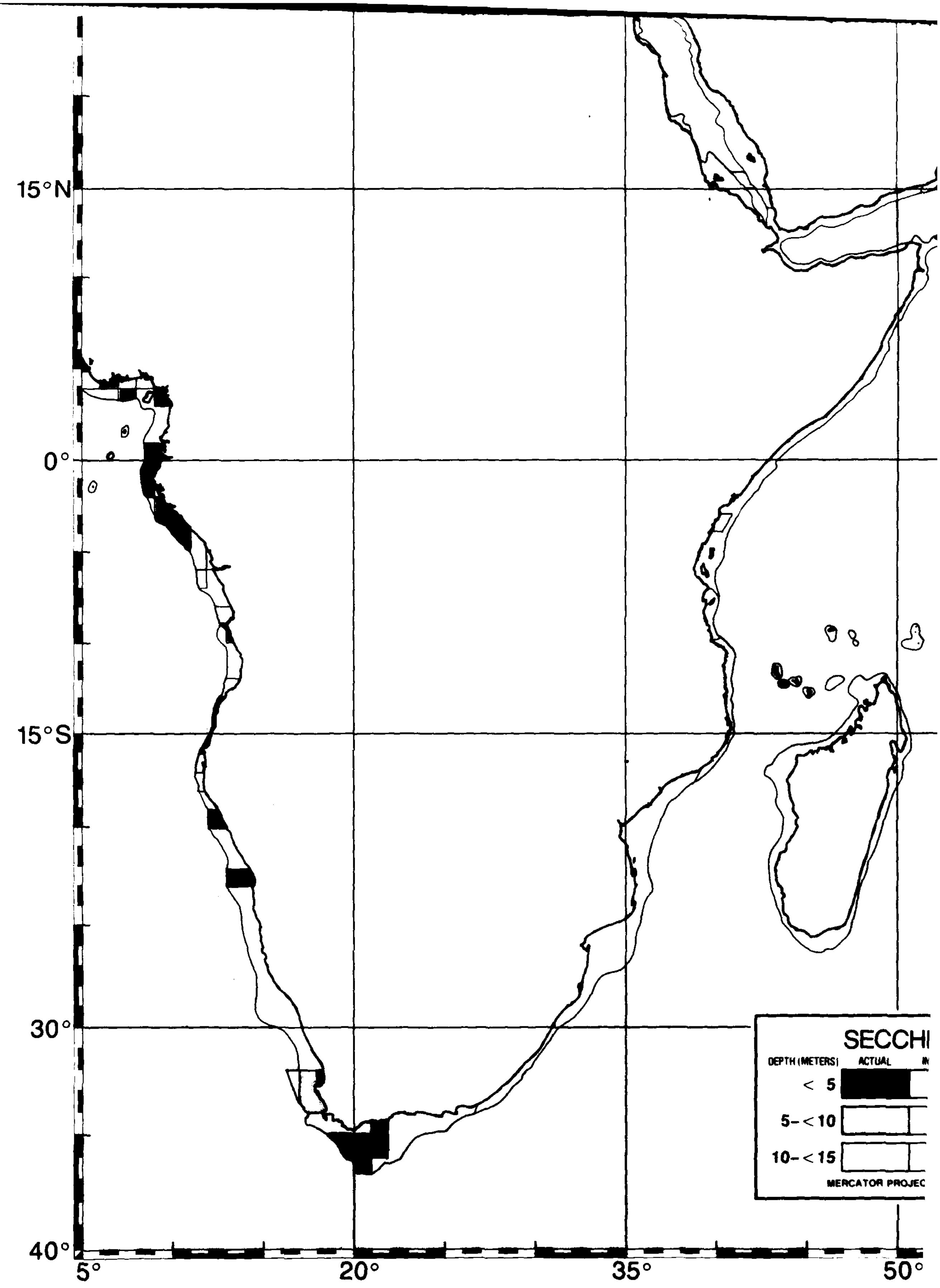

PLATE VI JANUARY—MARCH

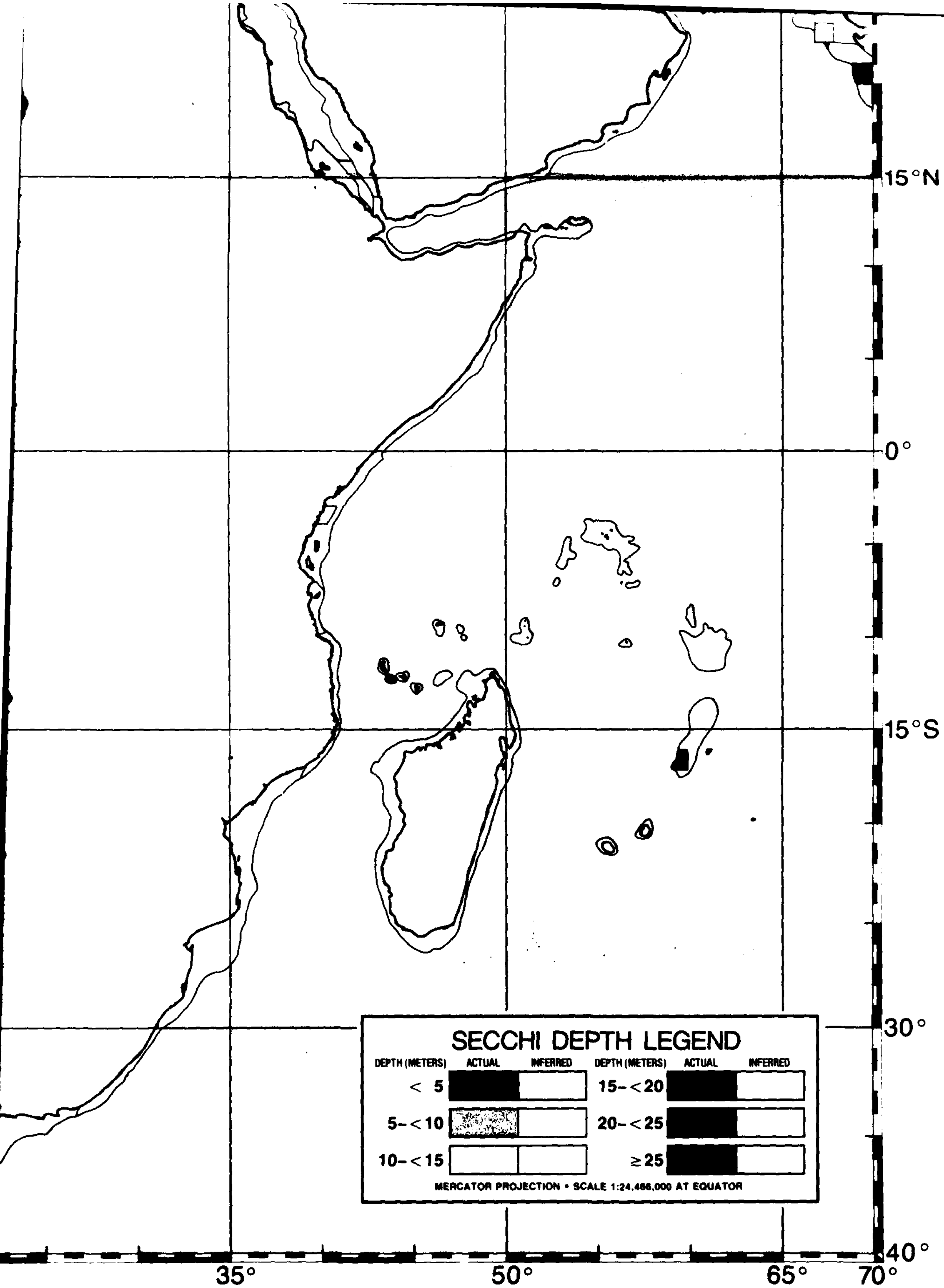

Compiled by: R.A. Arnone, F.A. Hilder, S.P. Tucker
Prepared for the Defense Mapping Agency by
the Naval Ocean Research and Development Activity
Remote Sensing Branch, NSTL, Mississippi

RCH

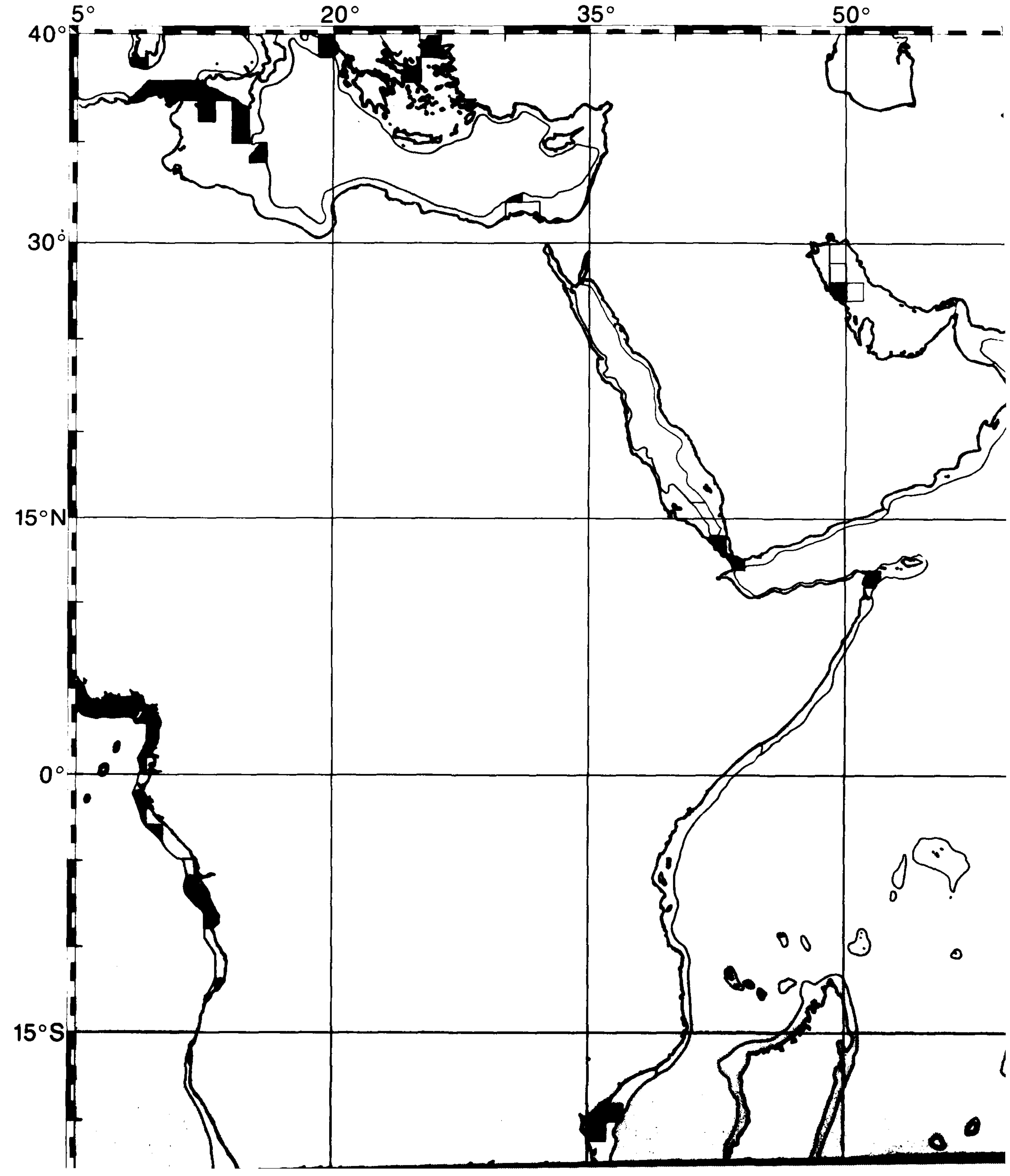
5°
20°
35°
50°
40°
30°
15°N
0°
15°S

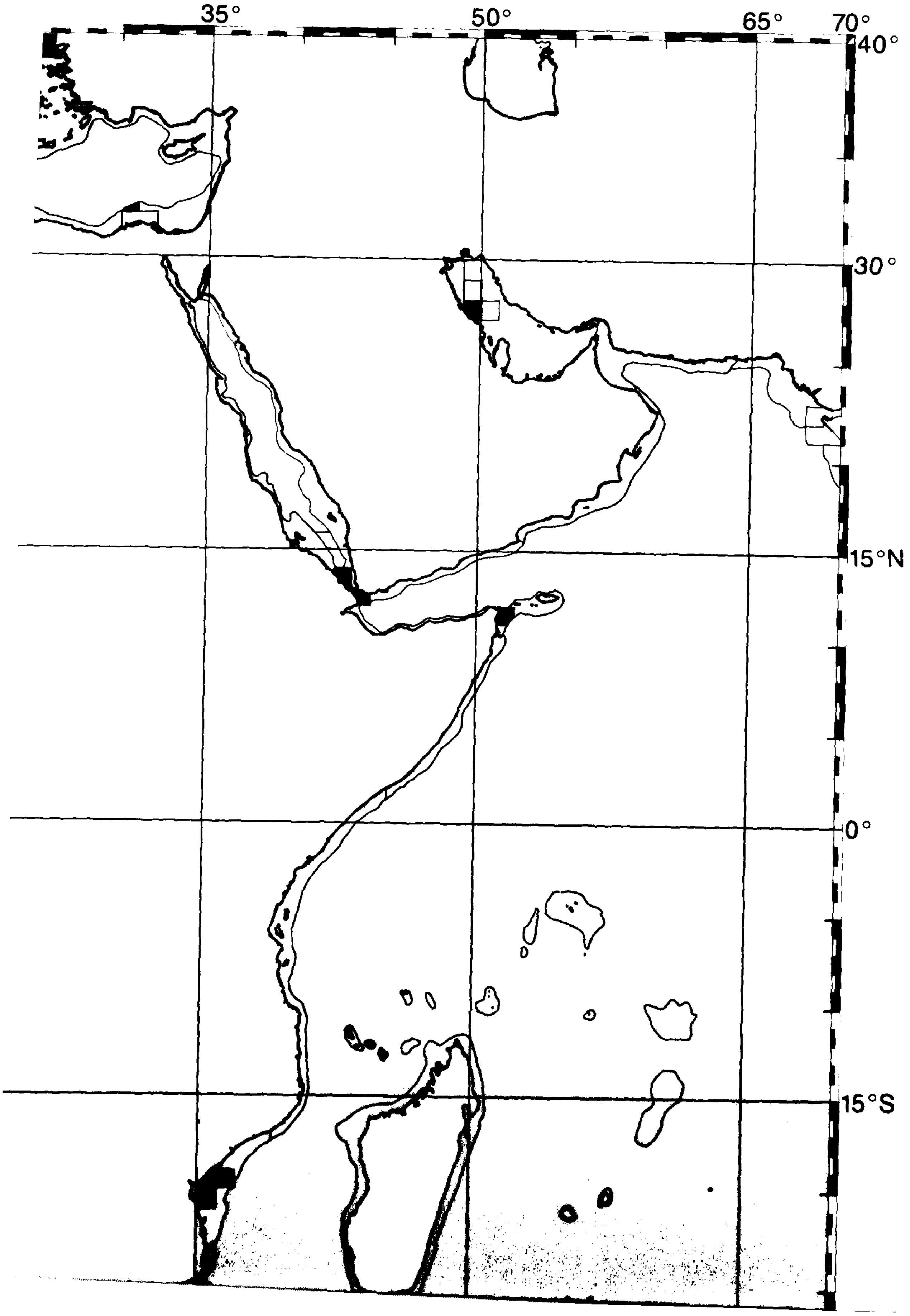
35°
50°
65°
70°
40°
30°
15°N
0°
15°S

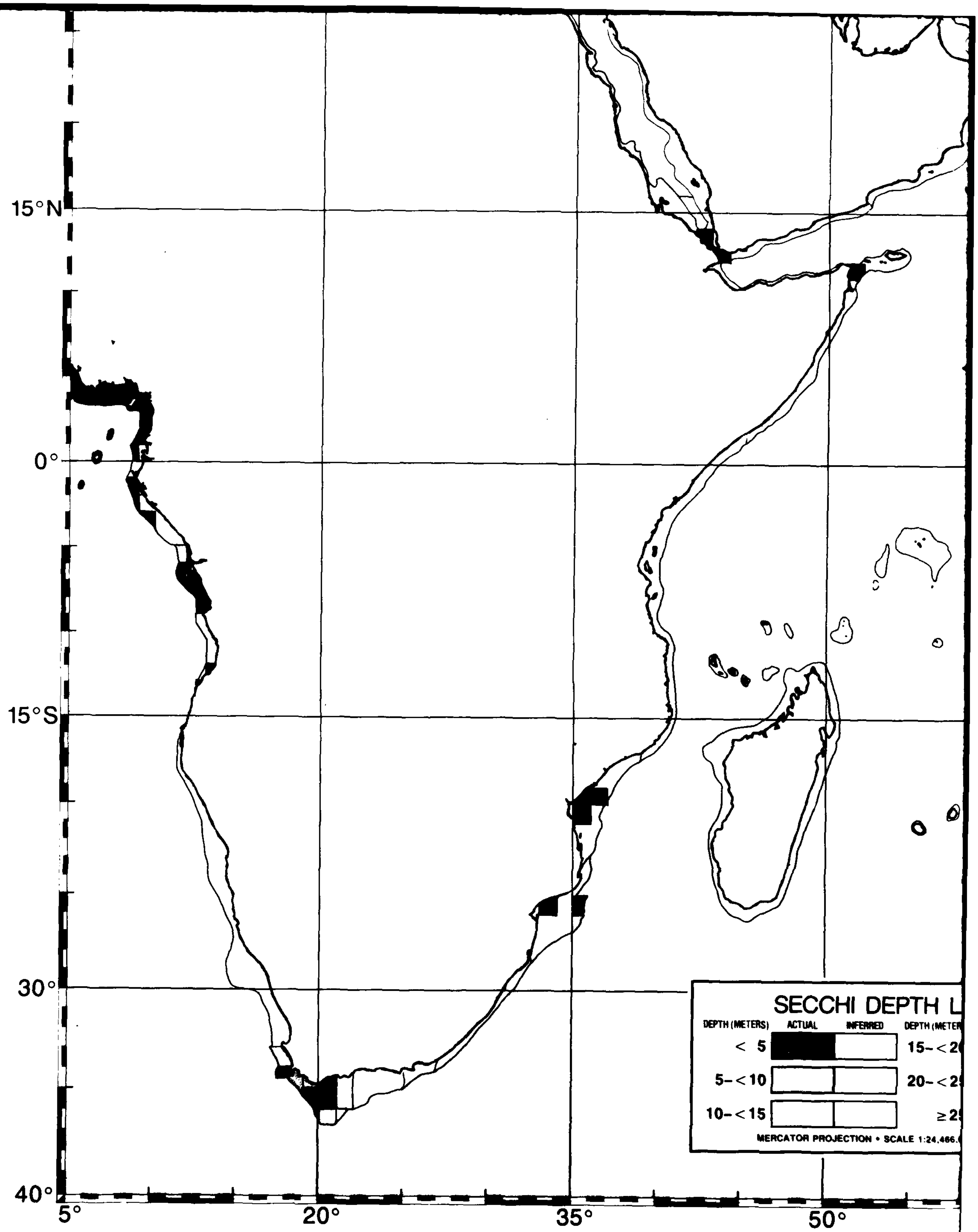

PLATE VII APRIL—JUNE

Compiled by: R.A. Ar
Prepared for the Defen
the Naval Ocean Resea
Remote Sensing Branch

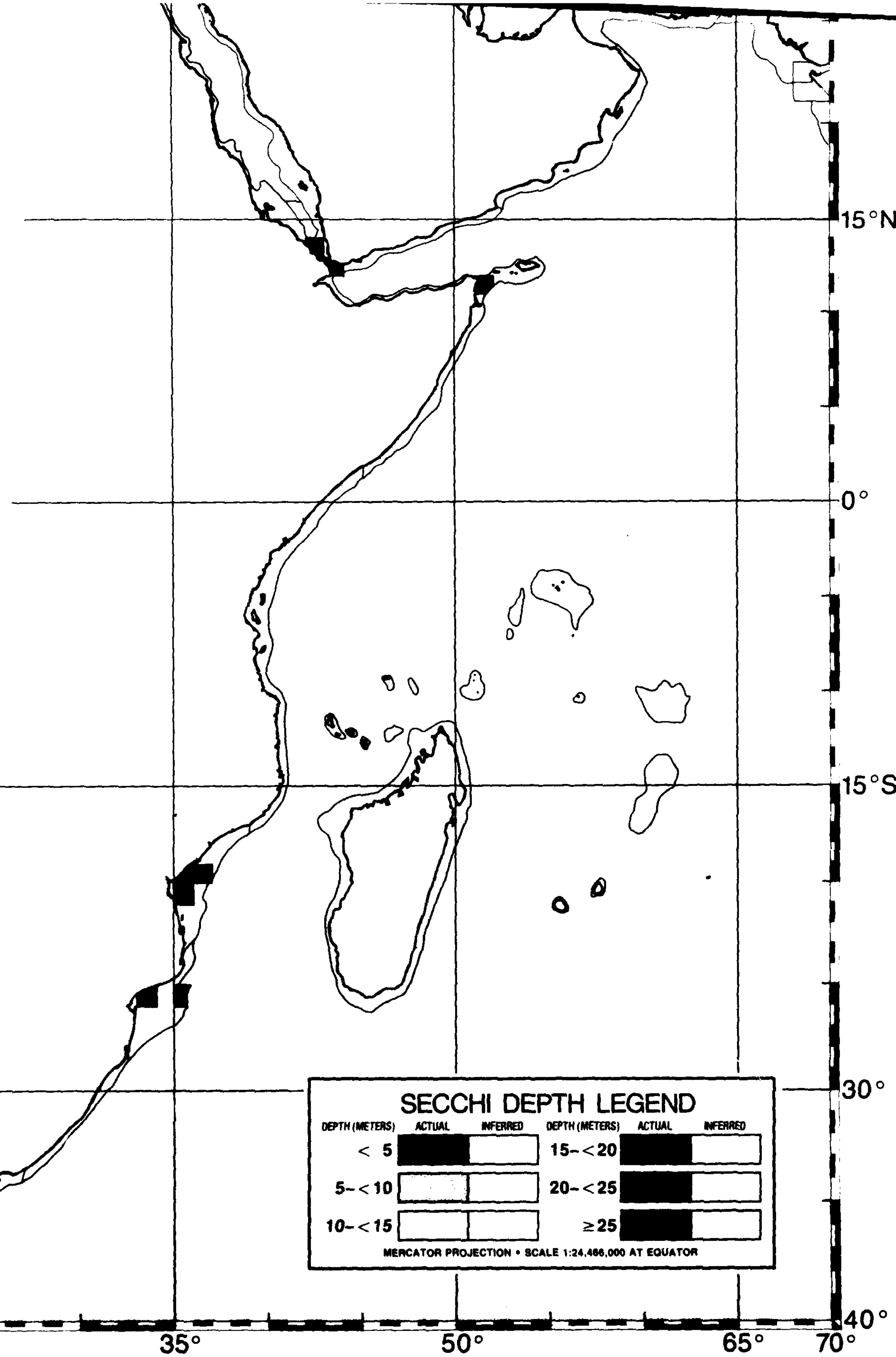

Compiled by: R.A. Arnone, F.A. Hilder, S.P. Tucker
Prepared for the Defense Mapping Agency by
the Naval Ocean Research and Development Activity
Remote Sensing Branch, NSTL, Mississippi

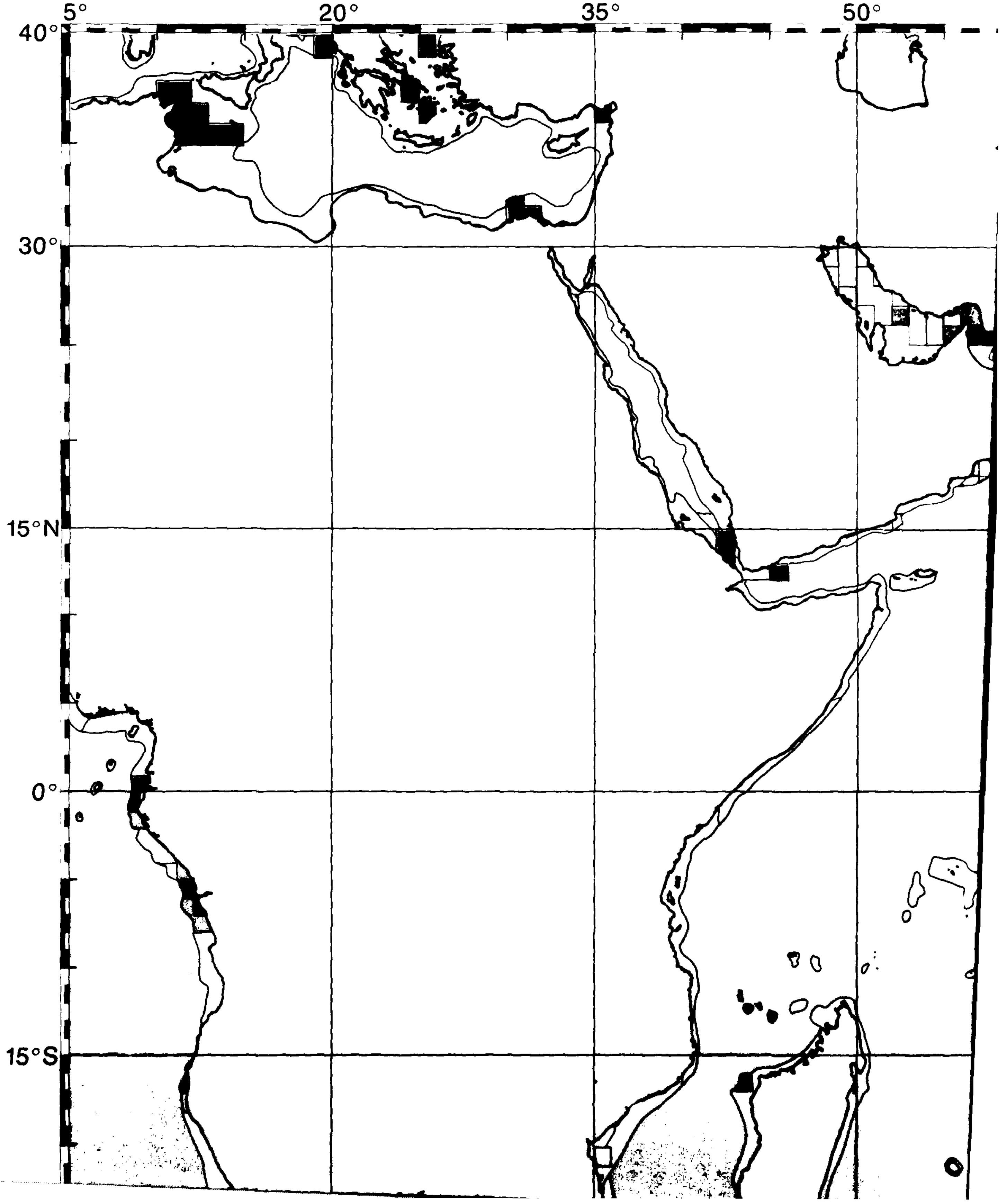
5°
20°
35°
50°
40°
30°
15°N
0°
15°S

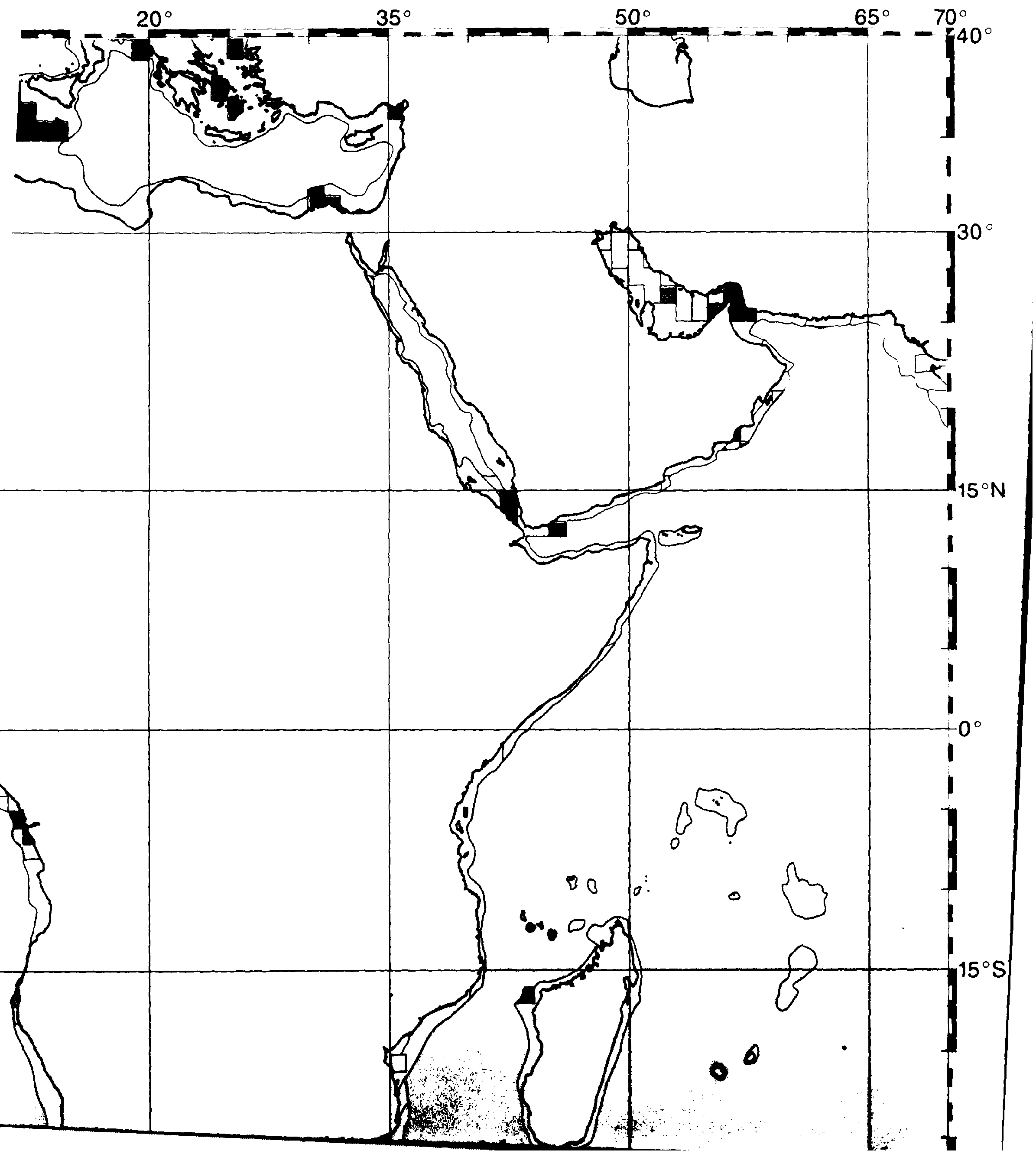

20°
35°
50°
65°
70°
40°
30°
15°N
0°
15°S

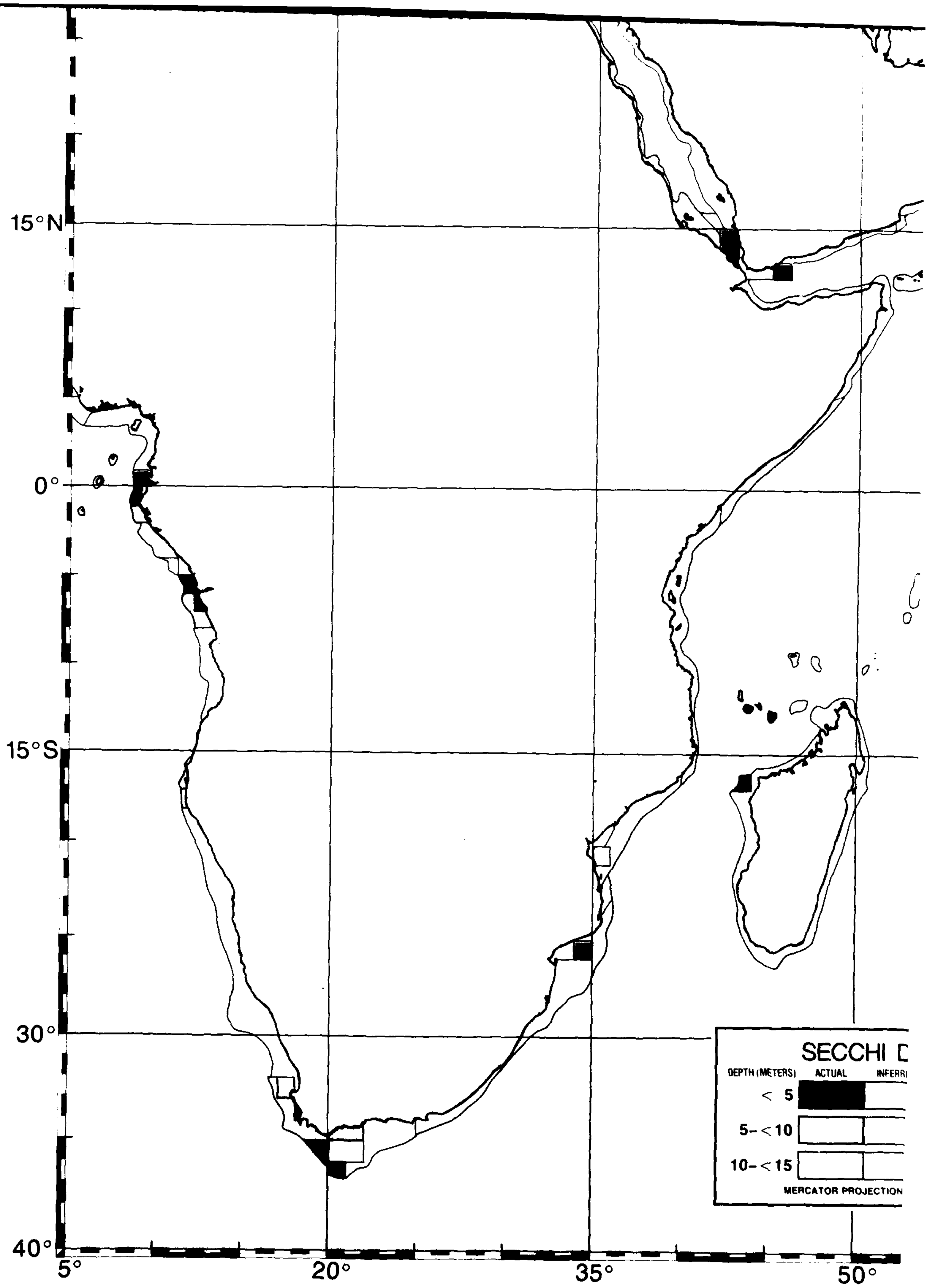

PLATE VIII JULY—SEPTEMBER

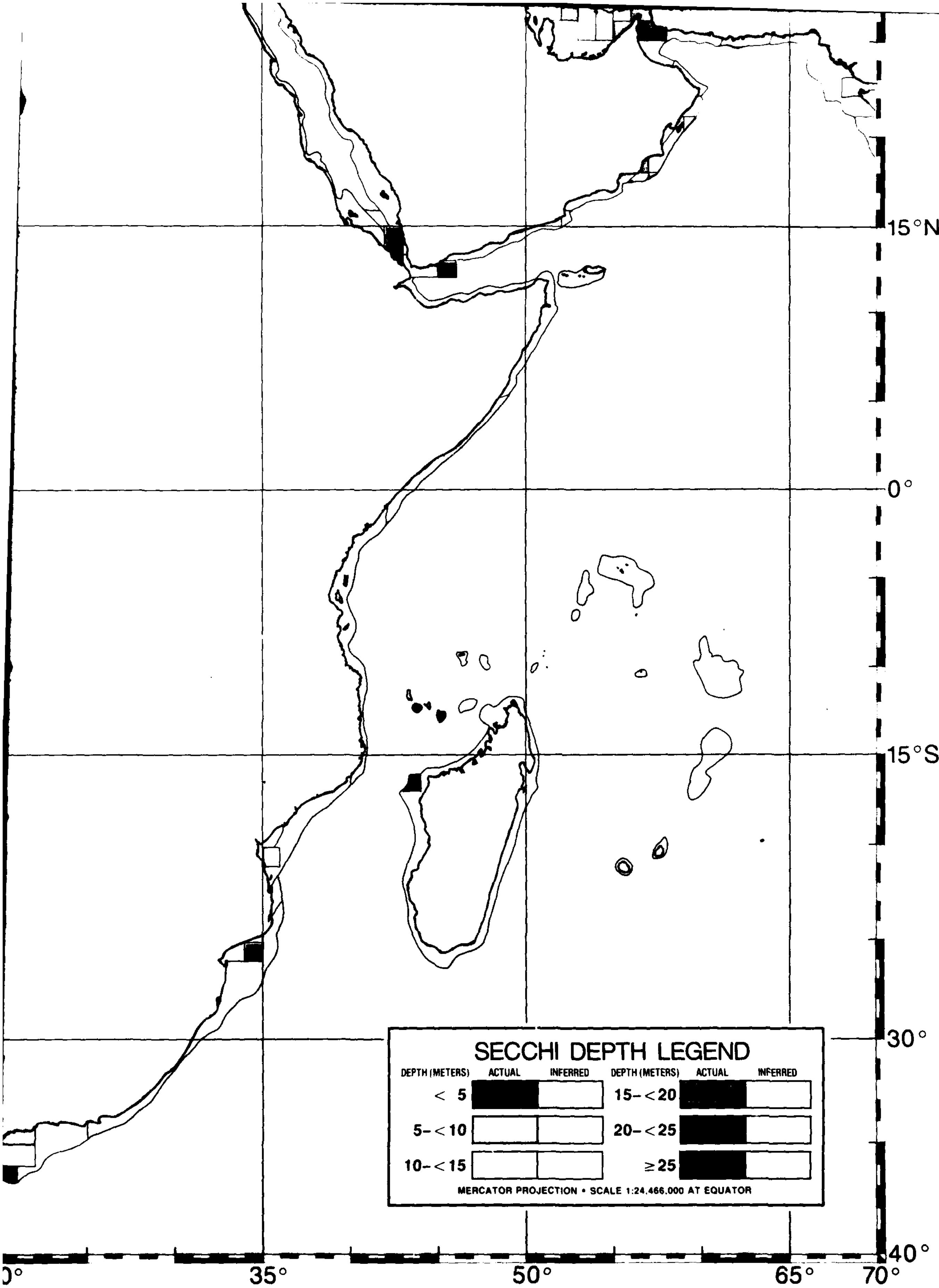

Compiled by: R.A. Arnone, F.A. Hilder, S.P. Tucker
Prepared for the Defense Mapping Agency by
the Naval Ocean Research and Development Activity
Remote Sensing Branch, NSTL, Mississippi

'TEMBER

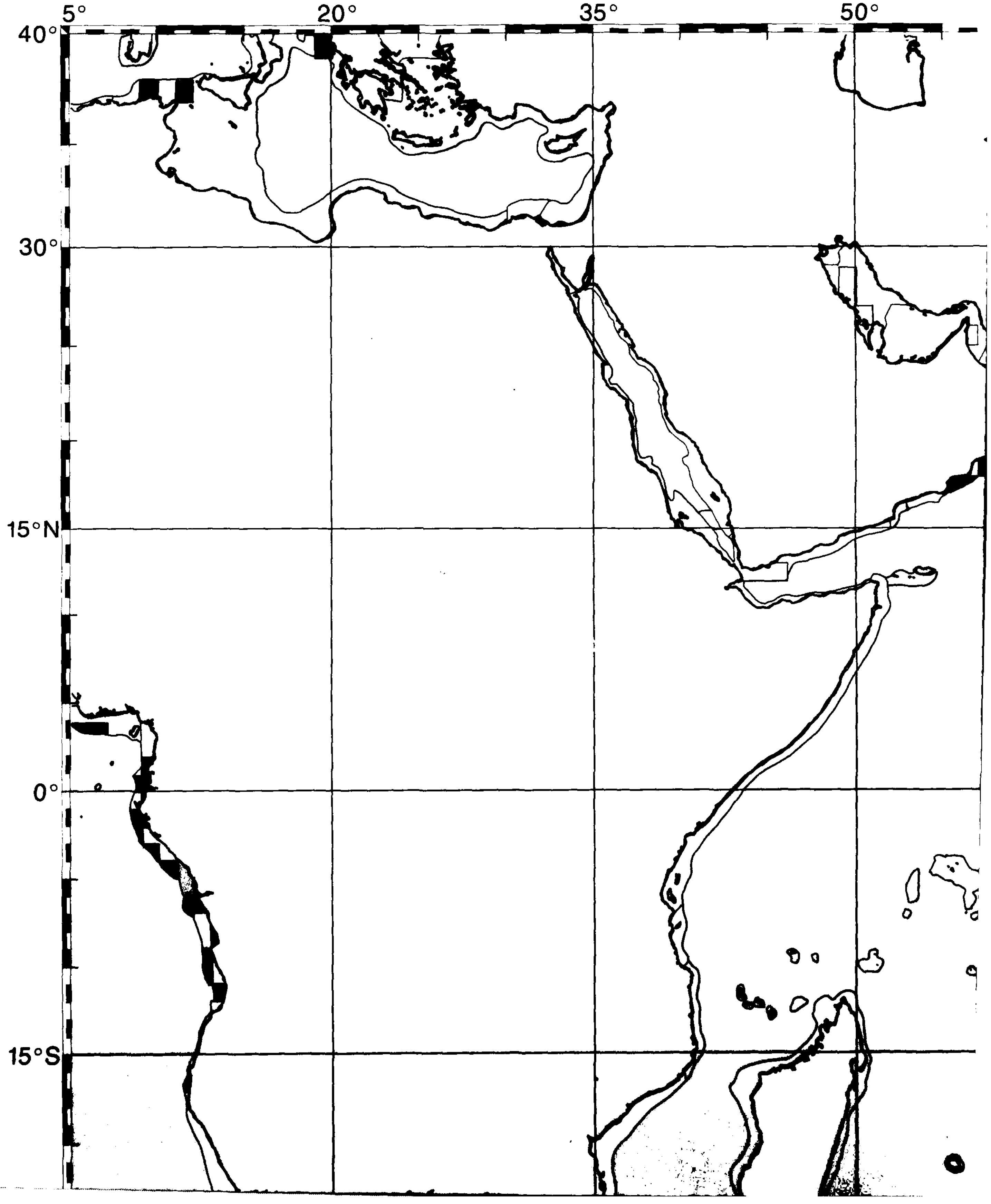
5°
20°
35°
50°
40°
30°
15°N
0°
15°S

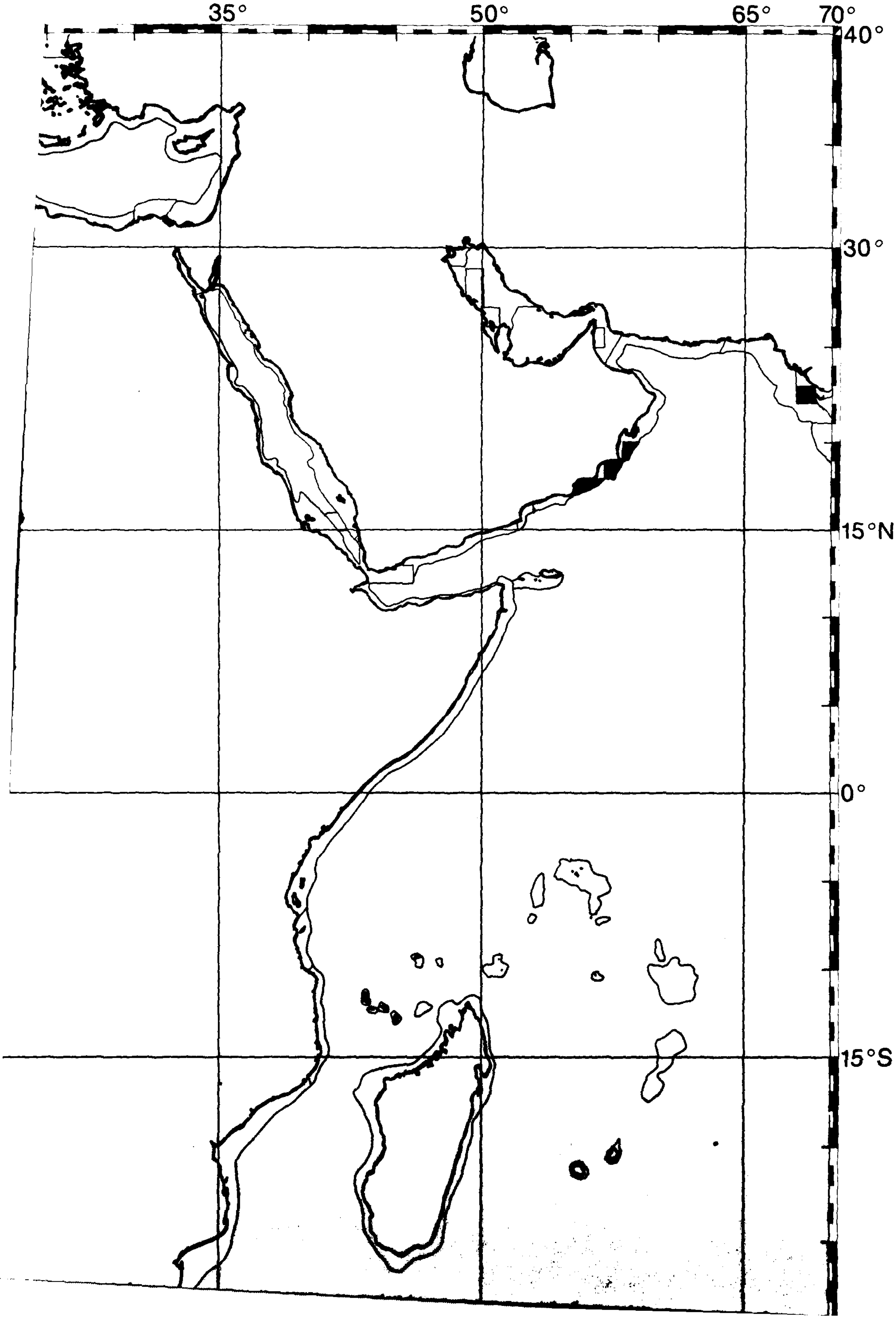
35°
50°
65°
70°
40°
30°
15°N
0°
15°S

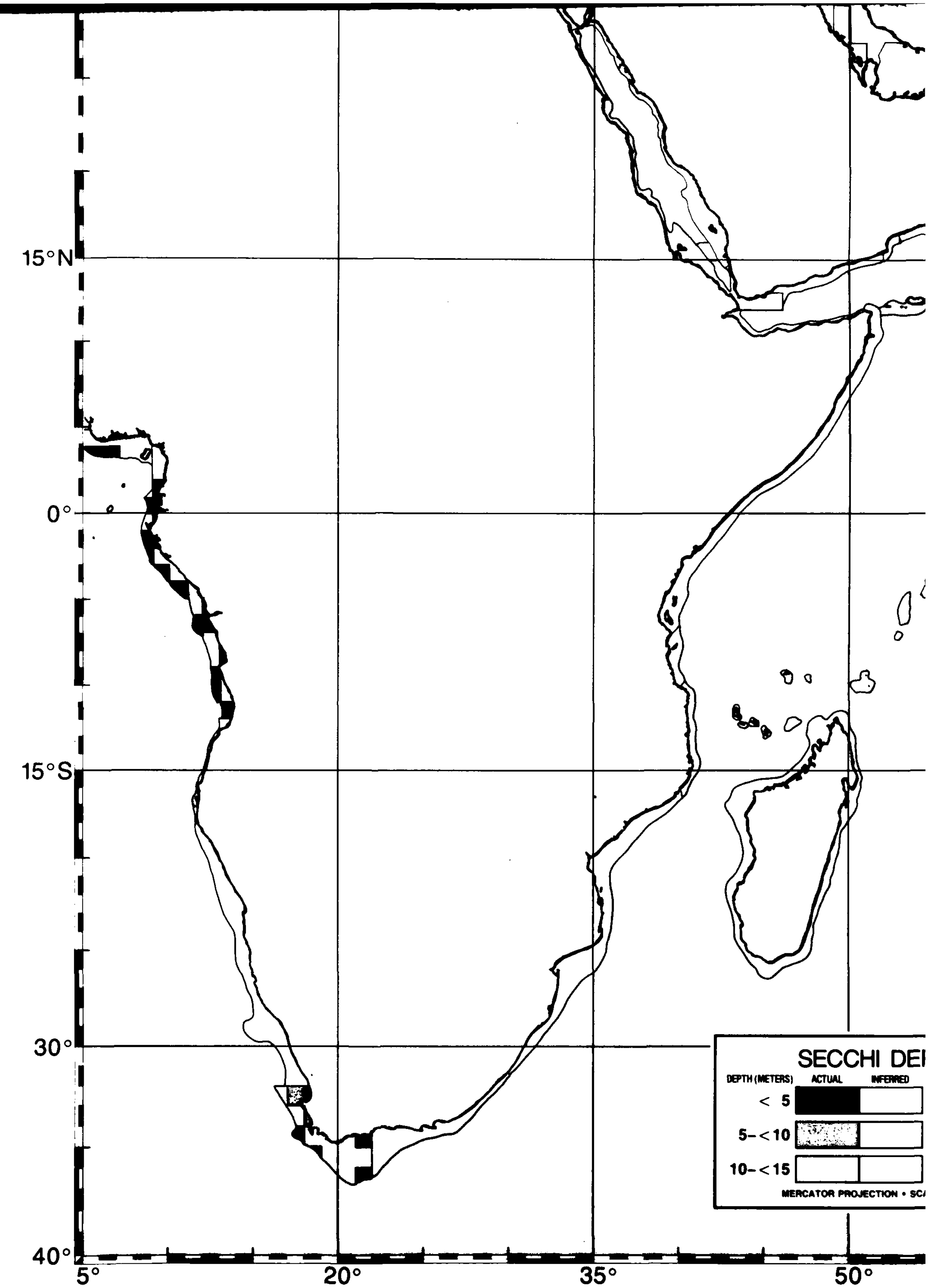

PLATE IX OCTOBER—DECEMBER

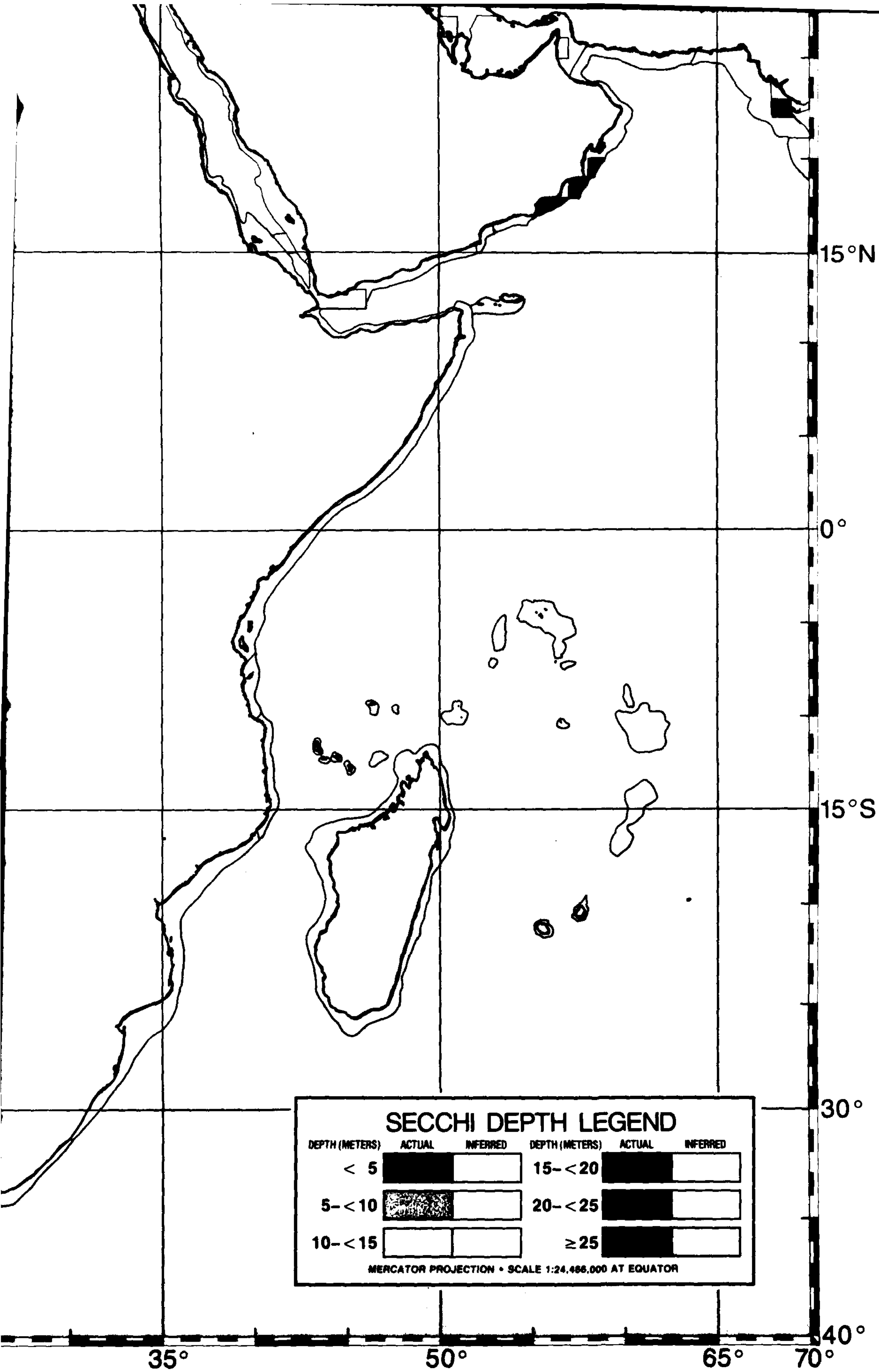

Compiled by: R.A. Arnone, F.A. Hilder, S.P. Tucker
Prepared for the Defense Mapping Agency by
the Naval Ocean Research and Development Activity
Remote Sensing Branch, NSTL, Mississippi

ER

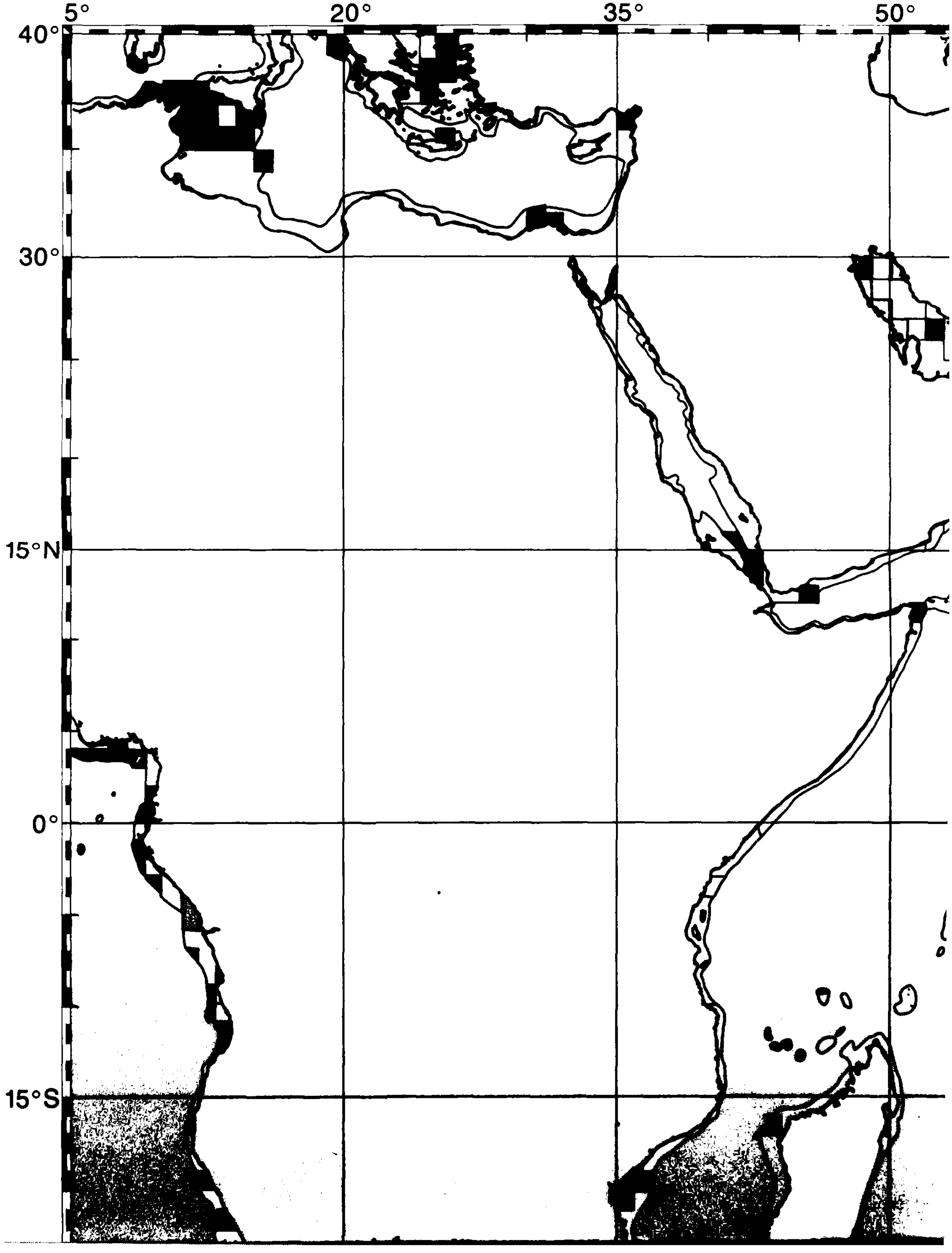
5°
20°
35°
50°
40°
30°
15°N
0°
15°S

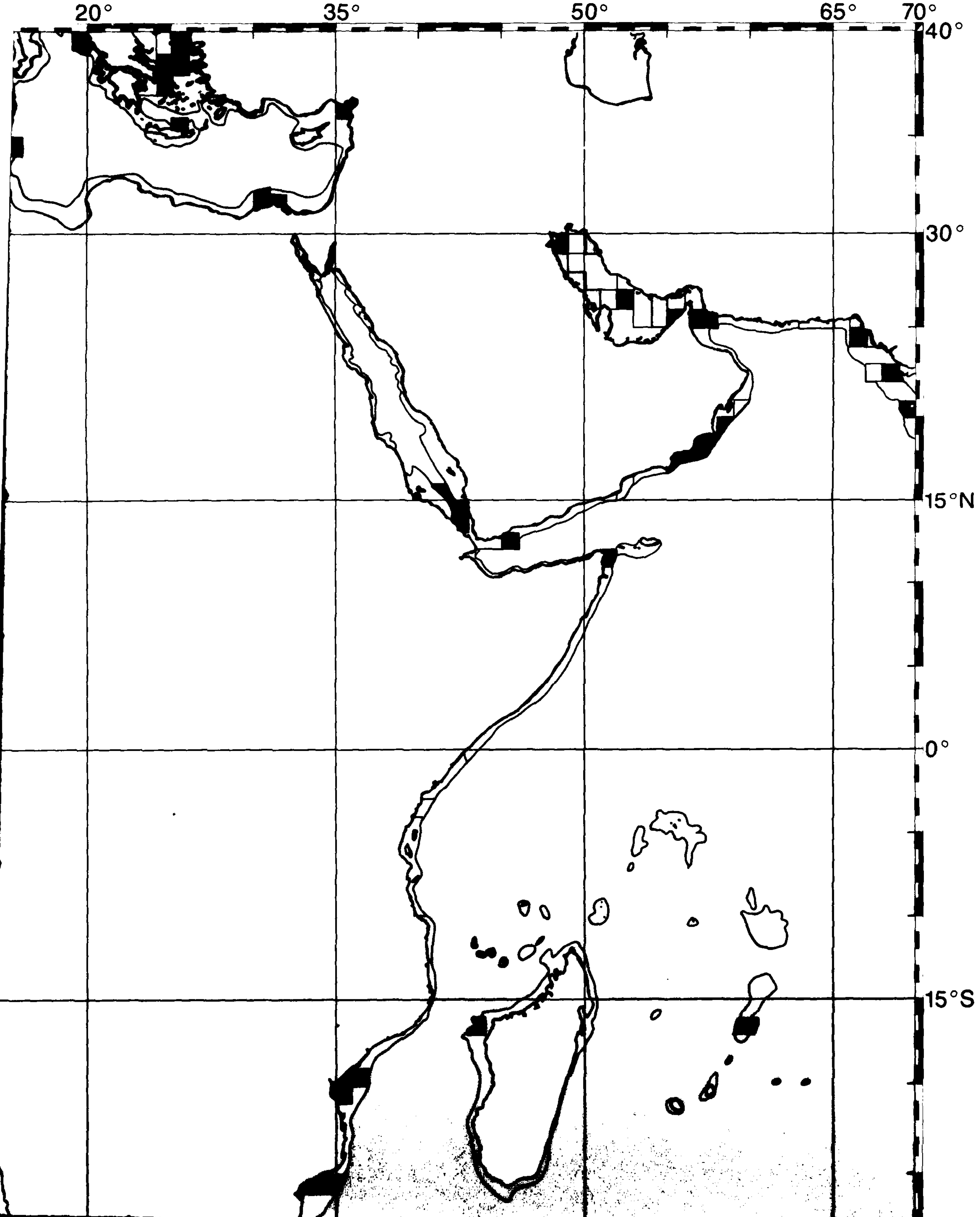
20°
35°
50°
65°
70°
40°
30°
15°N
0°
15°S

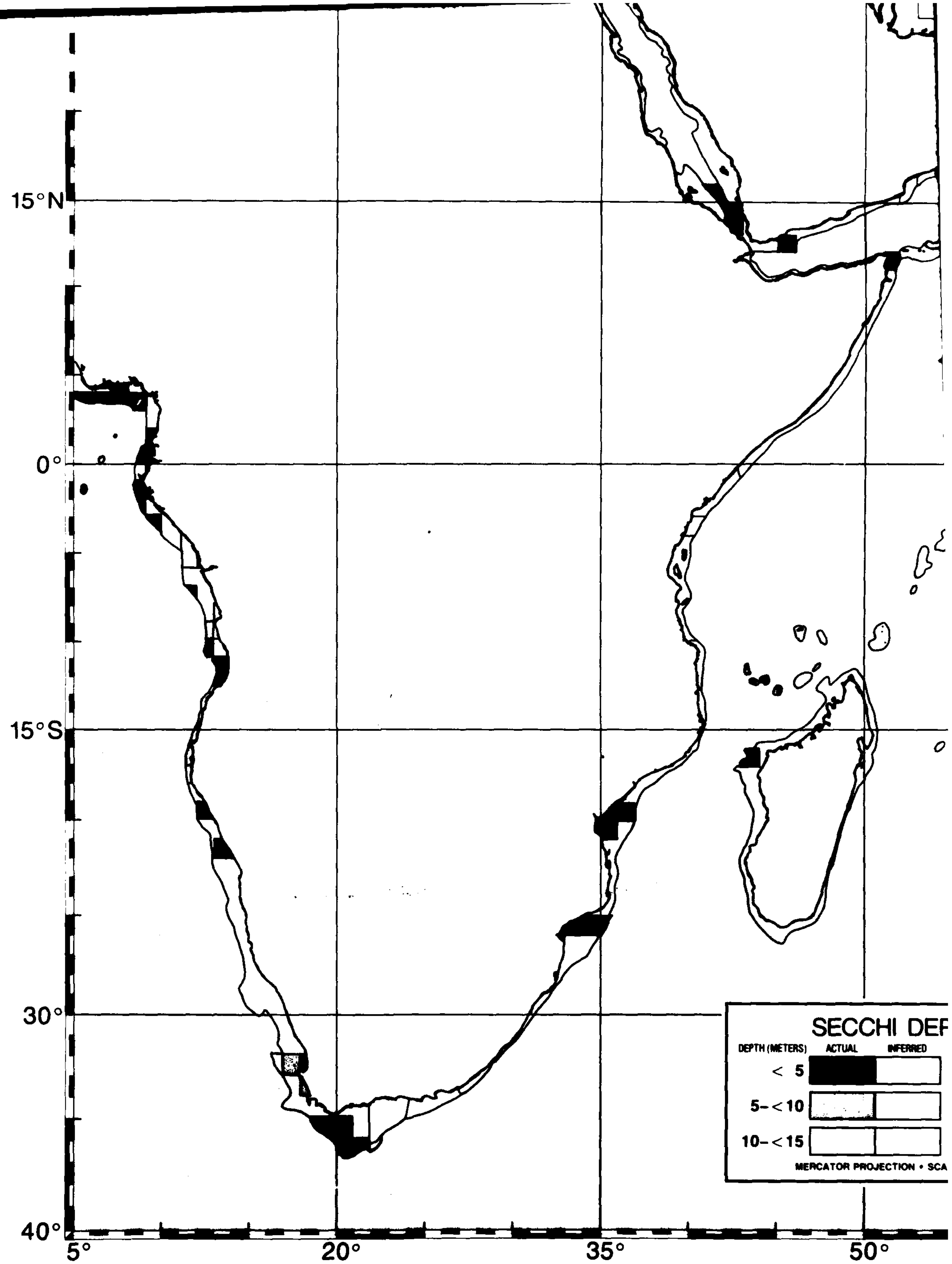

Compiled
Prepared
the Naval
Remote

PLATE X ANNUAL MEAN

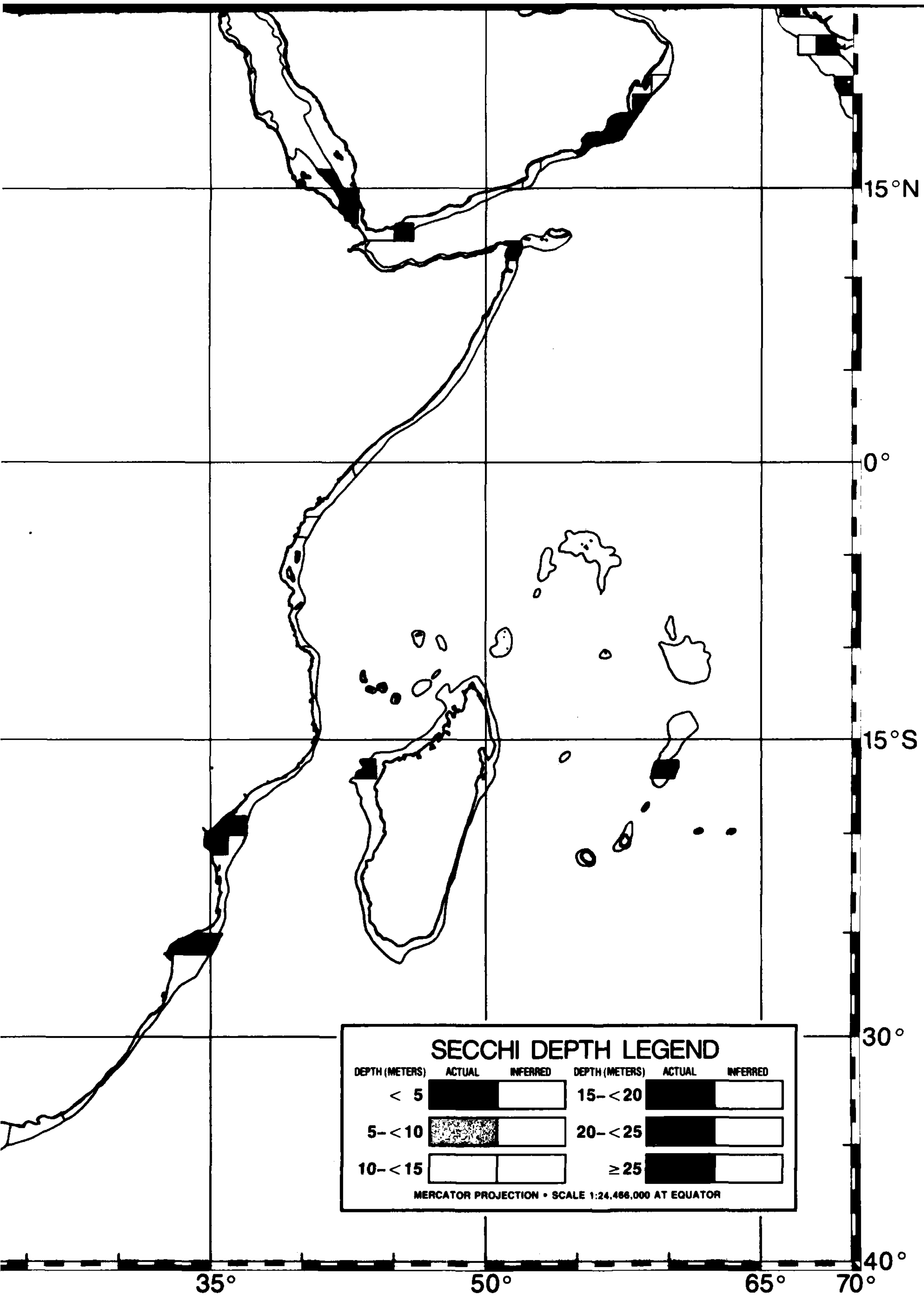

Compiled by: R.A. Arnone, F.A. Hilder, S.P. Tucker
Prepared for the Defense Mapping Agency by
the Naval Ocean Research and Development Activity
Remote Sensing Branch, NSTL, Mississippi

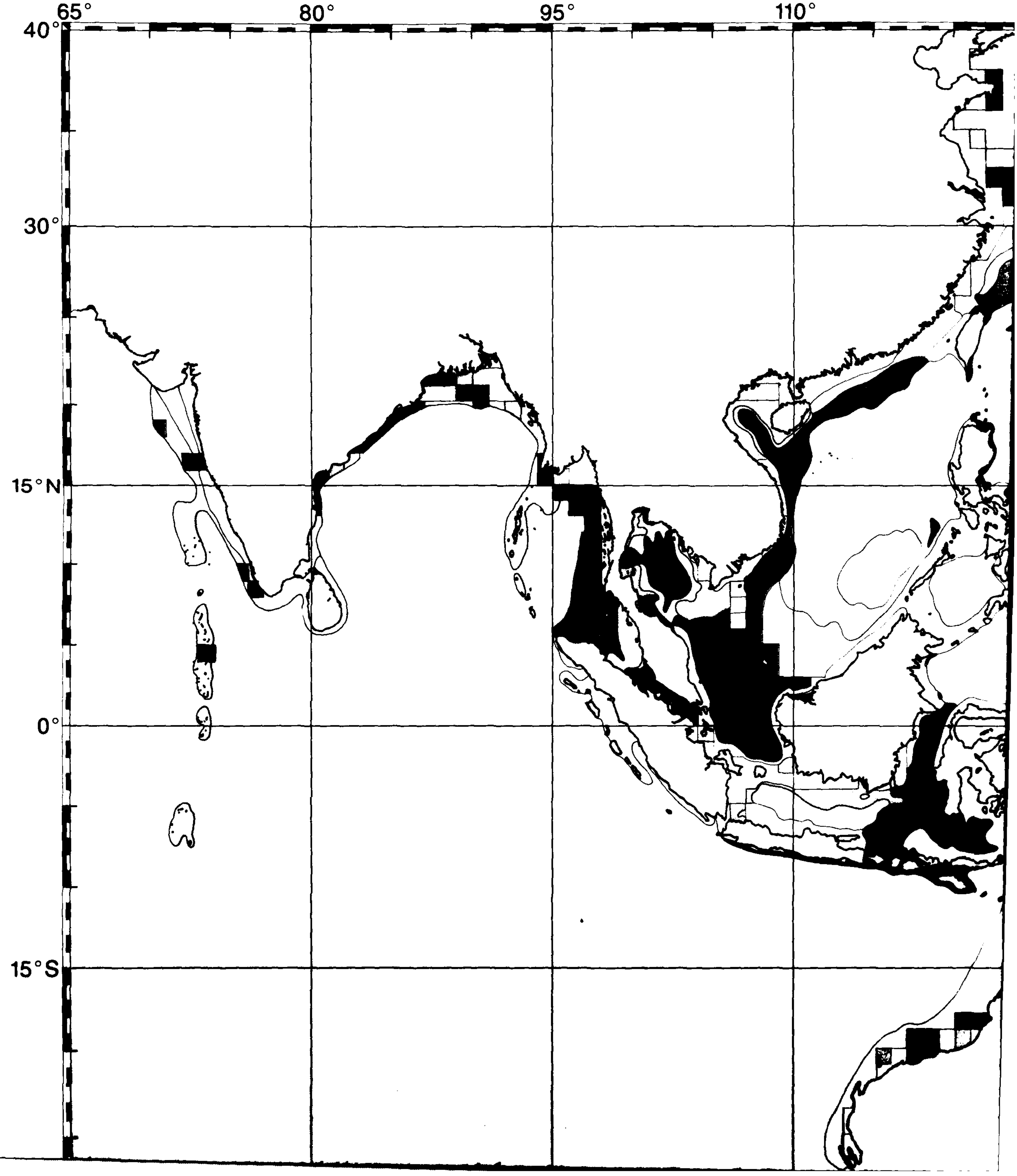

65°
80°
95°
110°
40°
30°
15°N
0°
15°S

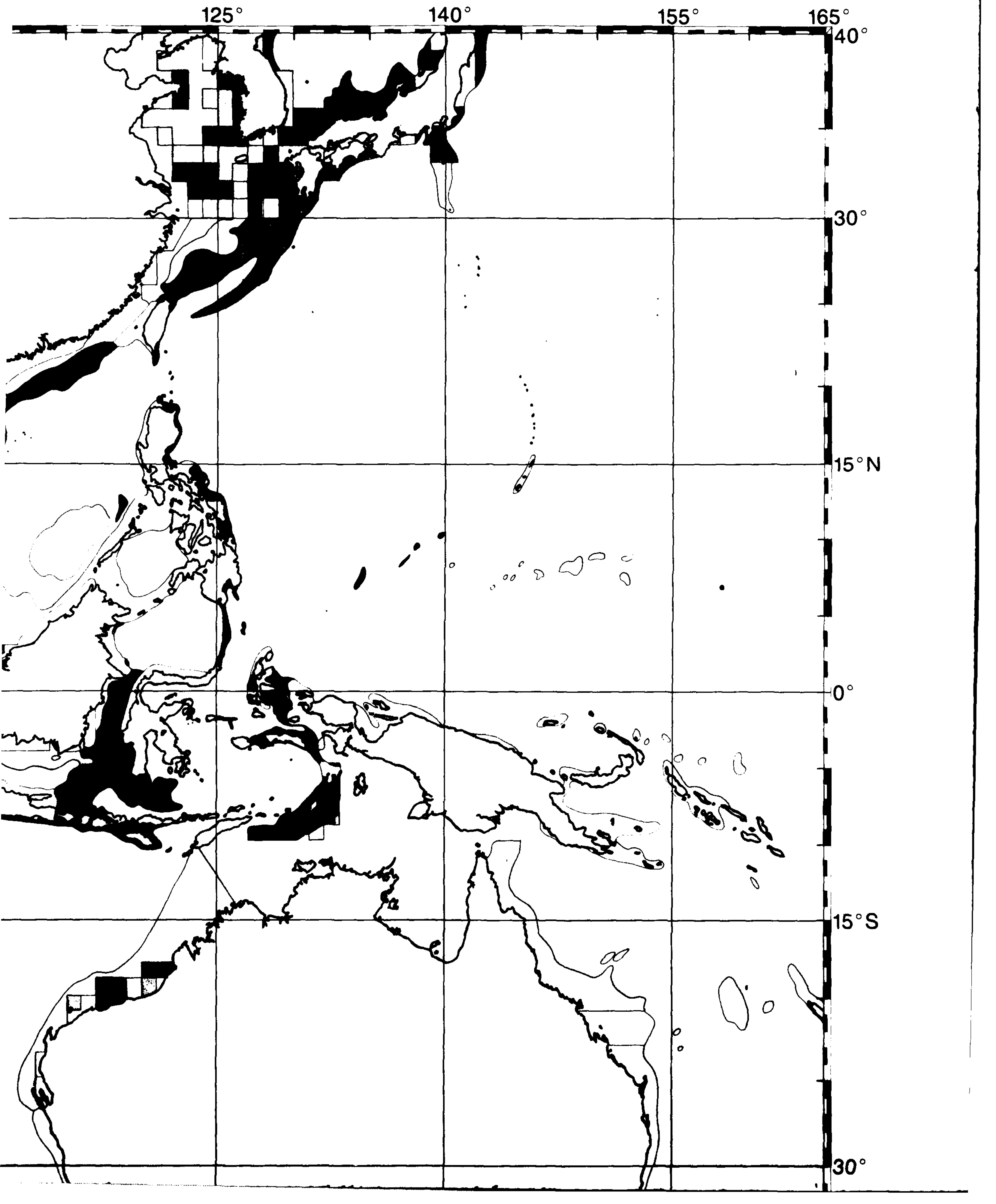

125°
140°
155°
165°
40°
30°
15°N
0°
15°S
30°

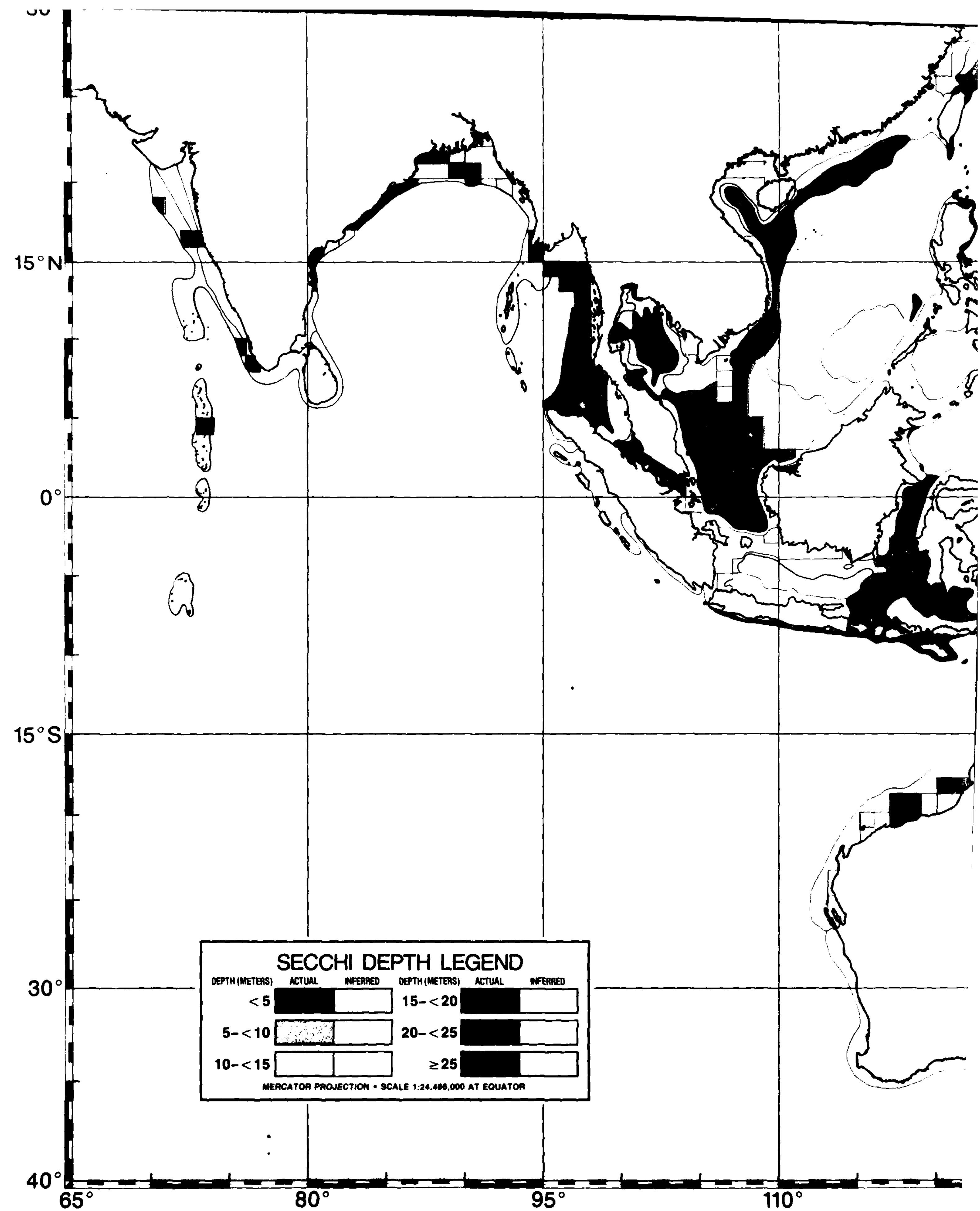

PLATE XI JANUARY—MARCH

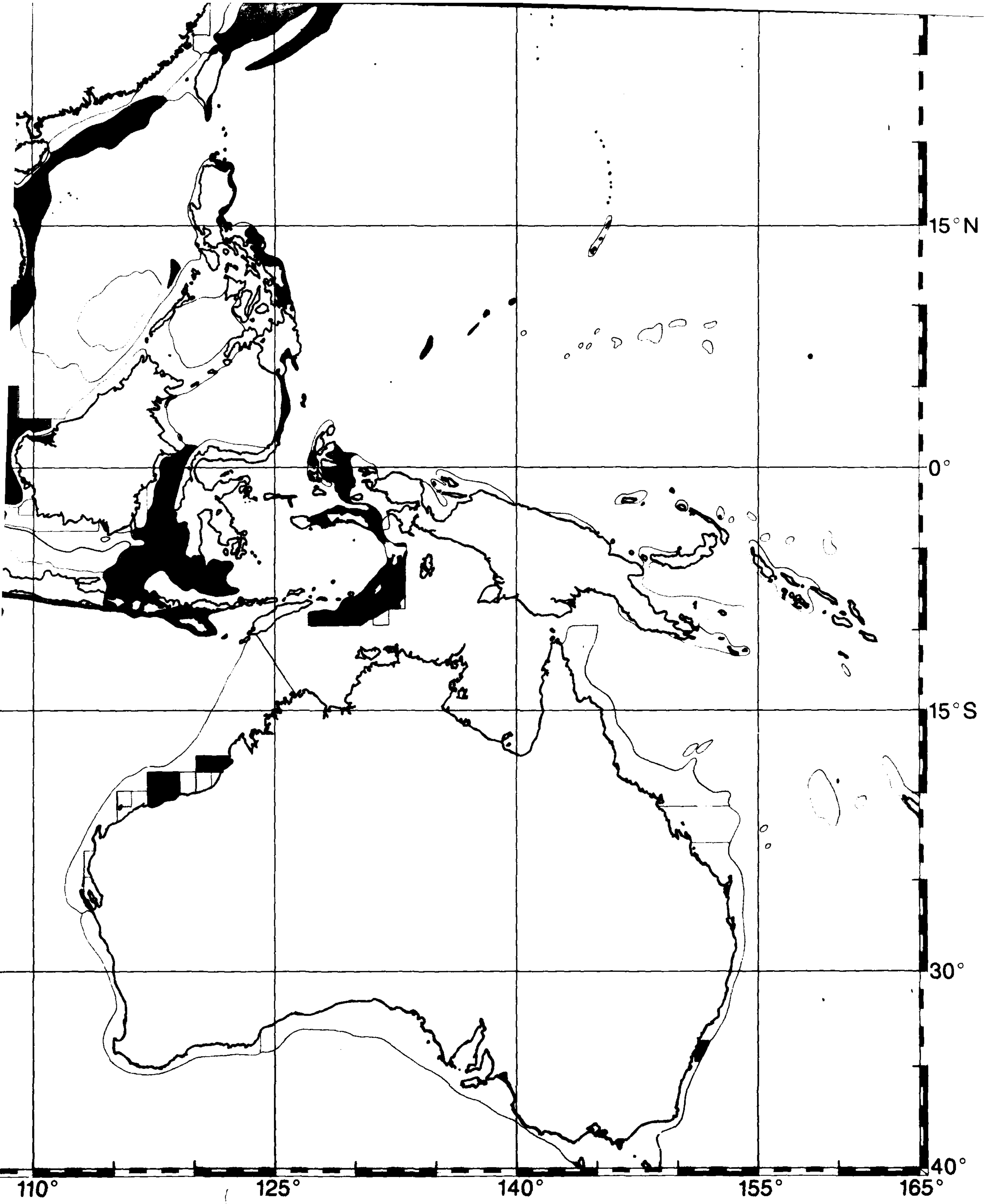

Compiled by: R.A. Arnone, F.A. Hilder, S.P. Tucker
Prepared for the Defense Mapping Agency by
the Naval Ocean Research and Development Activity
Remote Sensing Branch, NSTL, Mississippi

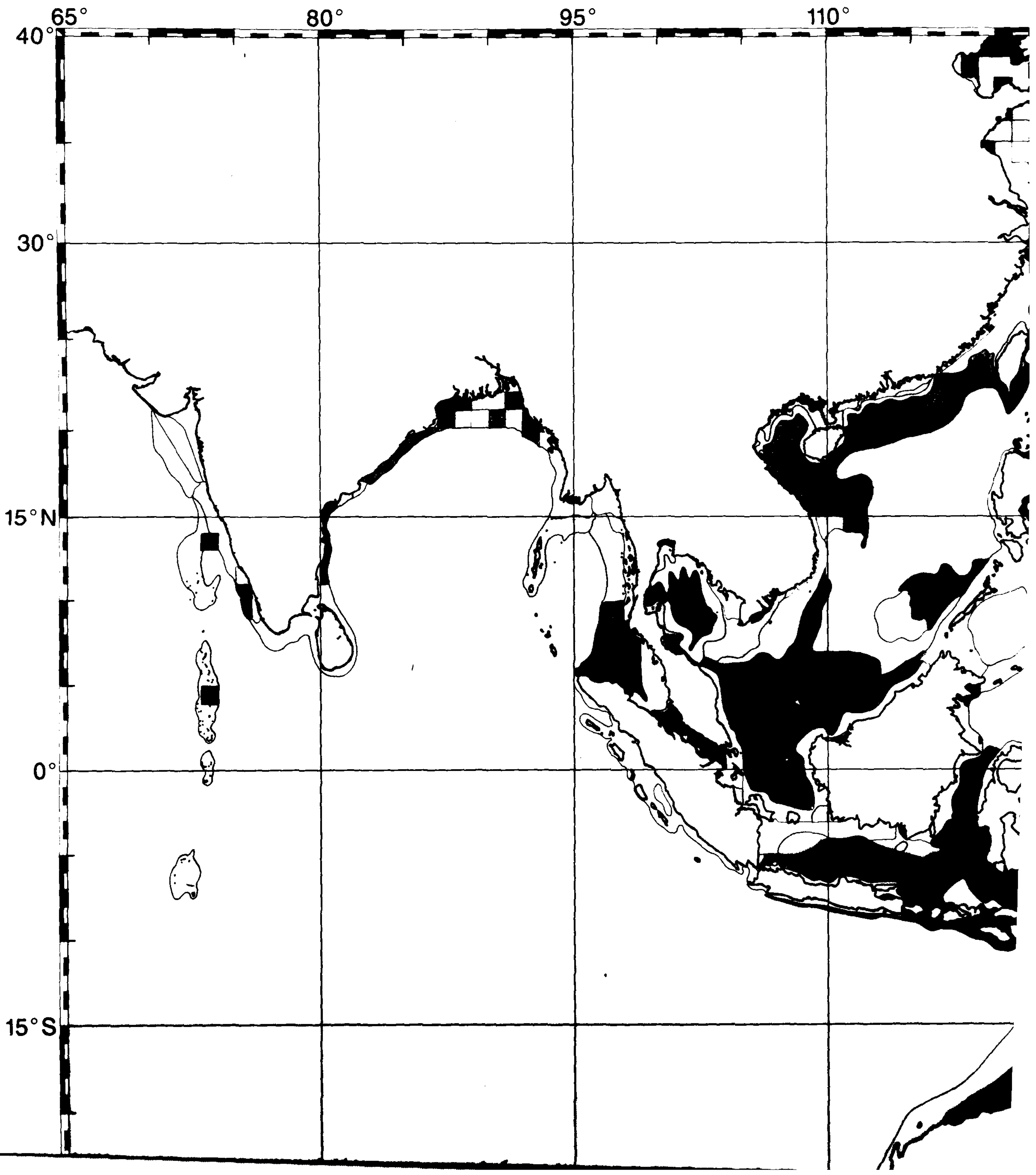
65°
80°
95°
110°
40°
30°
15°N
0°
15°S

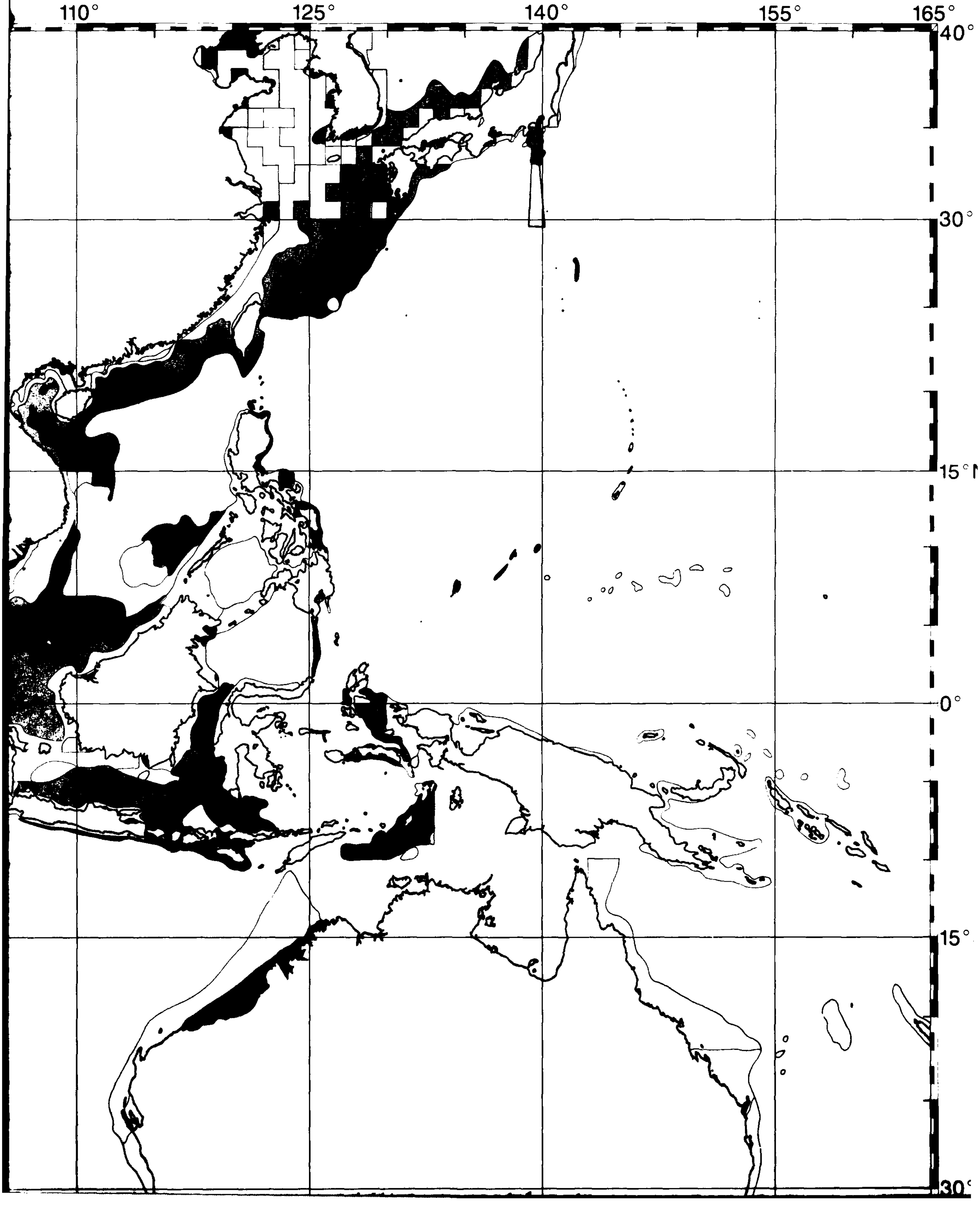
110°
125°
140°
155°
165°
40°
30°
15°
0°
15°
30°

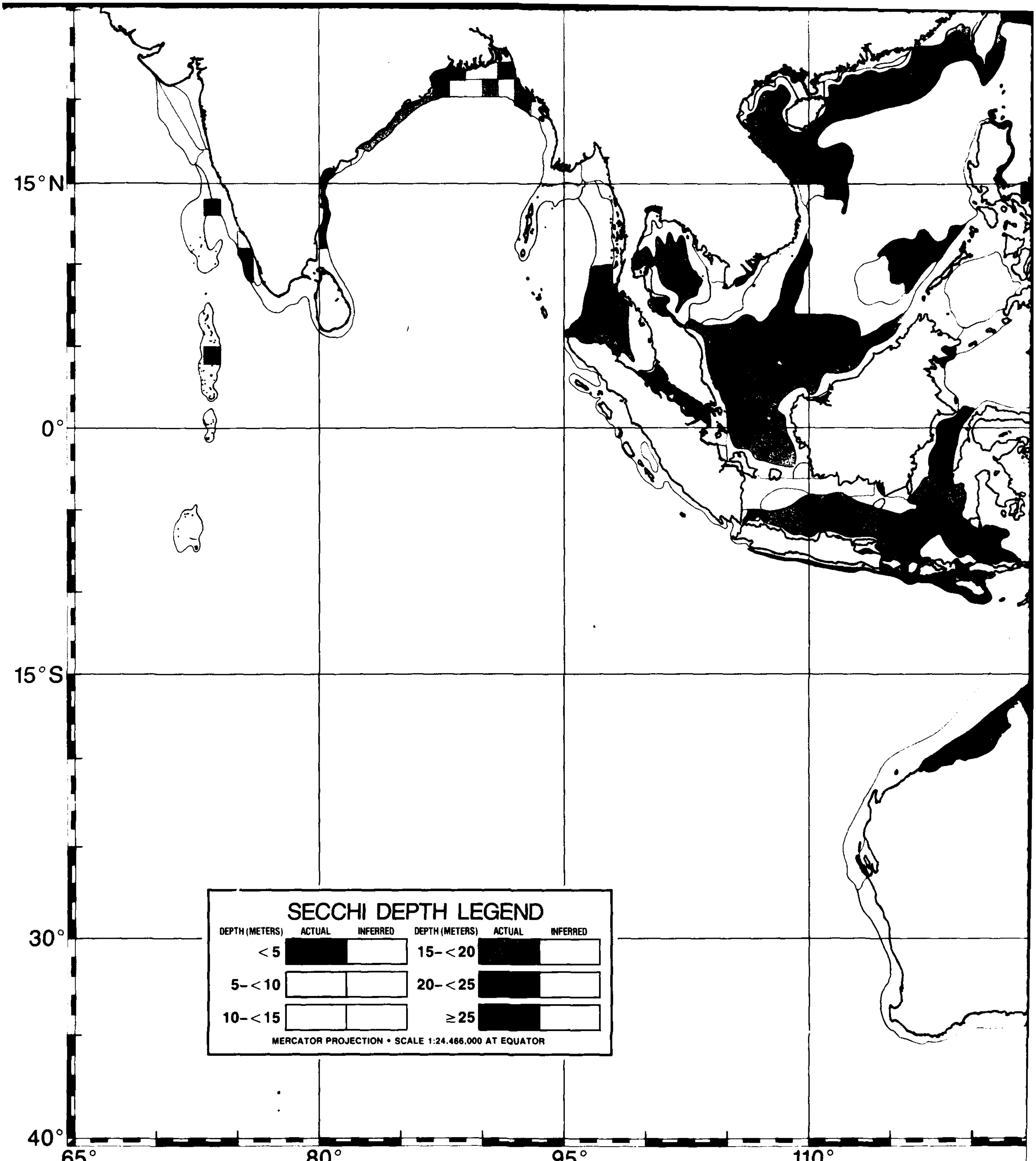

PLATE XII APRIL—JUNE

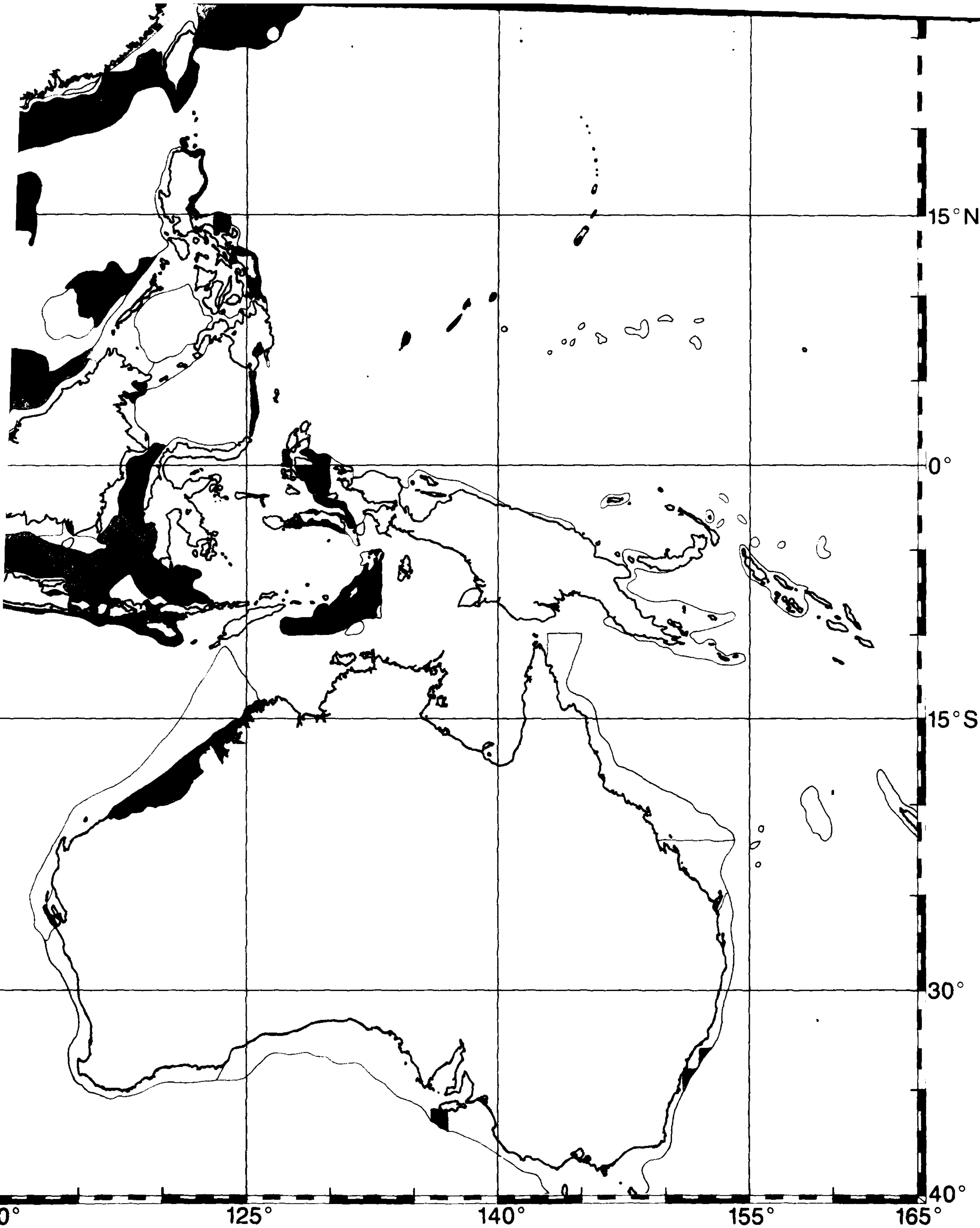

Compiled by: R.A. Arnone, F.A. Hilder, S.P. Tucker
Prepared for the Defense Mapping Agency by
the Naval Ocean Research and Development Activity
Remote Sensing Branch, NSTL, Mississippi

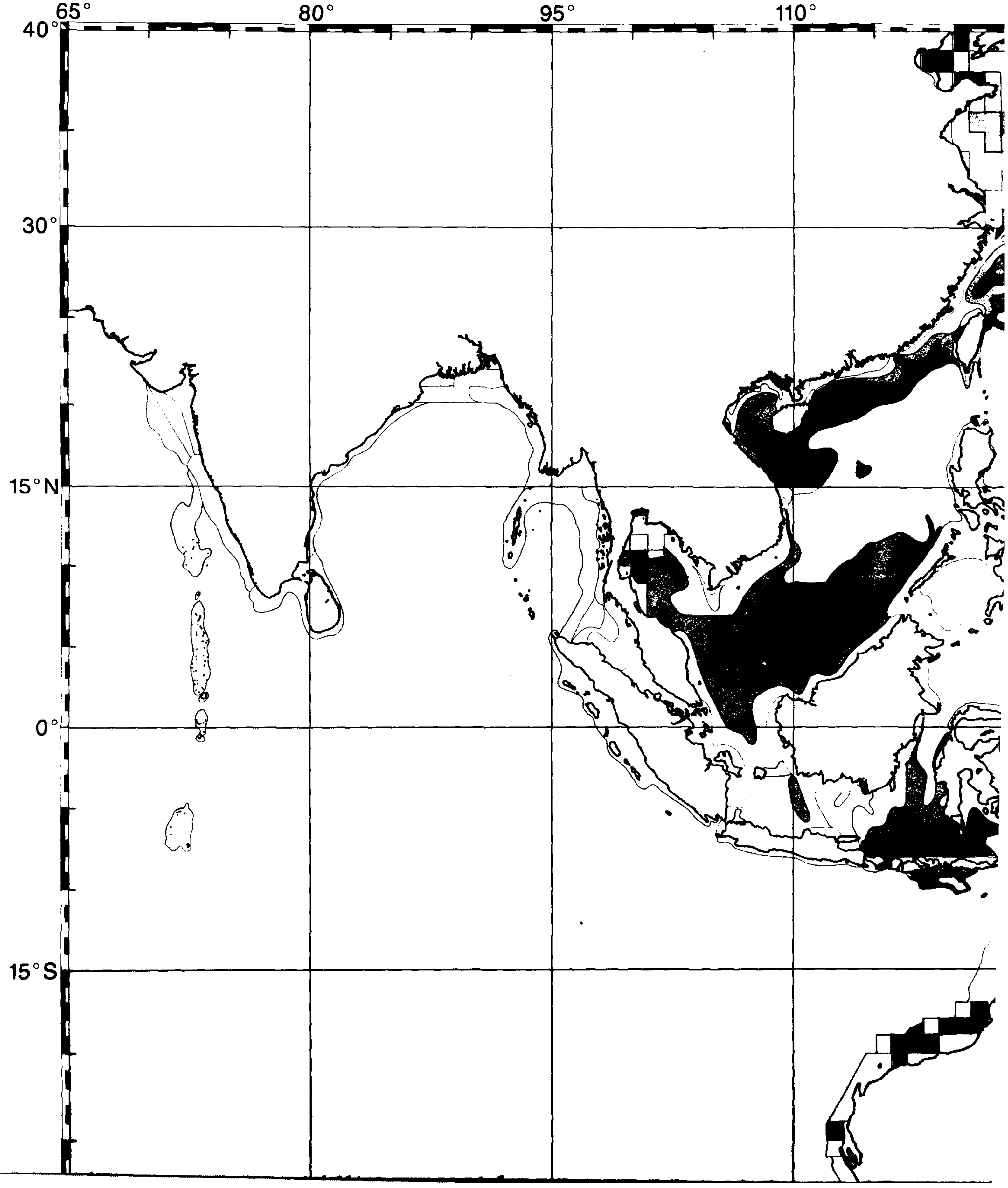
65°
80°
95°
110°
40°
30°
15° N
0°
15° S

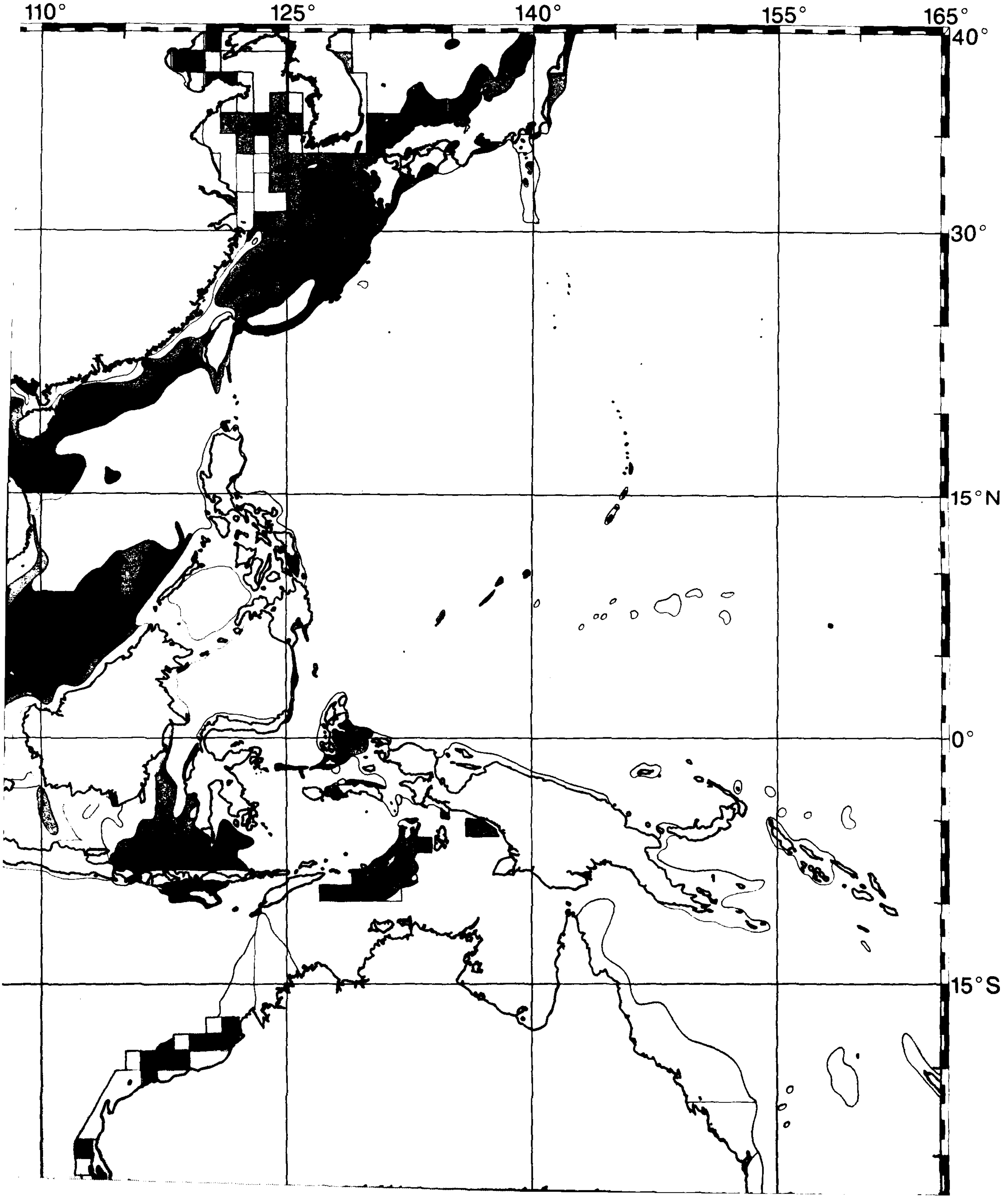

110°
125°
140°
155°
165°
40°
30°
15°N
0°
15°S

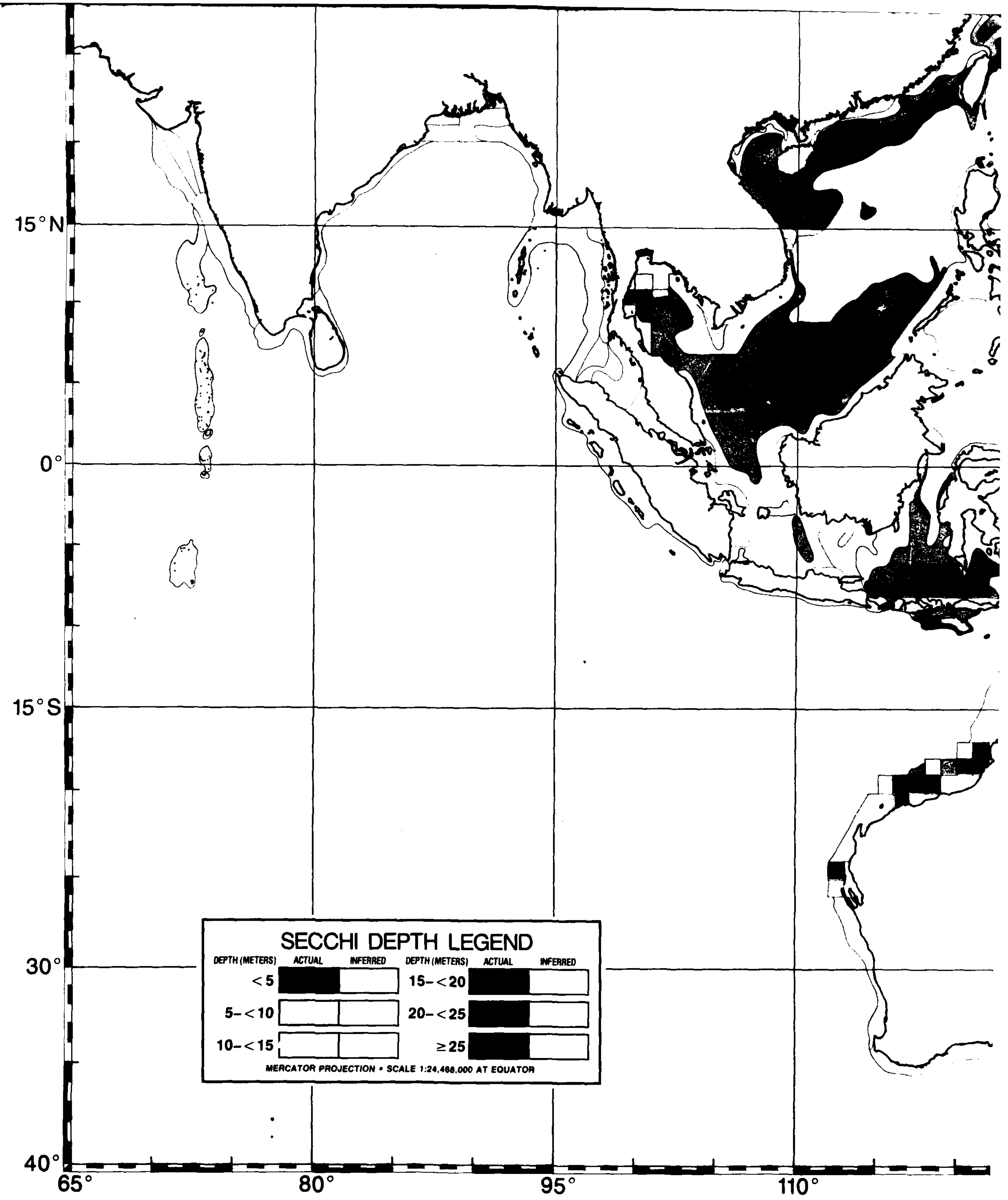

PLATE XIII JULY—SEPTEMBER

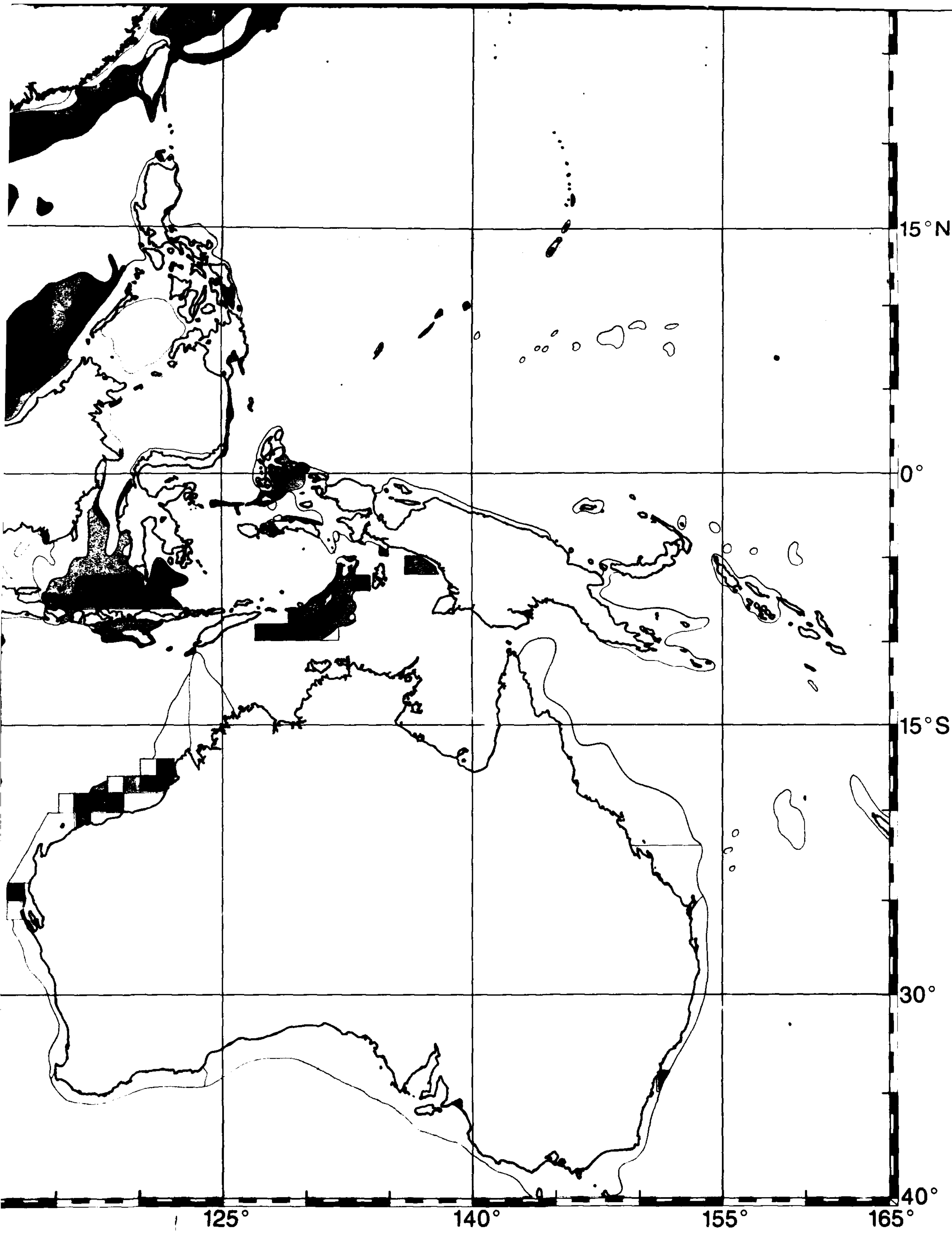

Compiled by: R.A. Arnone, F.A. Hilder, S.P. Tucker
Prepared for the Defense Mapping Agency by
the Naval Ocean Research and Development Activity
Remote Sensing Branch, NSTL, Mississippi

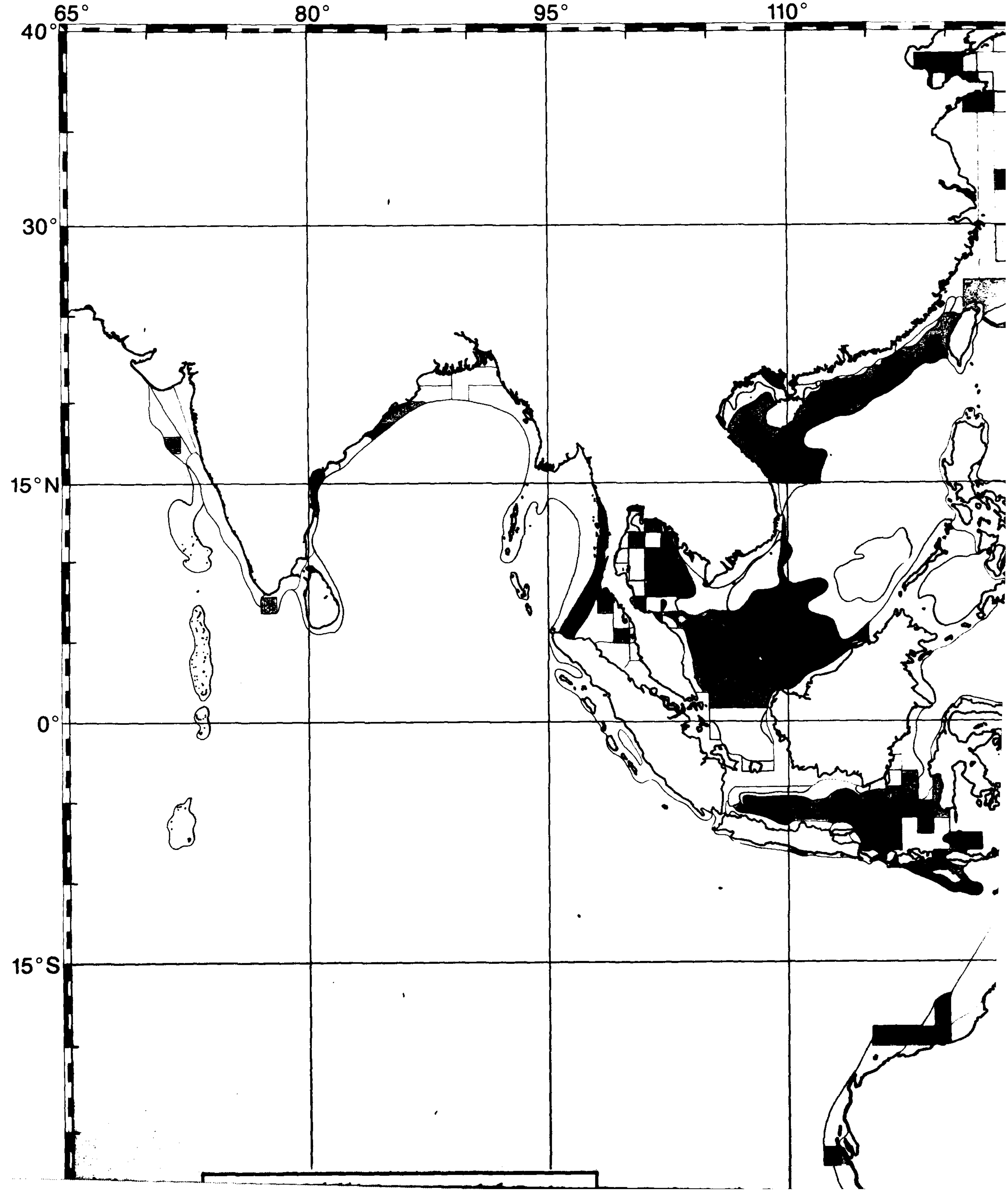

65°
80°
95°
110°
40°
30°
15°N
0°
15°S

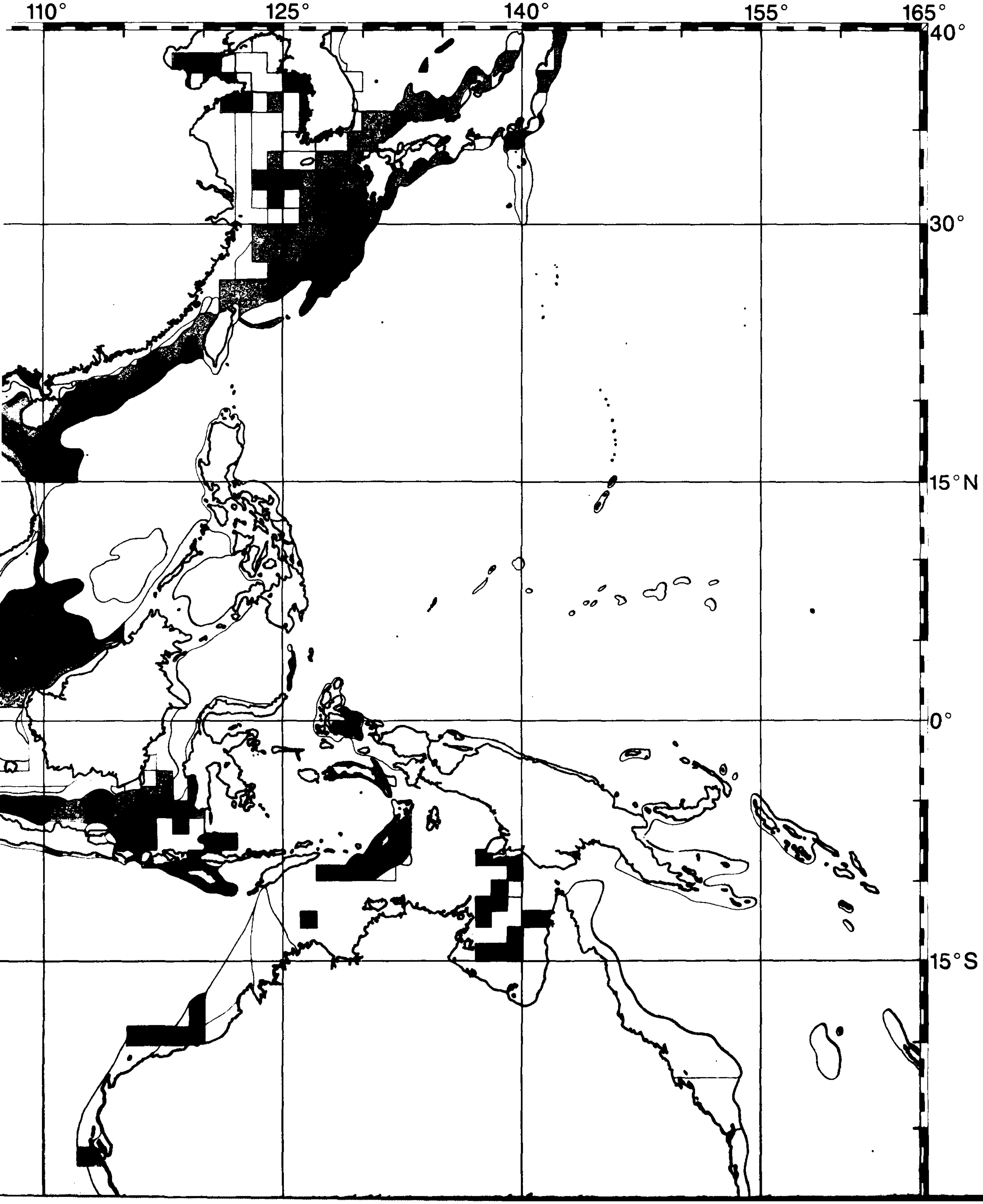

110°
125°
140°
155°
165°
40°
30°
15° N
0°
15° S

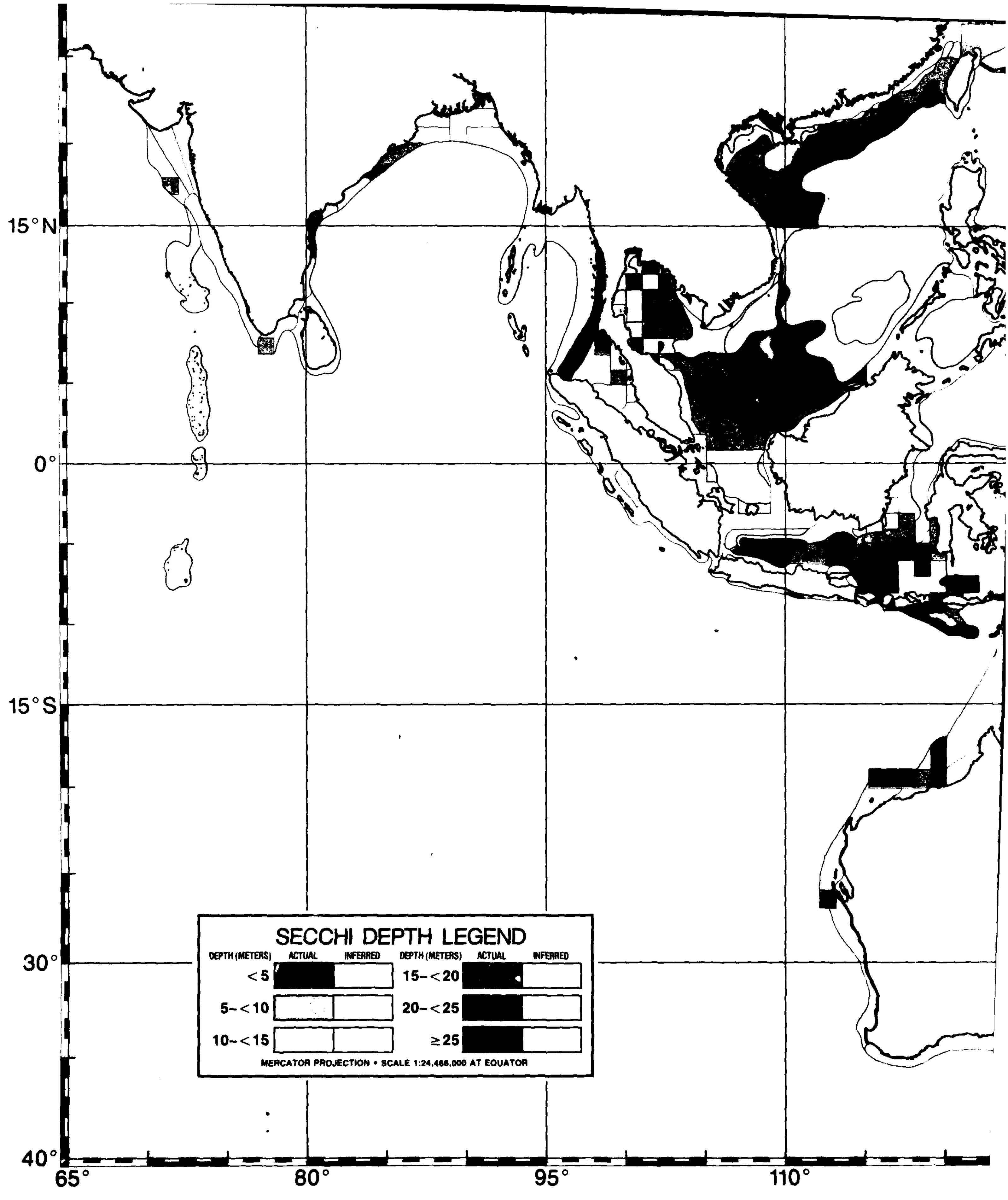

PLATE XIV OCTOBER—DECEMBER

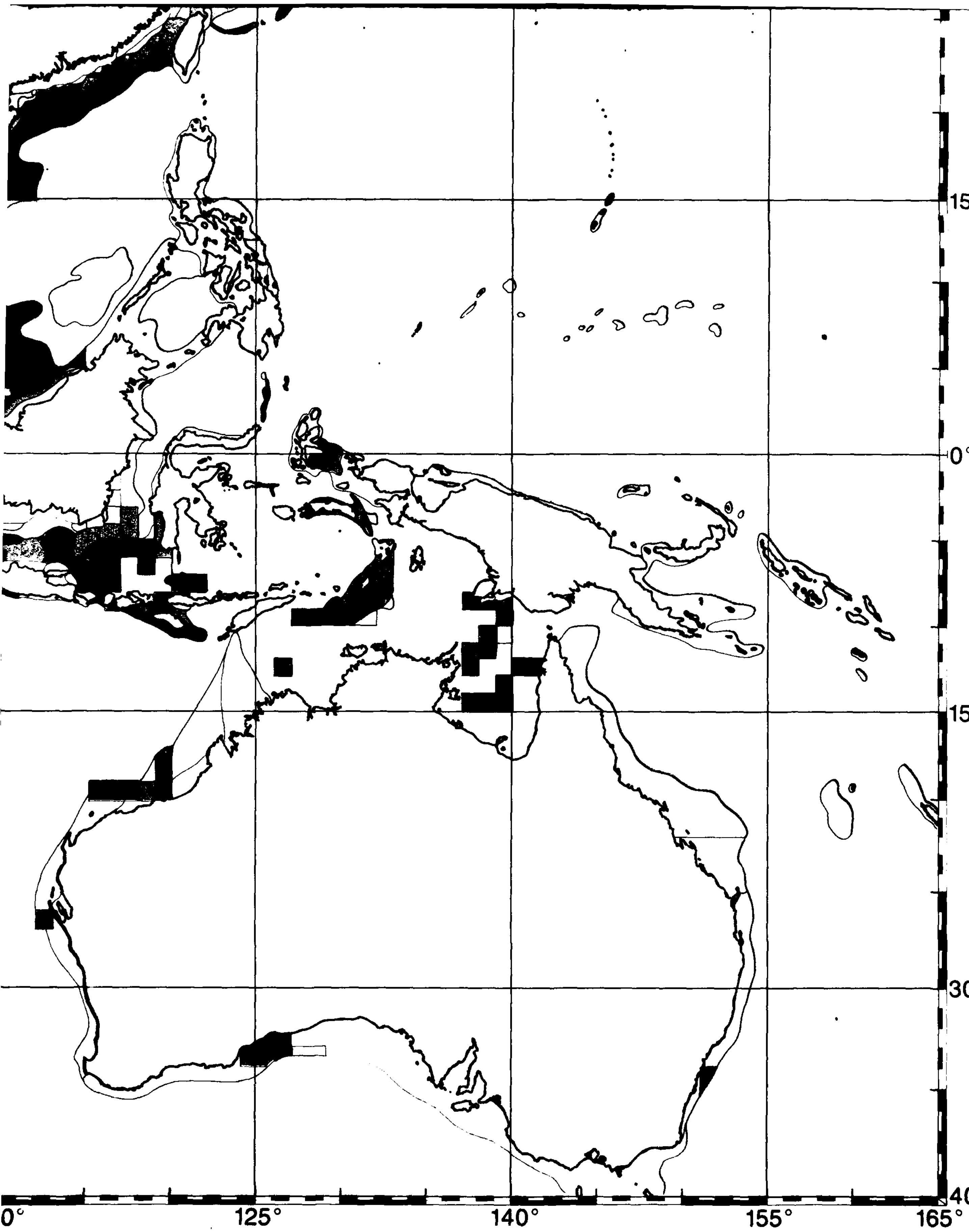

Compiled by: R.A. Arnone, F.A. Hilder, S.P. Tucker
Prepared for the Defense Mapping Agency by
the Naval Ocean Research and Development Activity
Remote Sensing Branch, NSTL, Mississippi

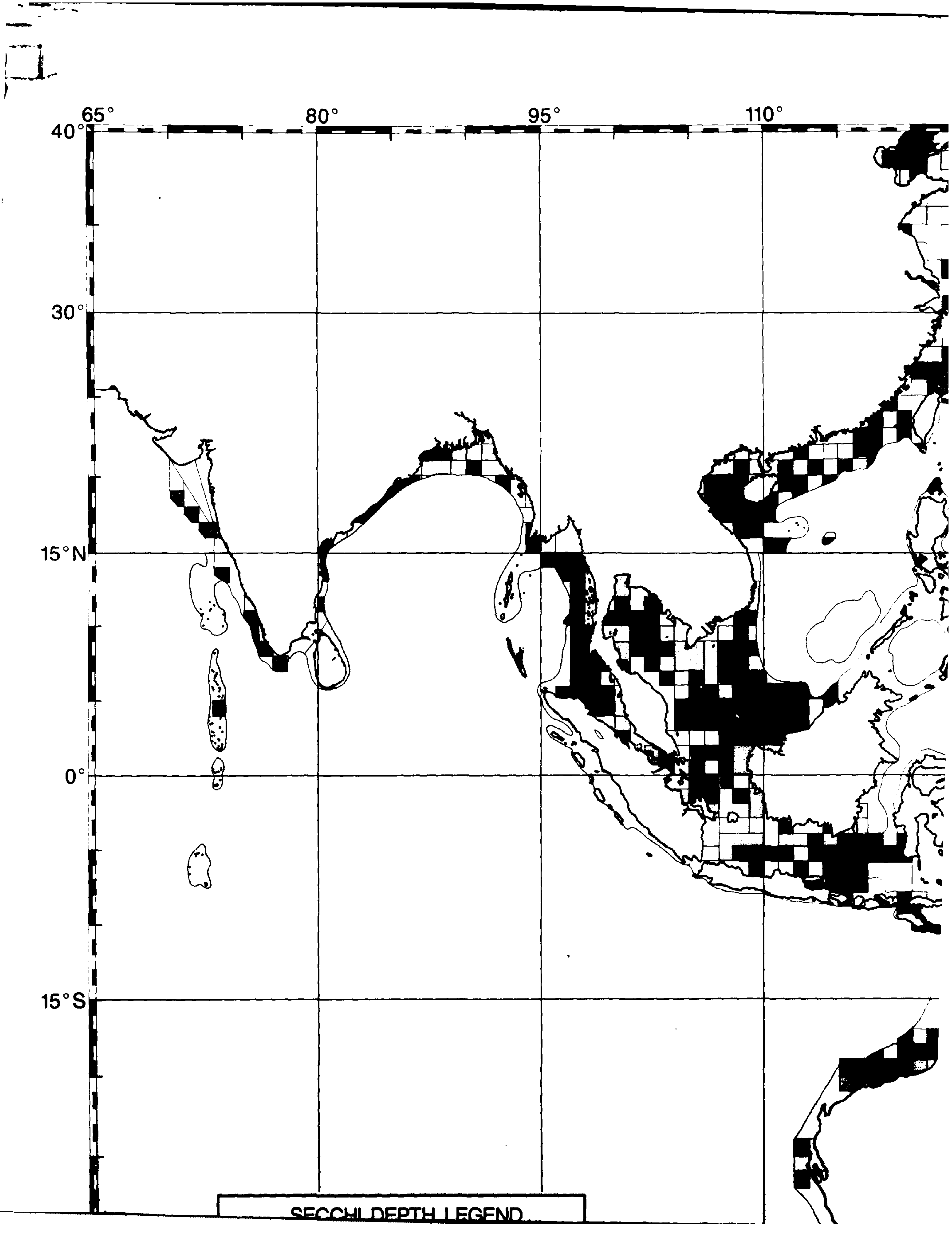
65°
80°
95°
110°
40°
30°
15°N
0°
15°S
SECCHI DEPTH LEGEND

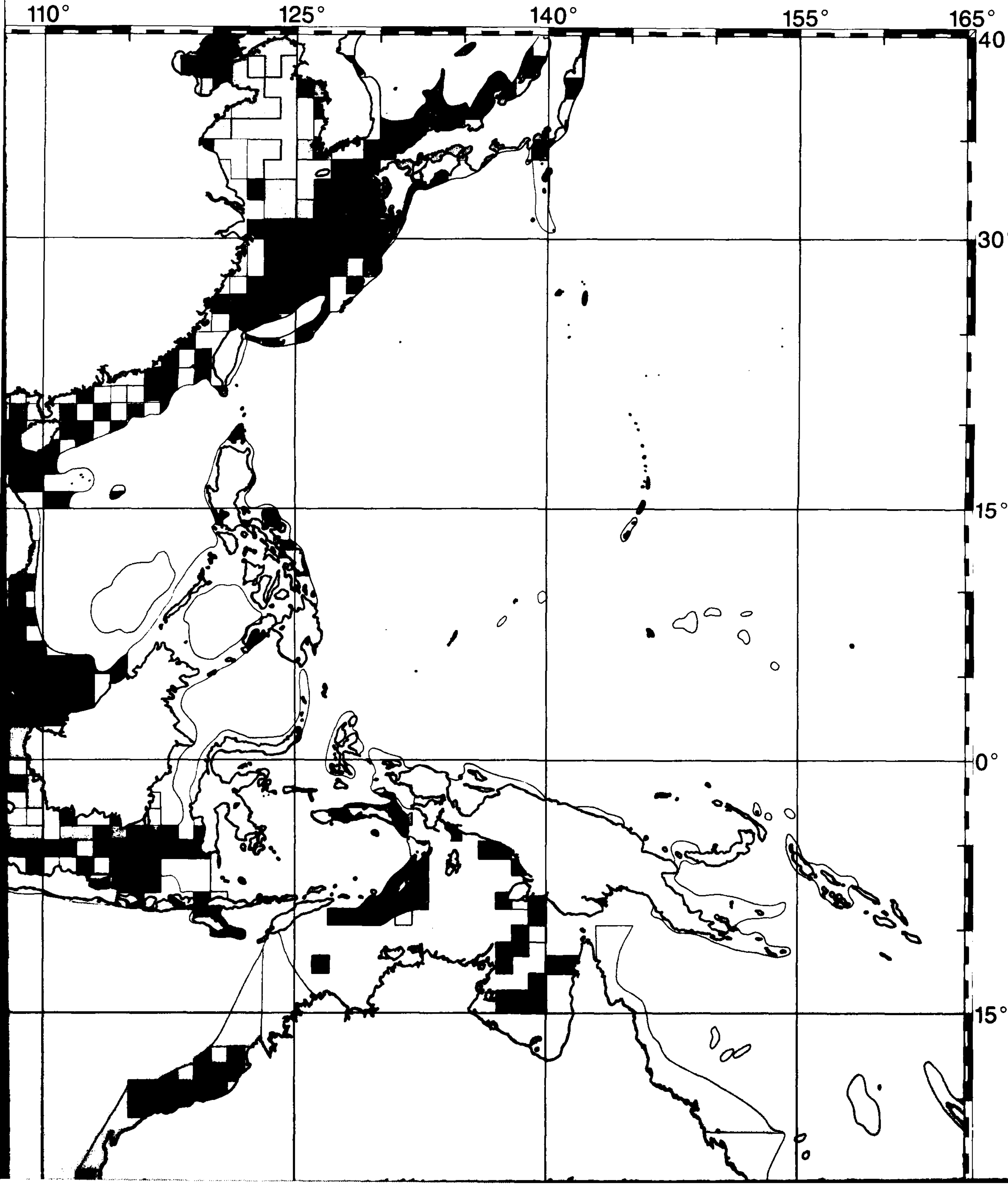

110°
125°
140°
155°
165°
40°
30°
15°N
0°
15°S

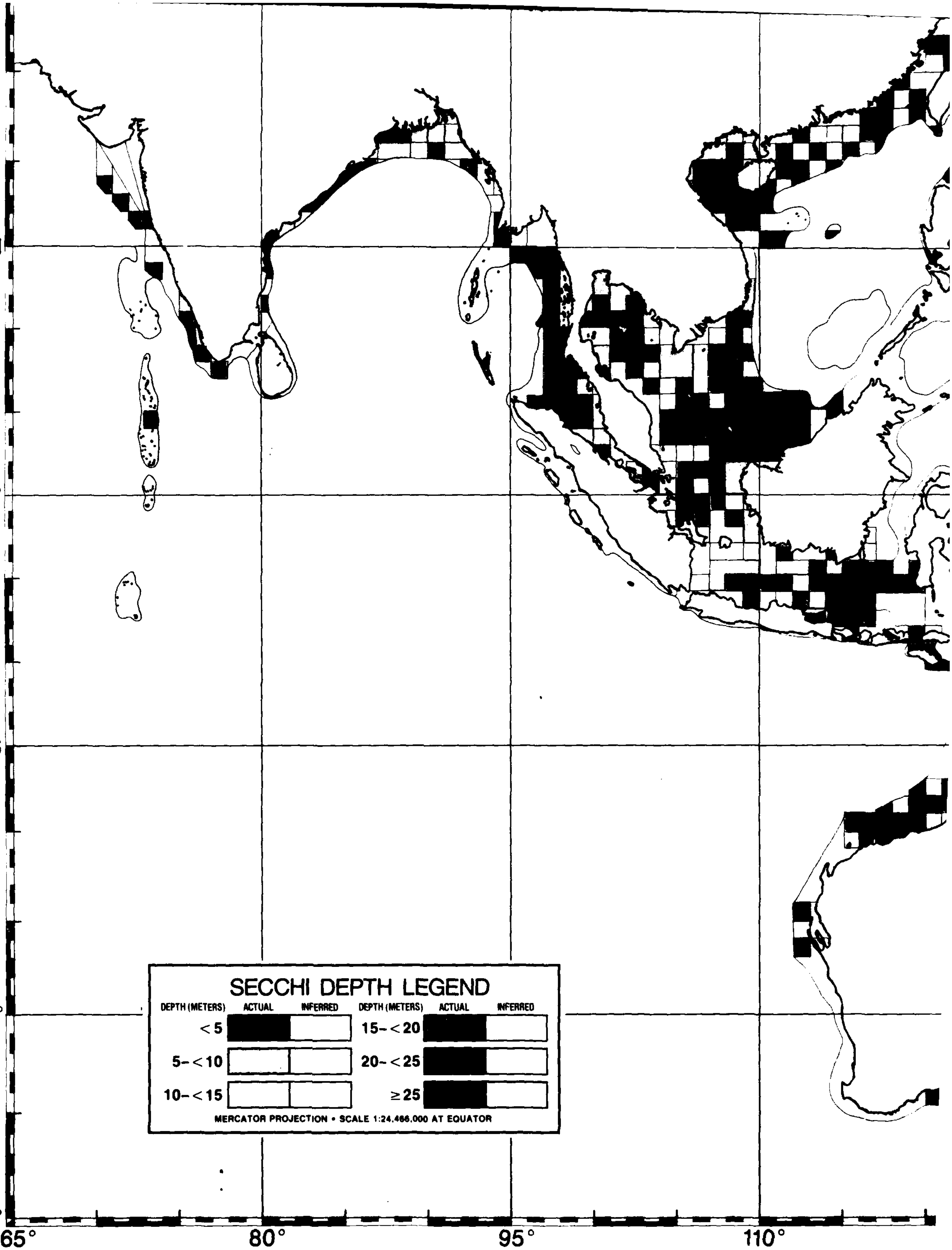

PLATE XV ANNUAL MEAN

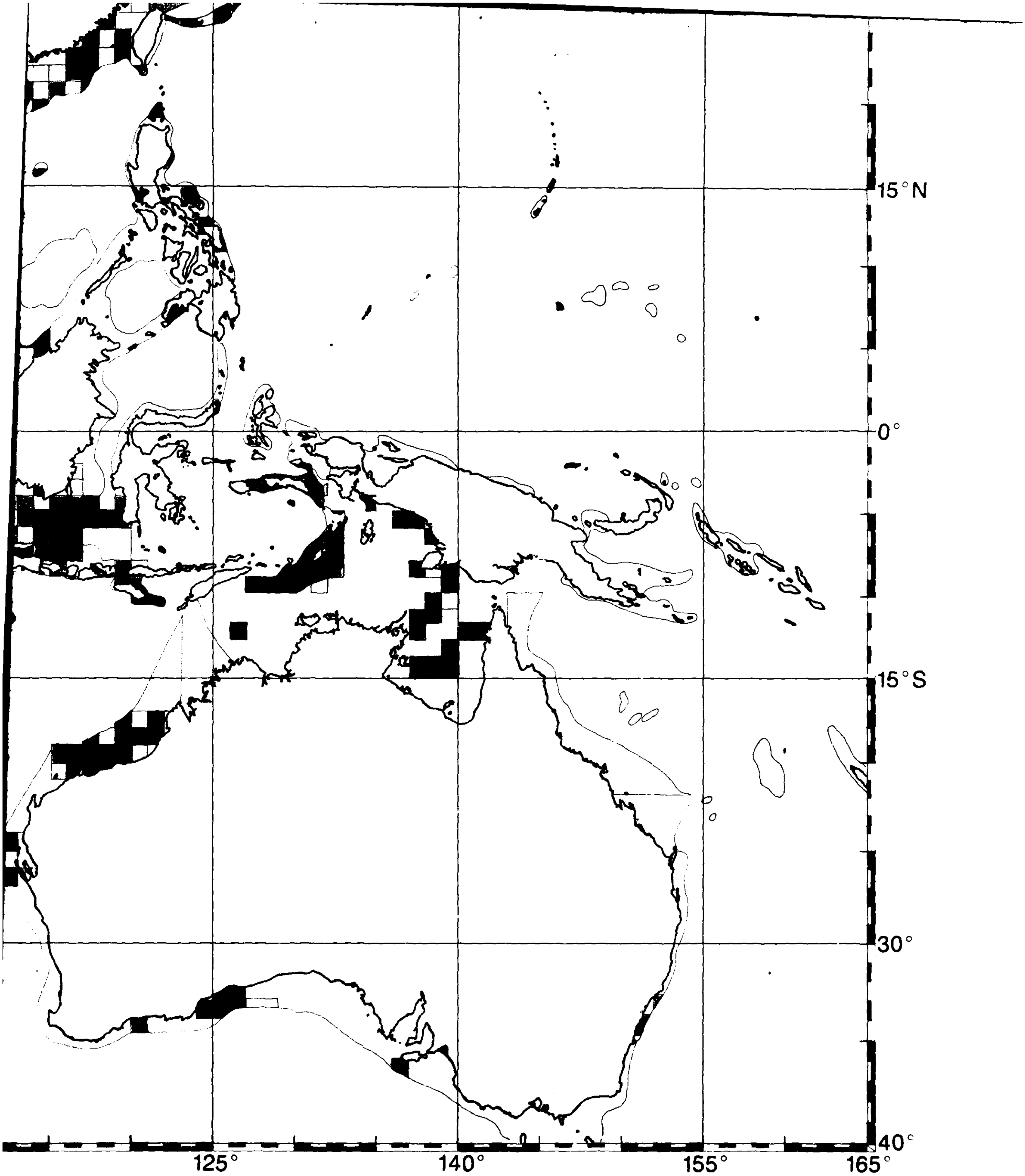

Compiled by: R.A. Arnone, F.A. Hilder, S.P. Tucker
Prepared for the Defense Mapping Agency by
the Naval Ocean Research and Development Activity
Remote Sensing Branch, NSTL, Mississippi

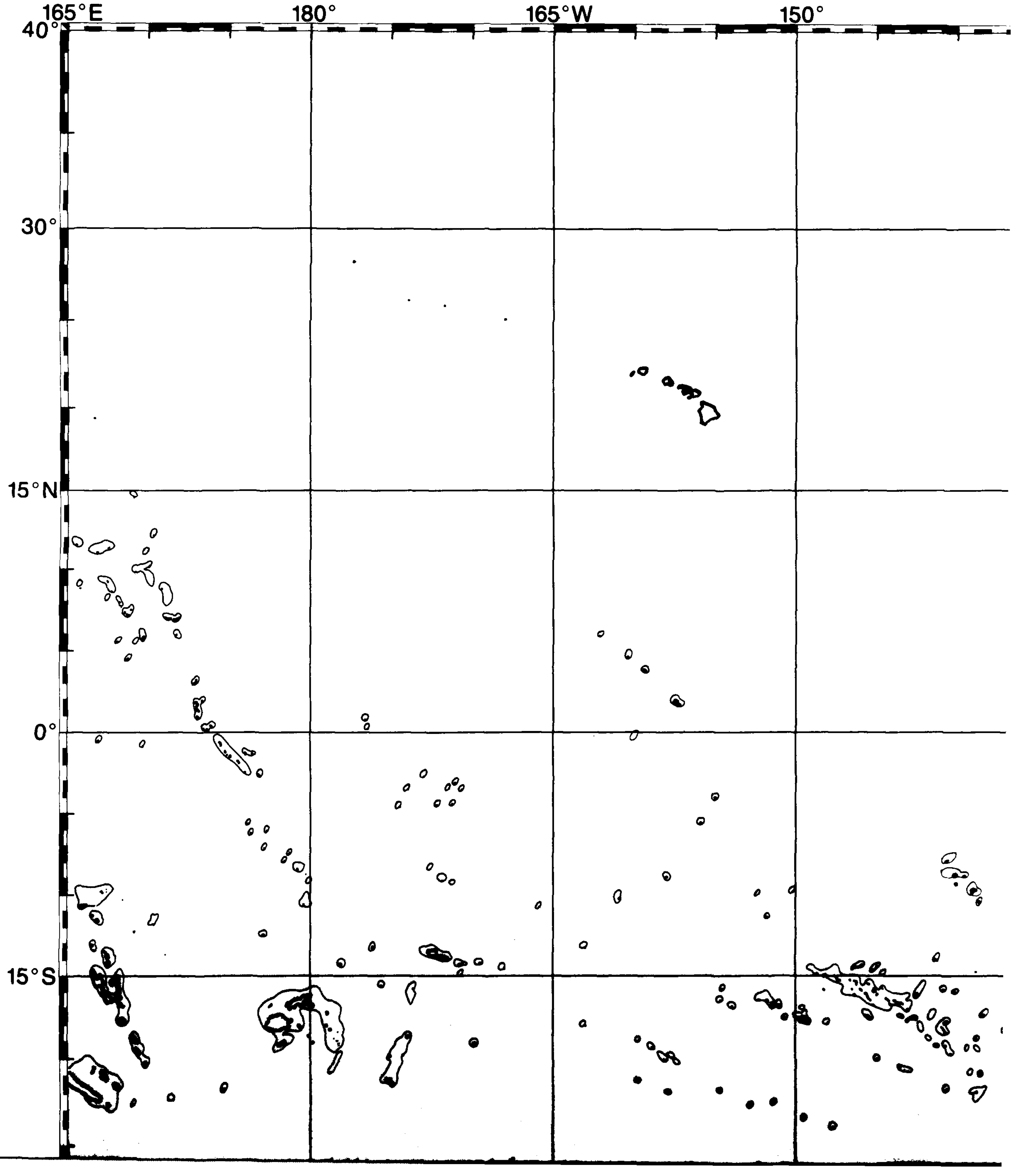
165°E
180°
165°W
150°
40°
30°
15°N
0°
15°S

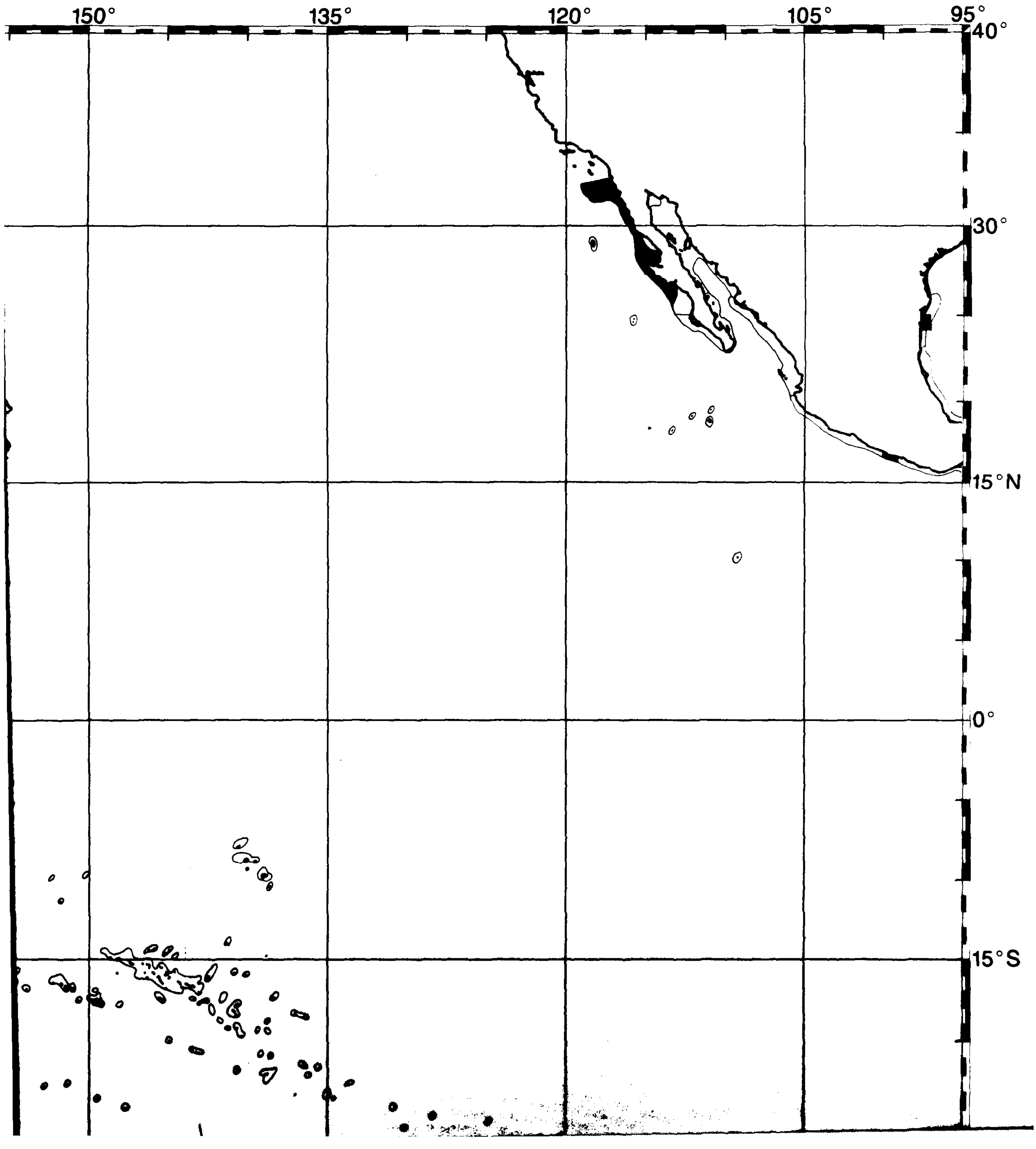
150°
135°
120°
105°
95°
40°
30°
15°N
0°
15°S

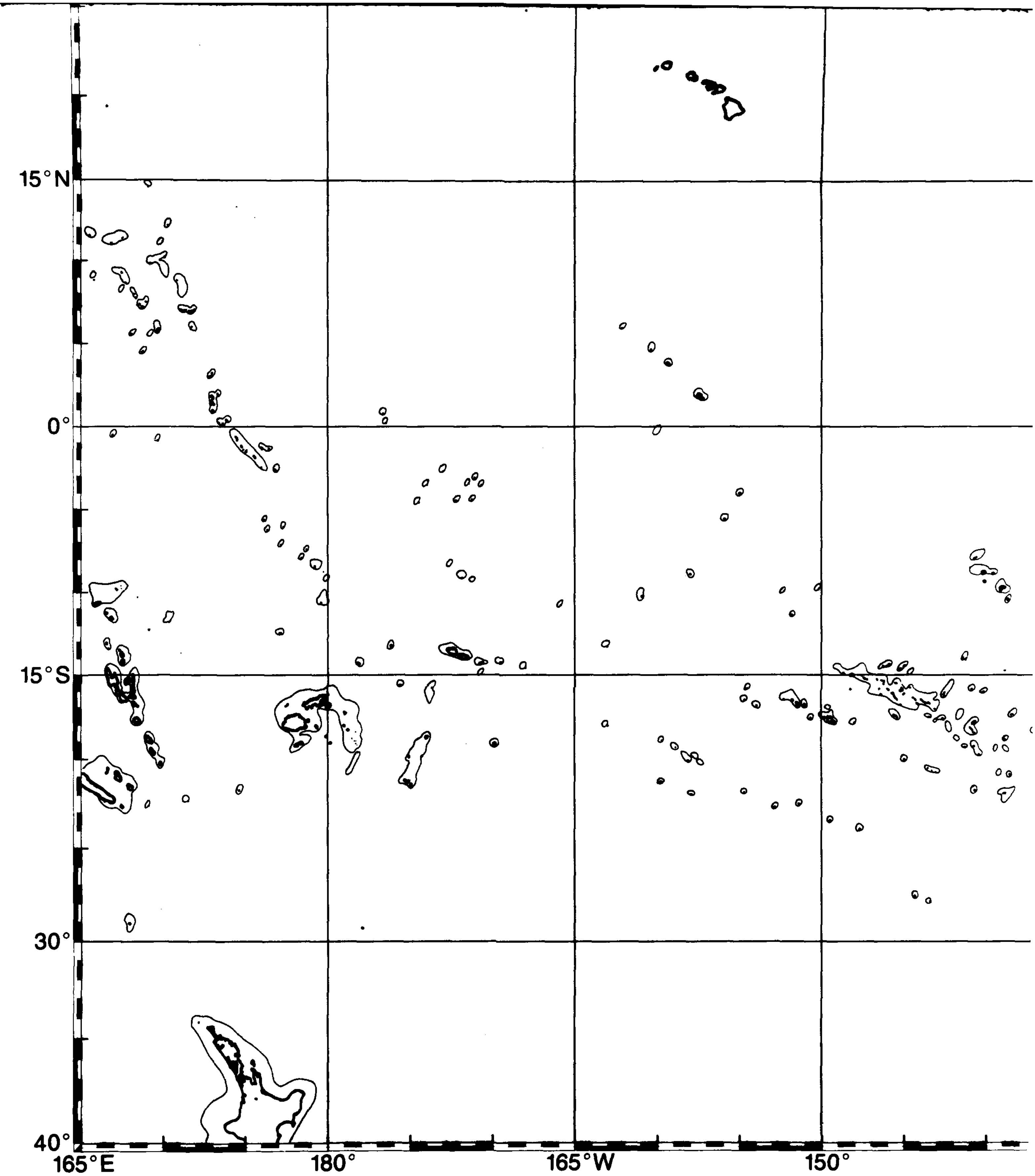

PLATE XVI JANUARY—MARCH

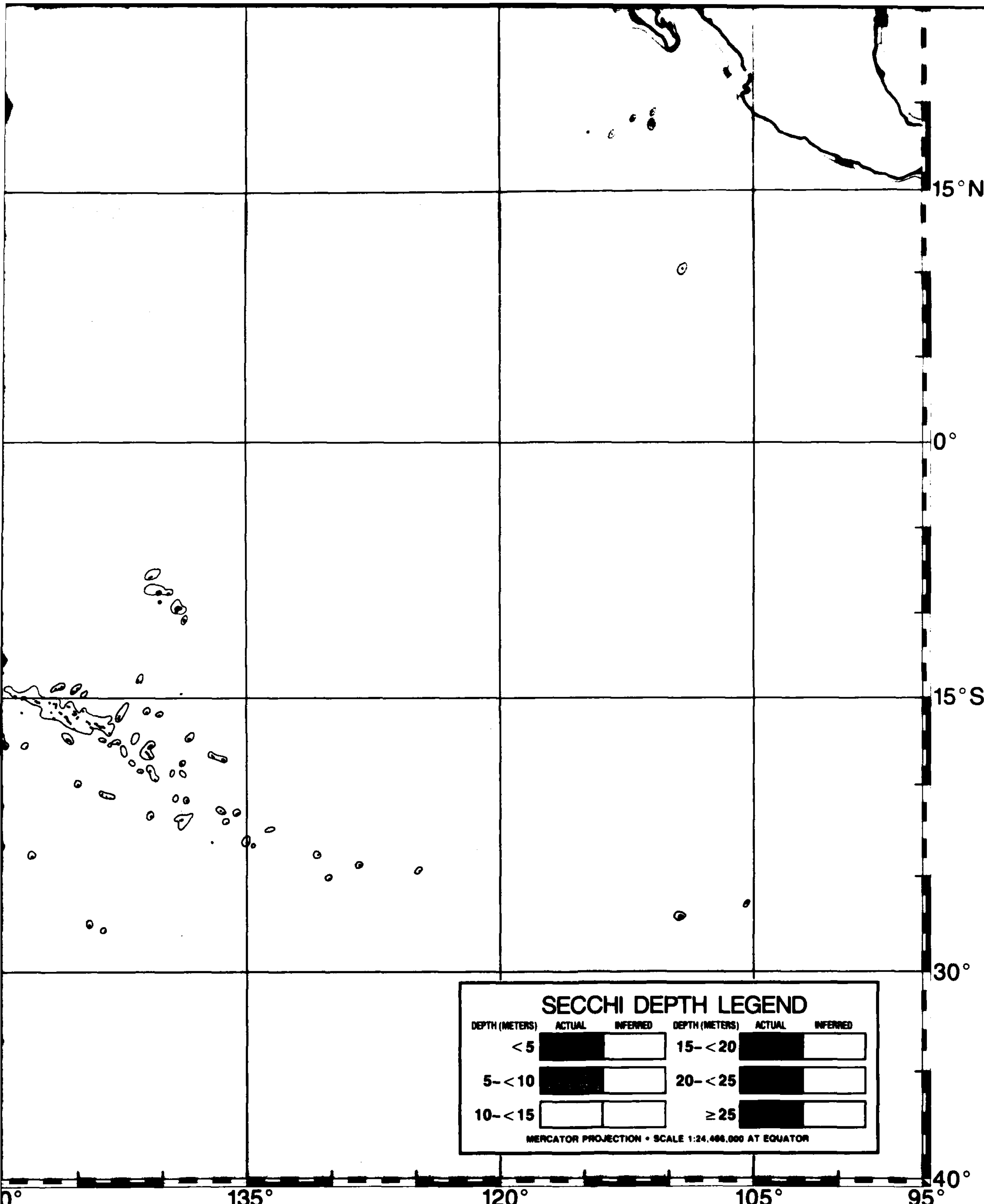

Compiled by: R.A. Arnone, F.A. Hilder, S.P. Tucker
Prepared for the Defense Mapping Agency by
the Naval Ocean Research and Development Activity
Remote Sensing Branch, NSTL, Mississippi

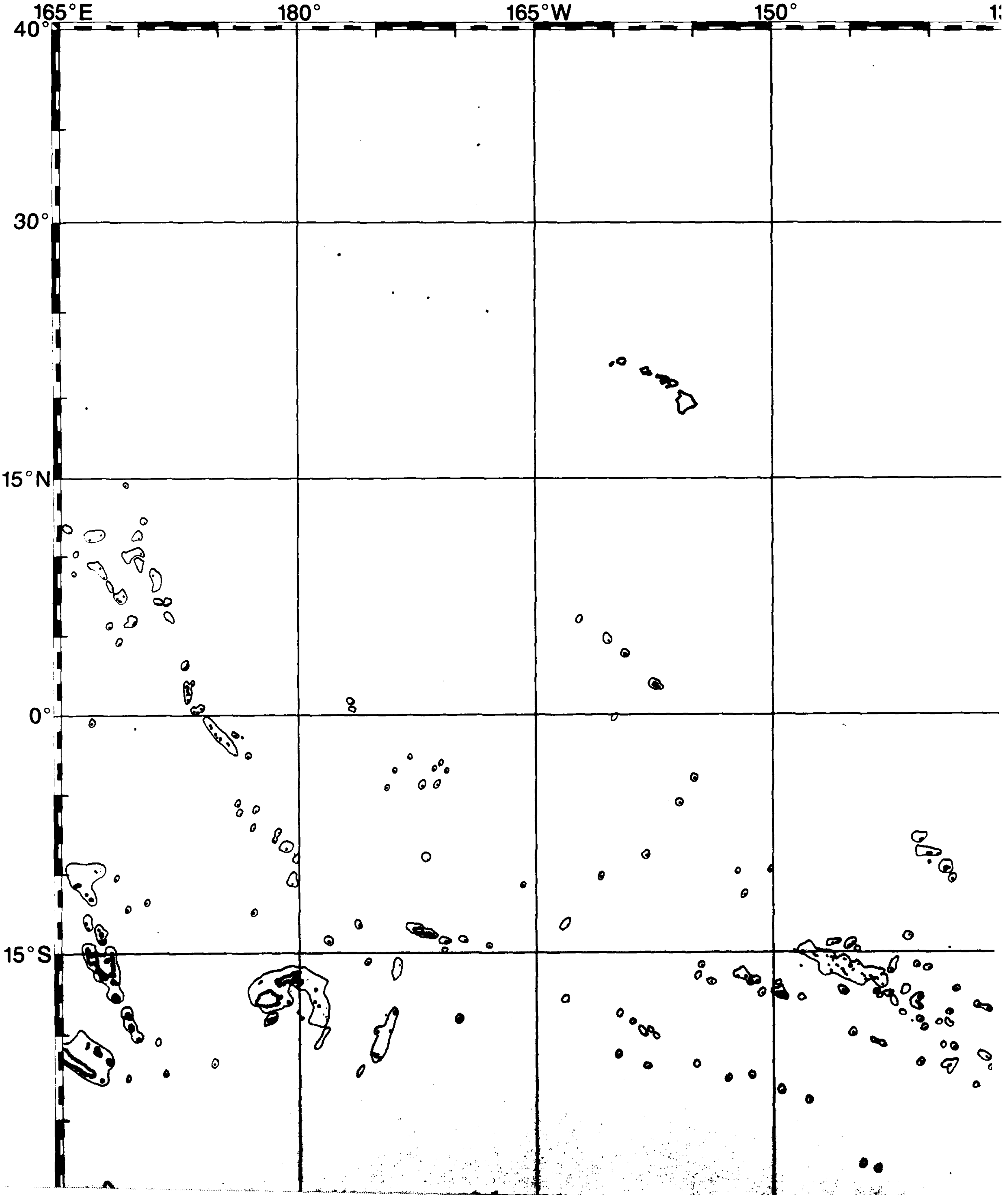
165°E
180°
165°W
150°
40°
30°
15°N
0°
15°S

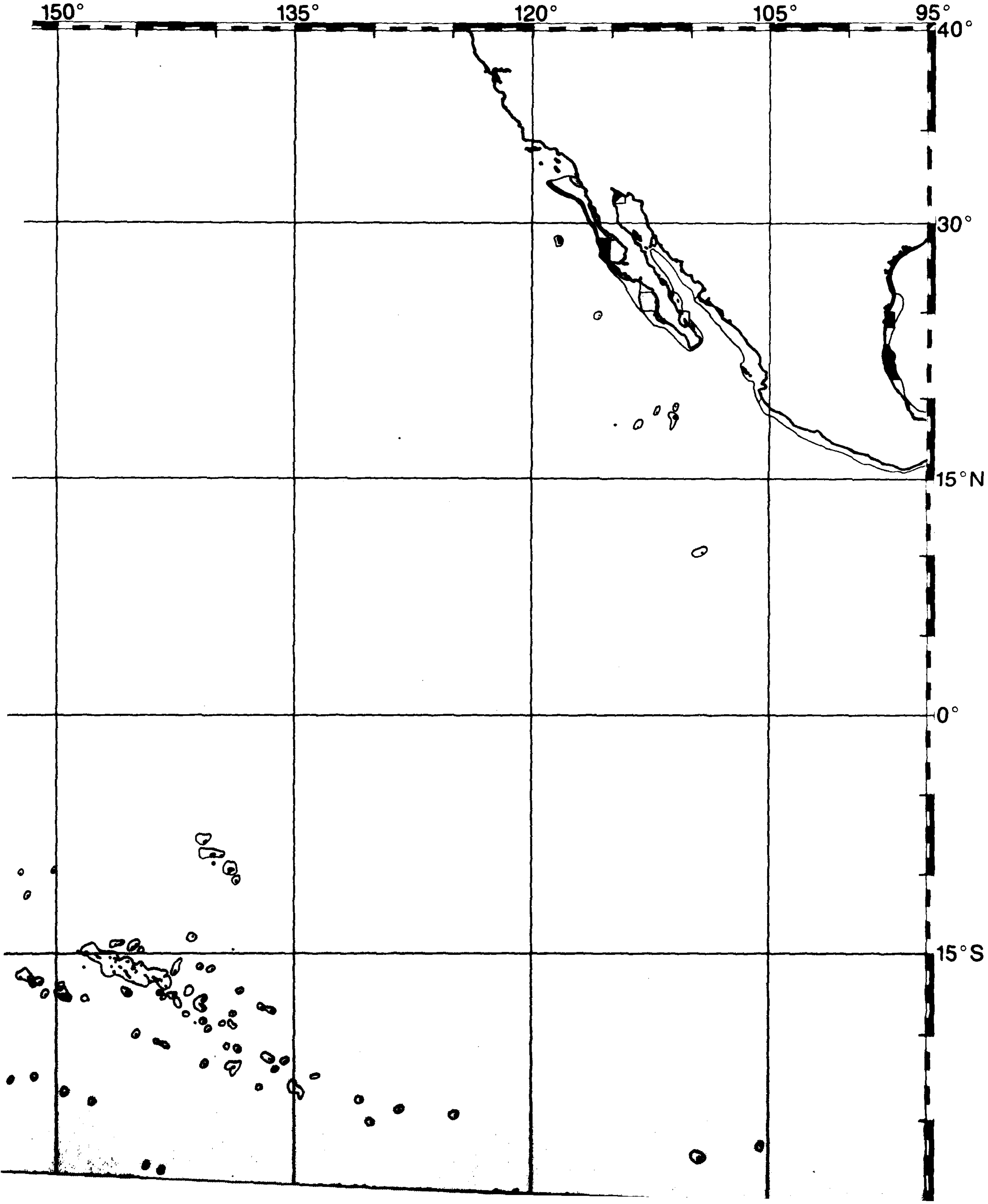
150°
135°
120°
105°
95°
40°
30°
15°N
0°
15°S

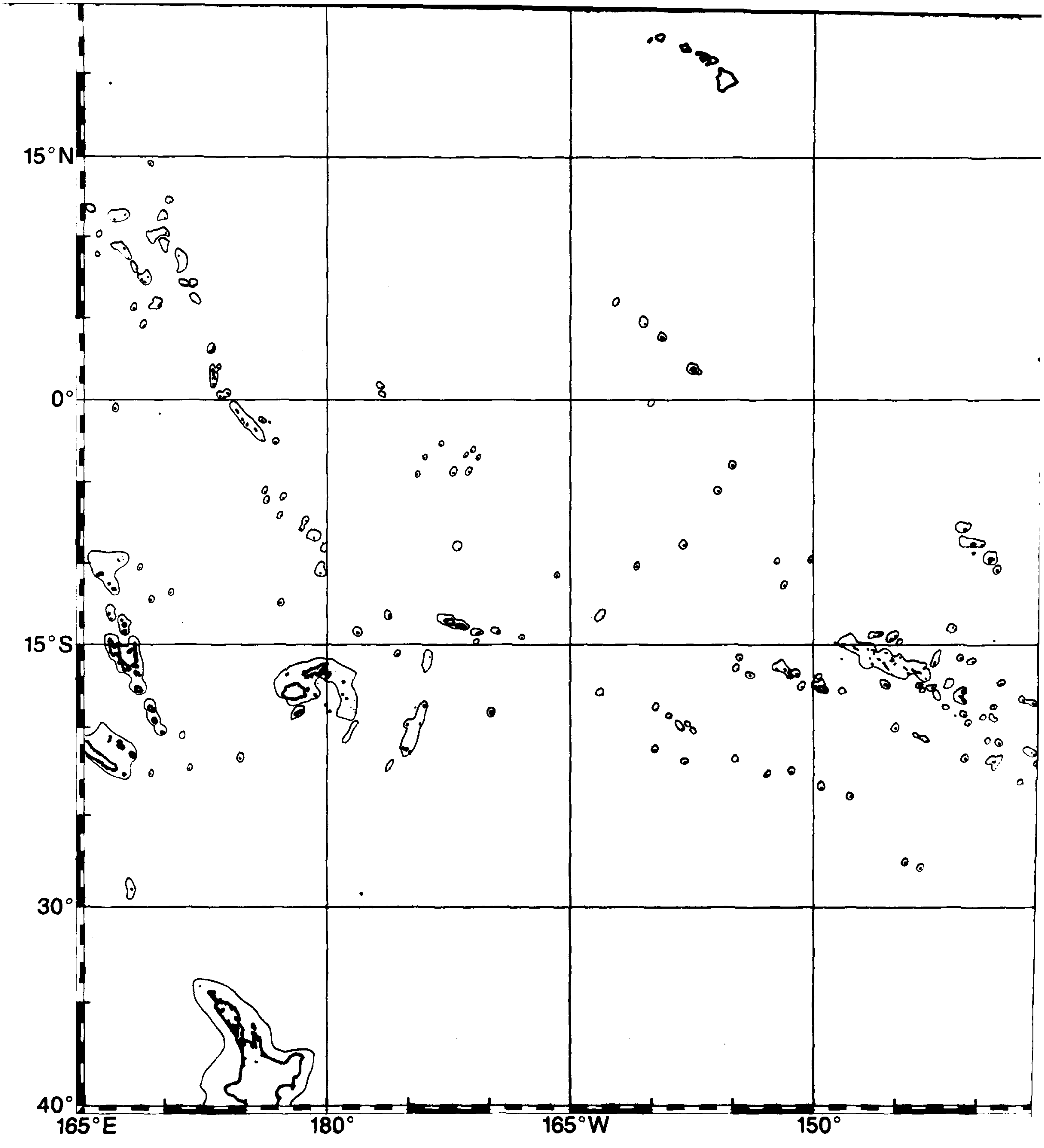

PLATE XVII APRIL—JUNE

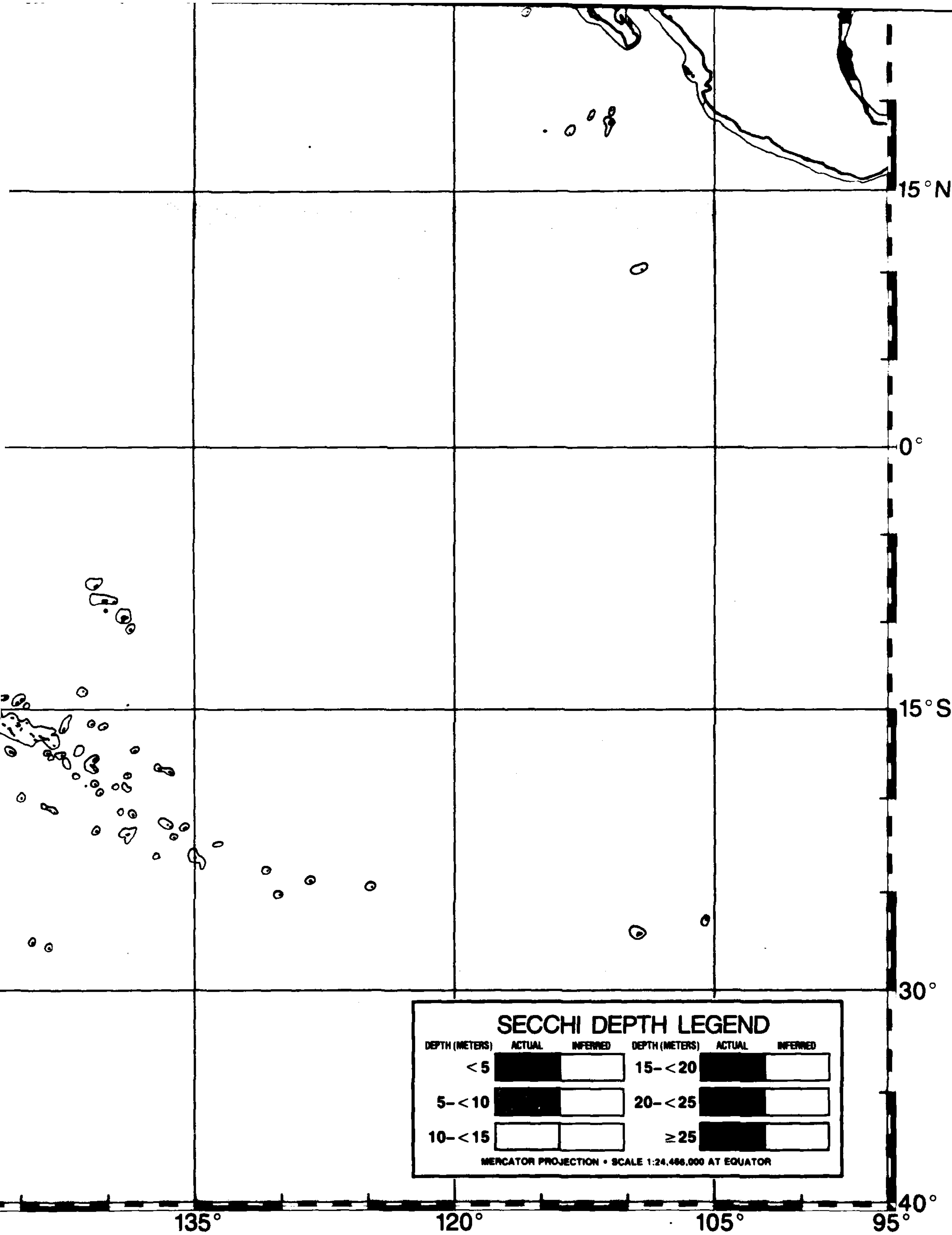

Compiled by: R.A. Arnone, F.A. Hilder, S.P. Tucker
Prepared for the Defense Mapping Agency by
the Naval Ocean Research and Development Activity
Remote Sensing Branch, NSTL, Mississippi

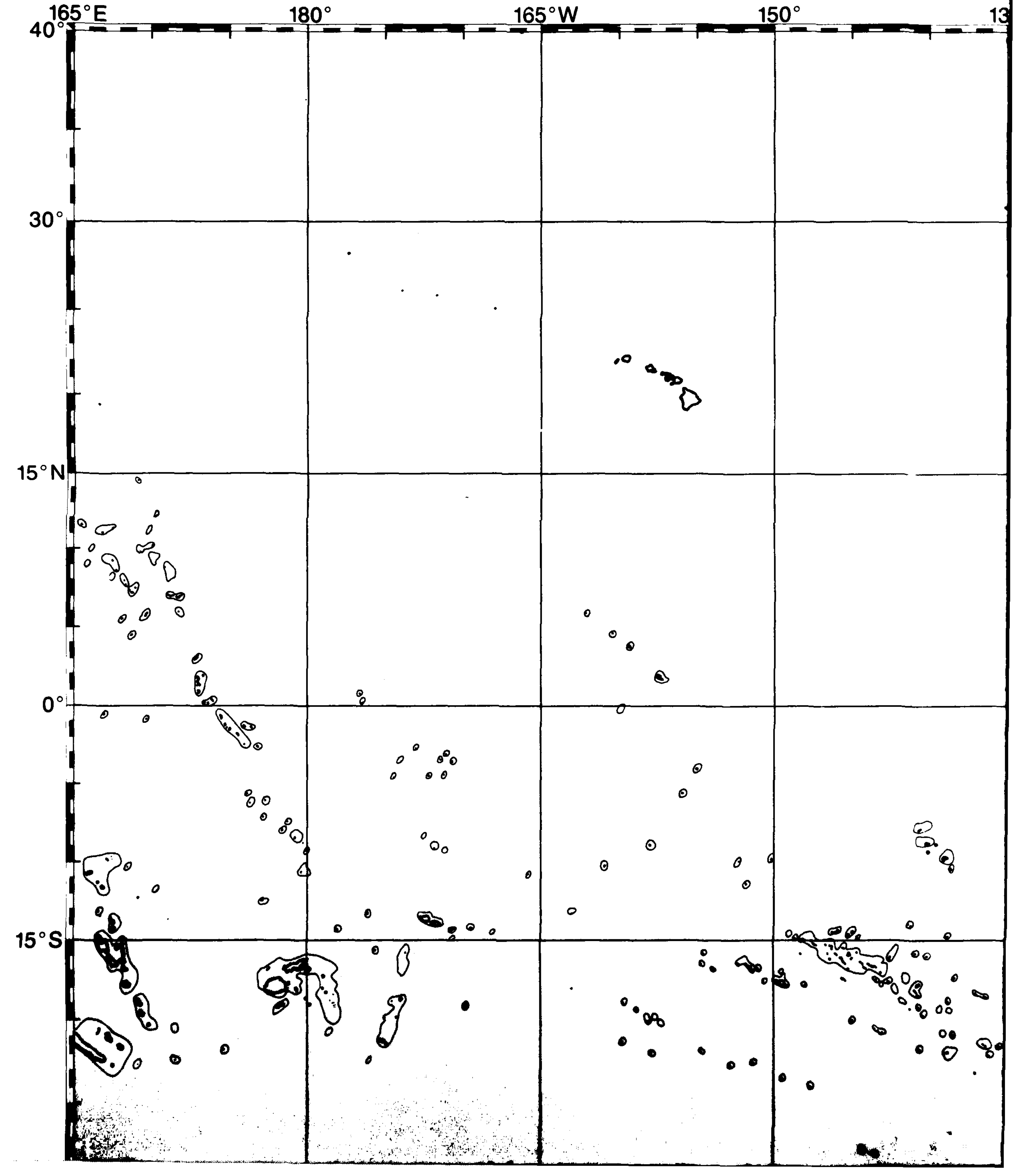
165°E
180°
165°W
150°
13
40°
30°
15°N
0°
15°S

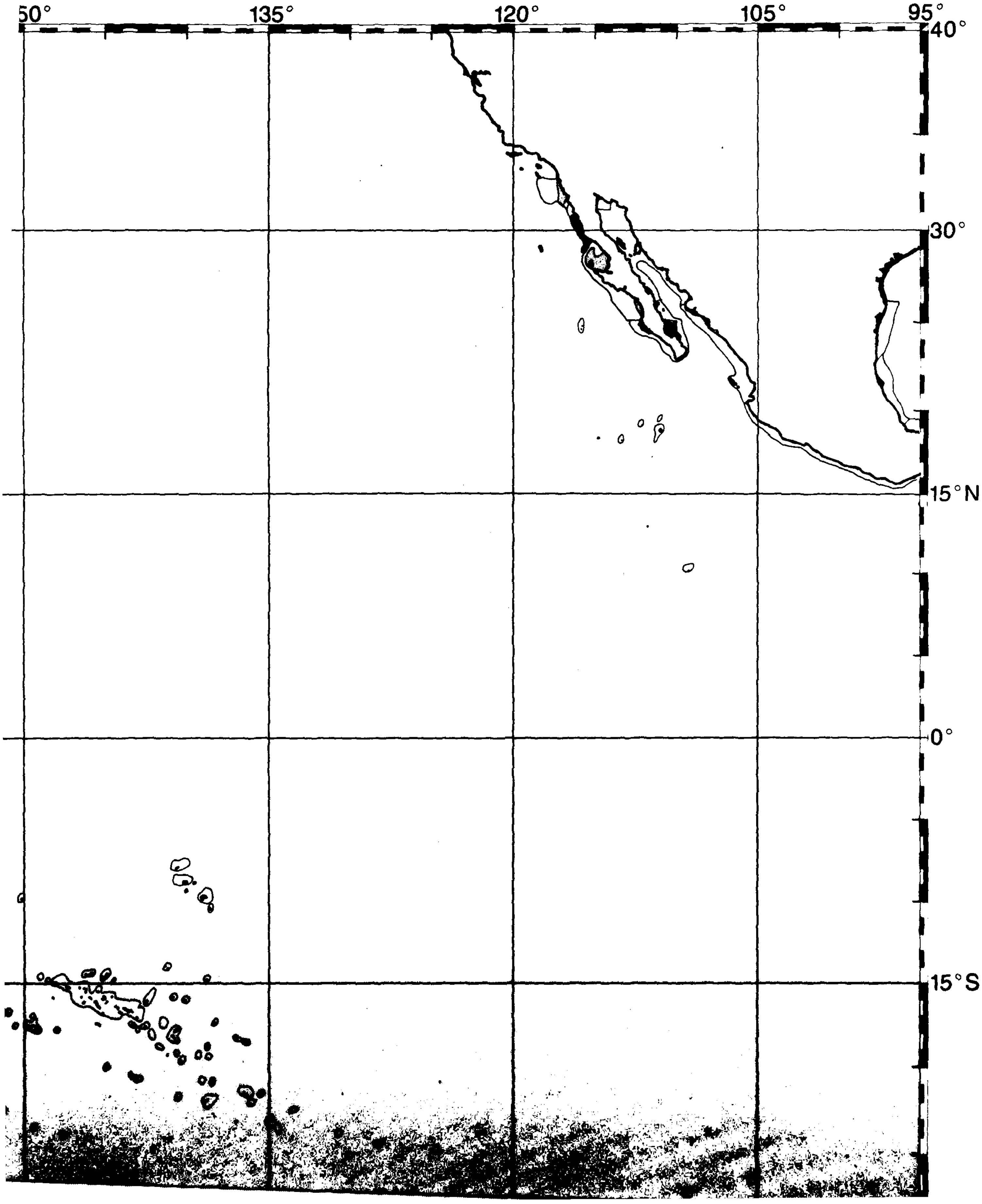

50°
135°
120°
105°
95°
40°
30°
15°N
0°
15°S

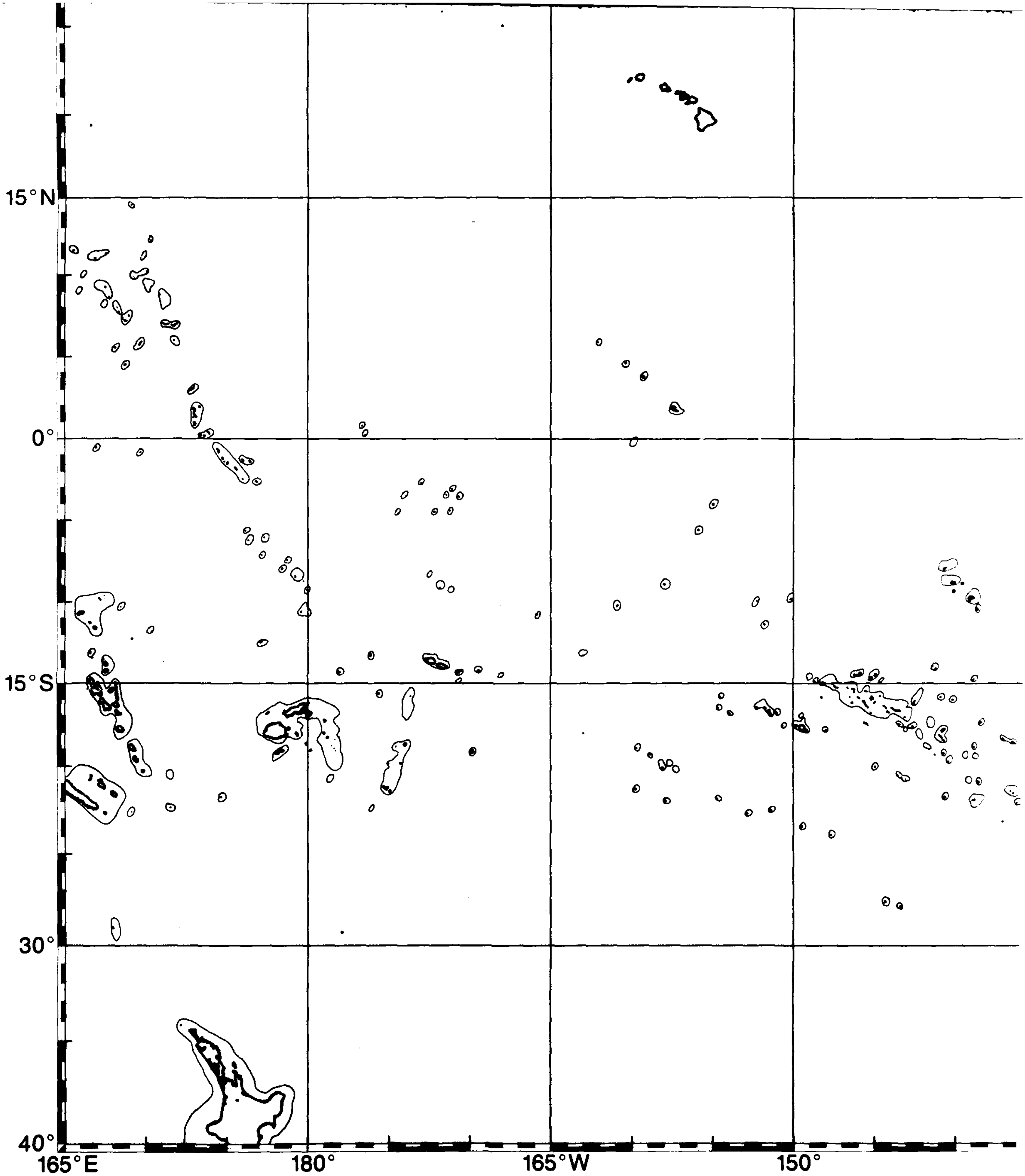

PLATE XVIII JULY—SEPTEMBER

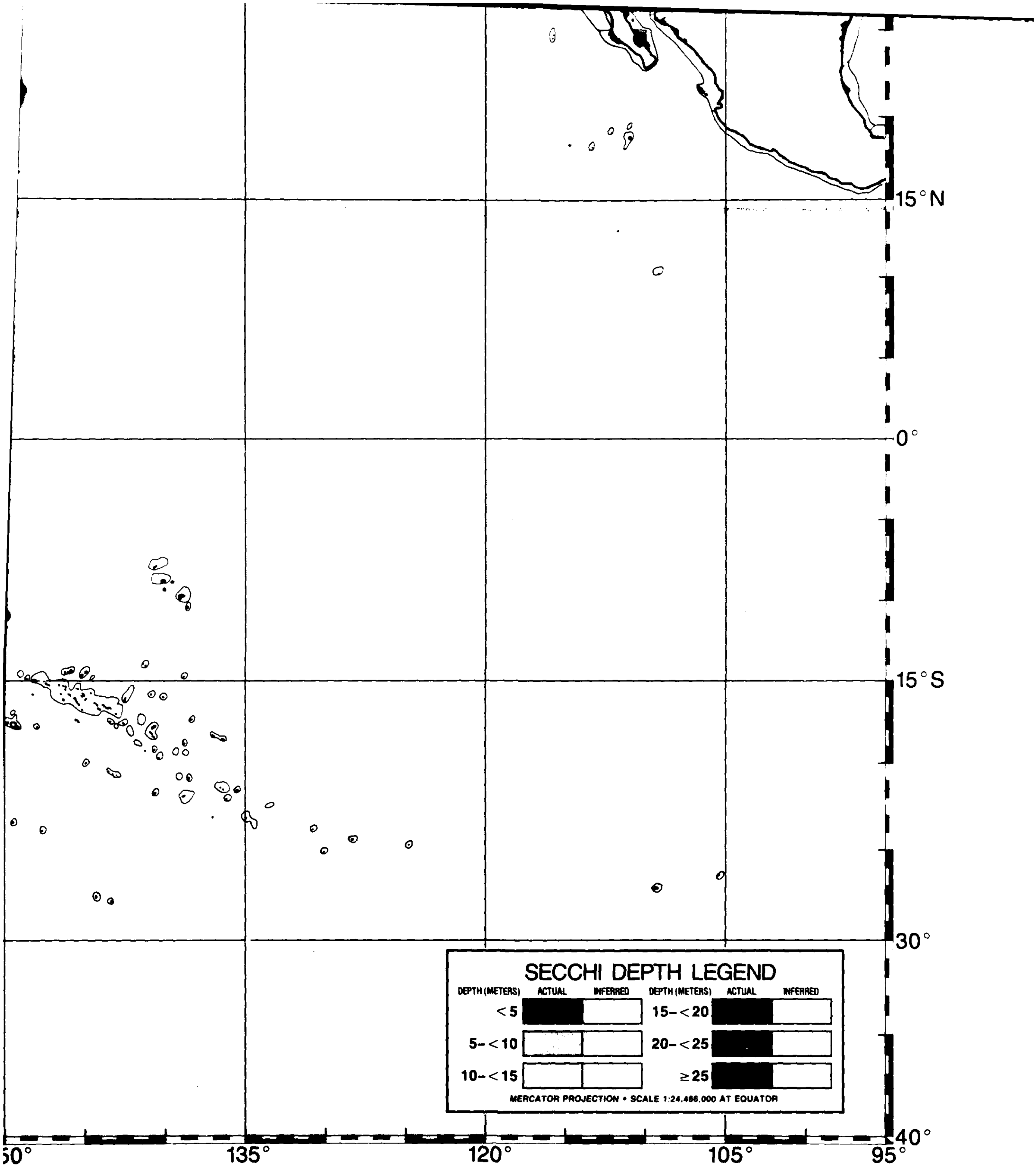

Compiled by: R.A. Arnone, F.A. Hilder, S.P. Tucker
Prepared for the Defense Mapping Agency by
the Naval Ocean Research and Development Activity
Remote Sensing Branch, NSTL, Mississippi

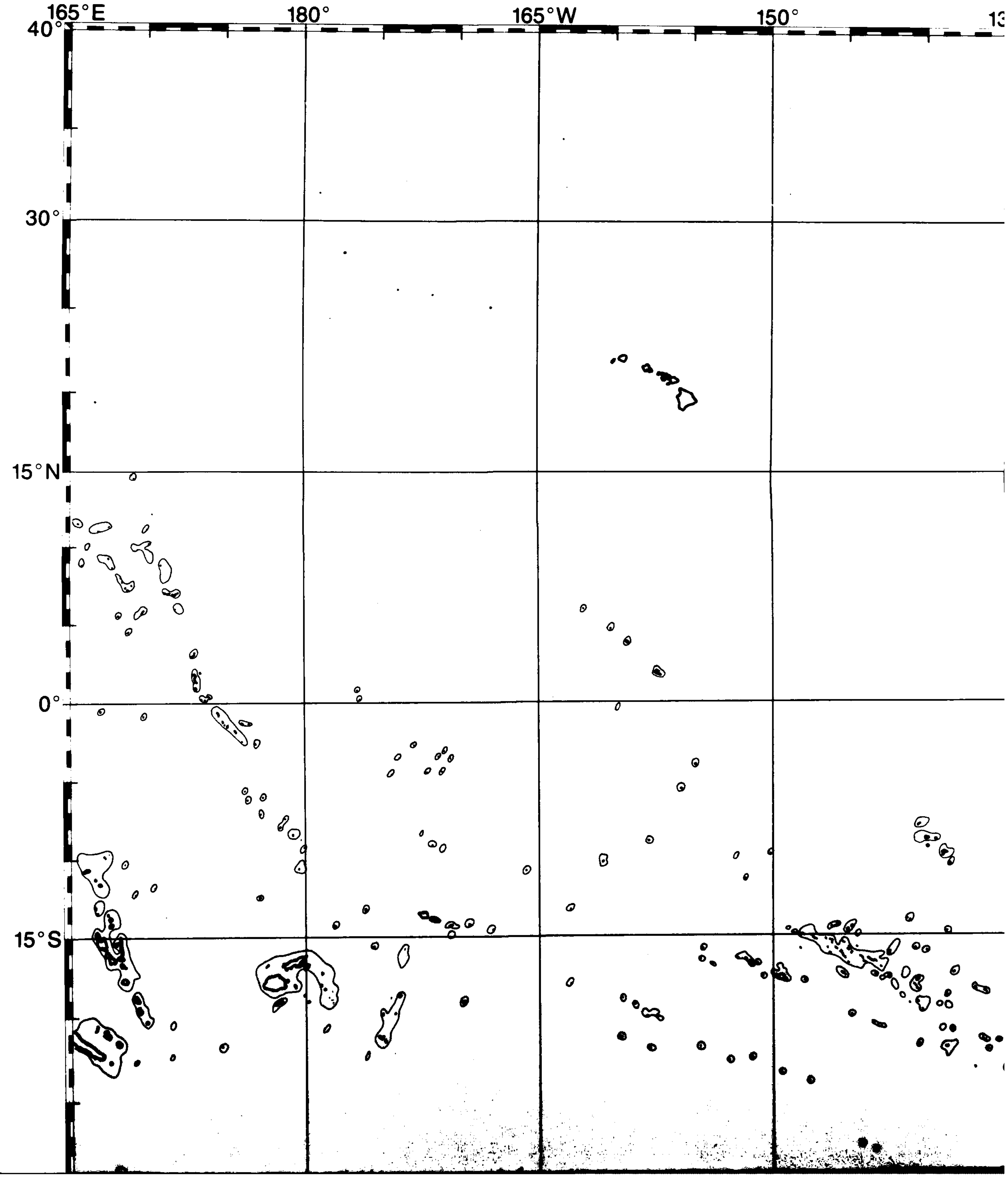

165°E
180°
165°W
150°
40°
30°
15°N
0°
15°S

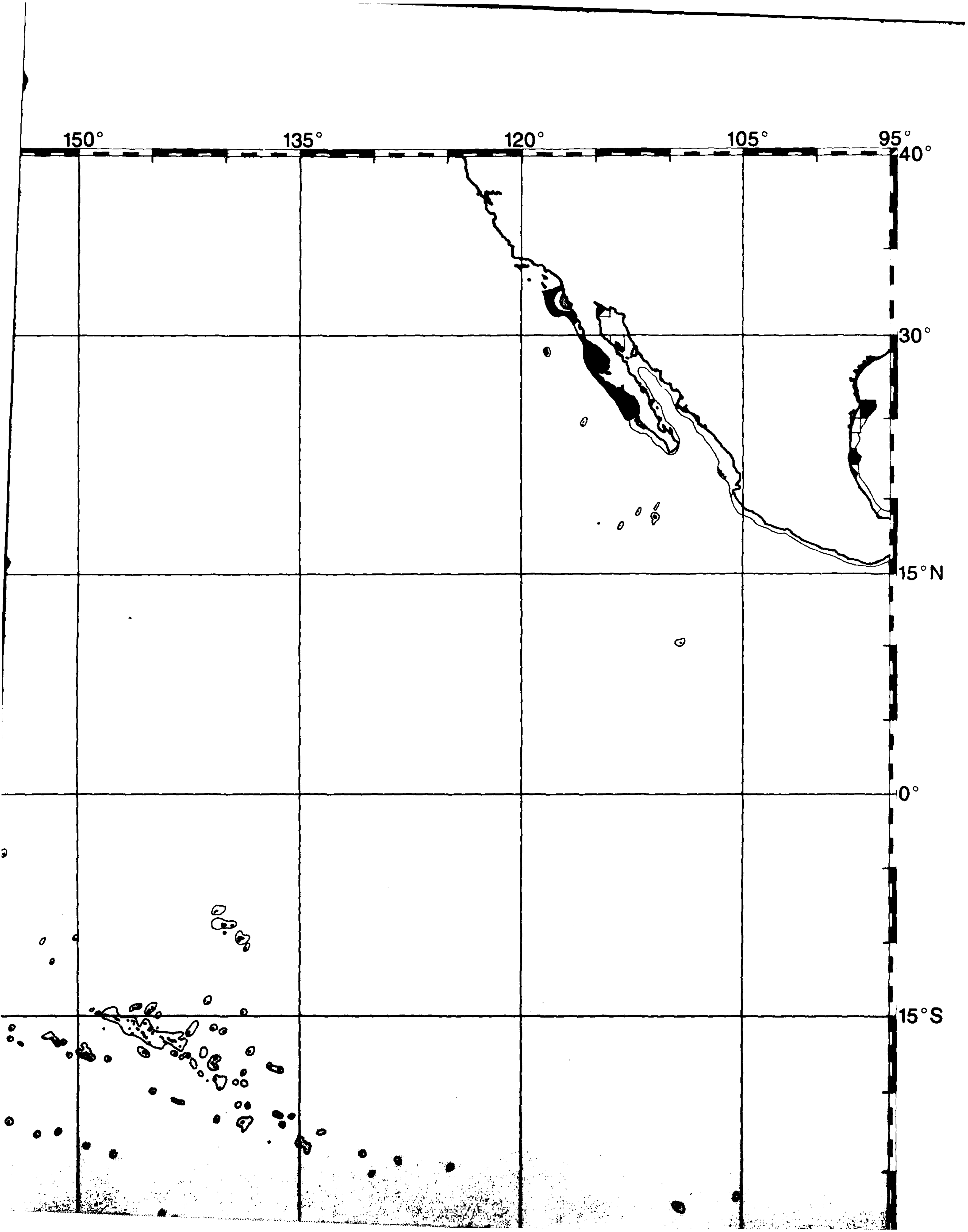
150°
135°
120°
105°
95°
40°
30°
15°N
0°
15°S

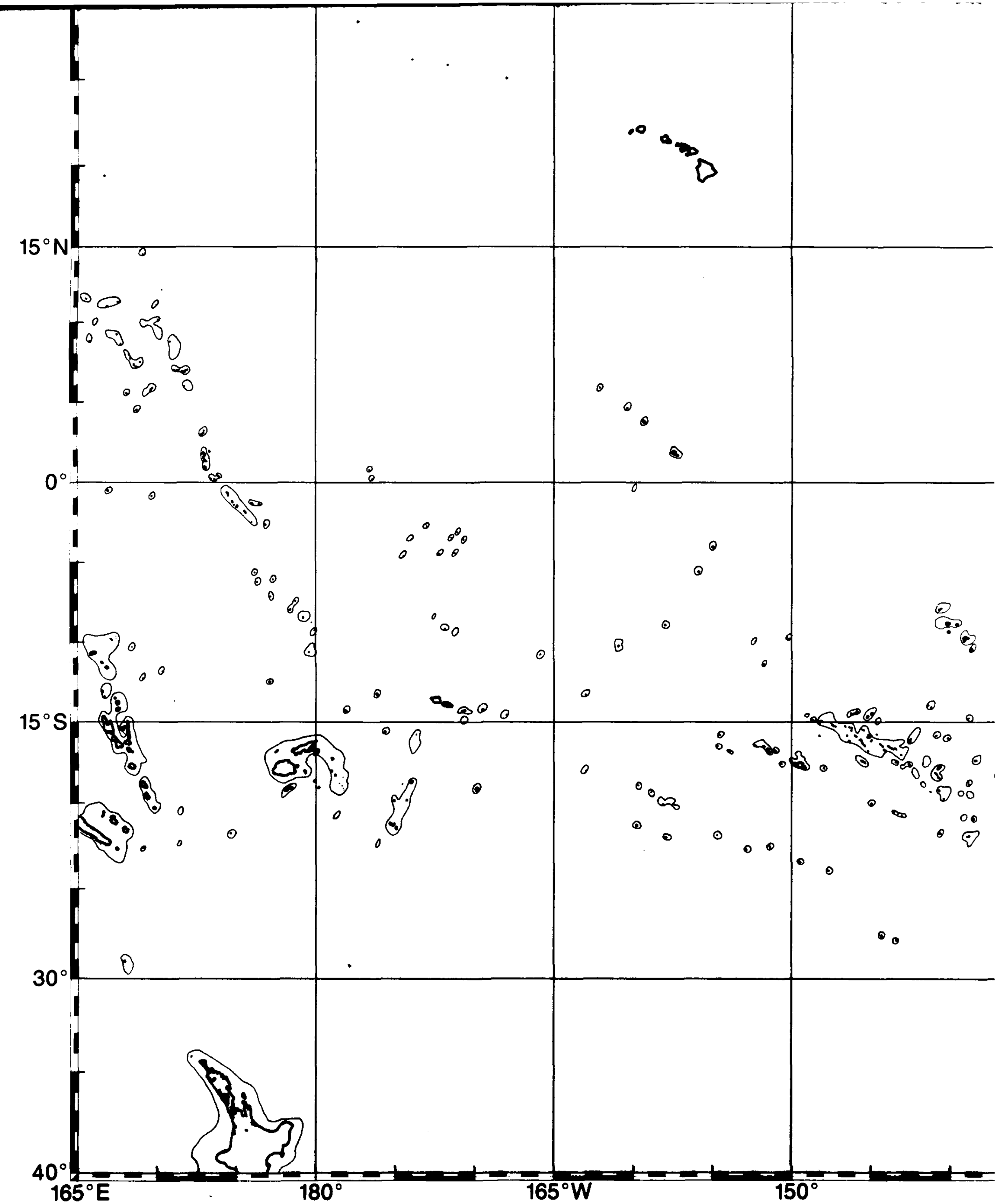

PLATE XIX OCTOBER—DECEMBER

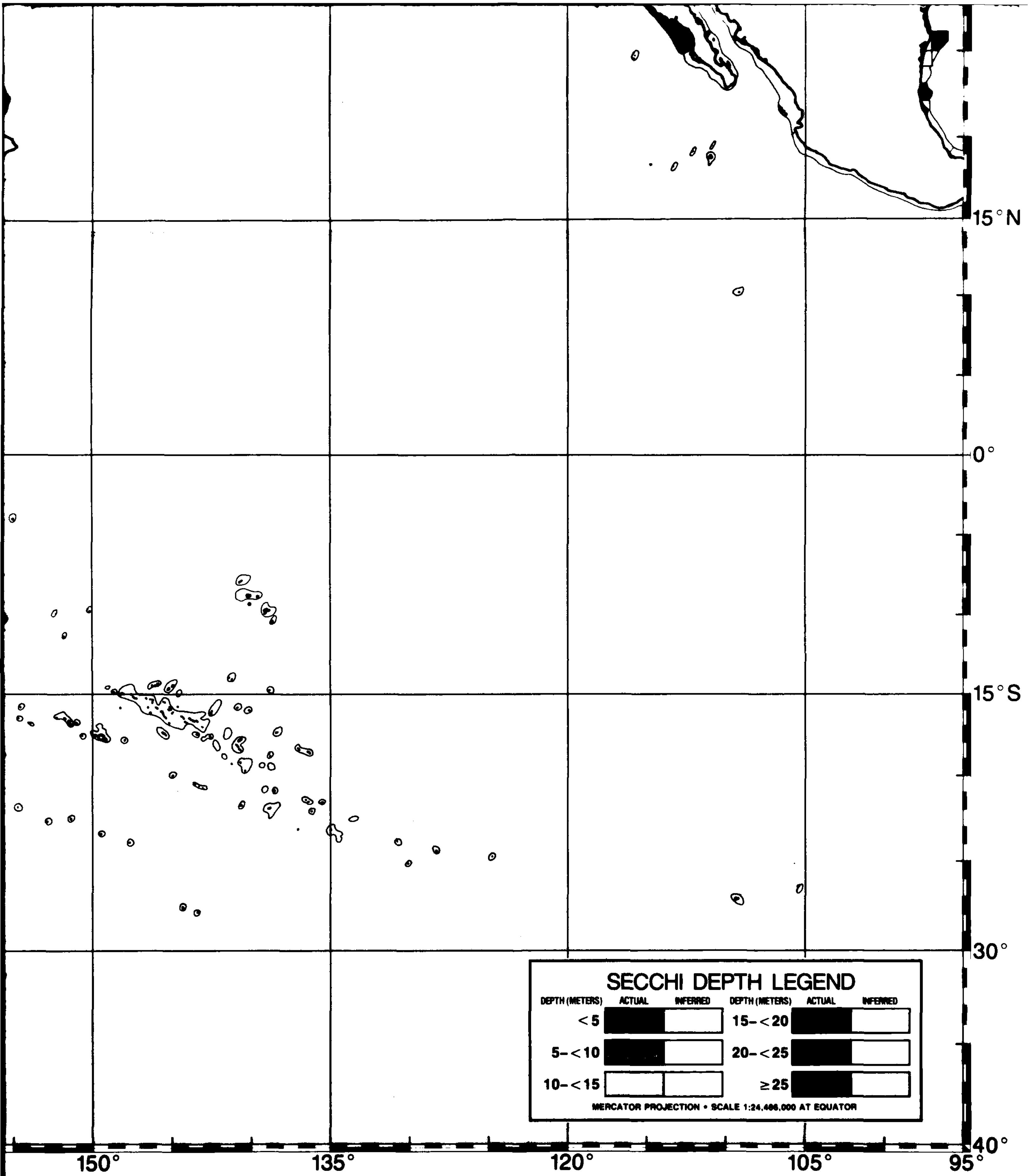

Compiled by: R.A. Arnone, F.A. Hilder, S.P. Tucker
Prepared for the Defense Mapping Agency by
the Naval Ocean Research and Development Activity
Remote Sensing Branch, NSTL, Mississippi

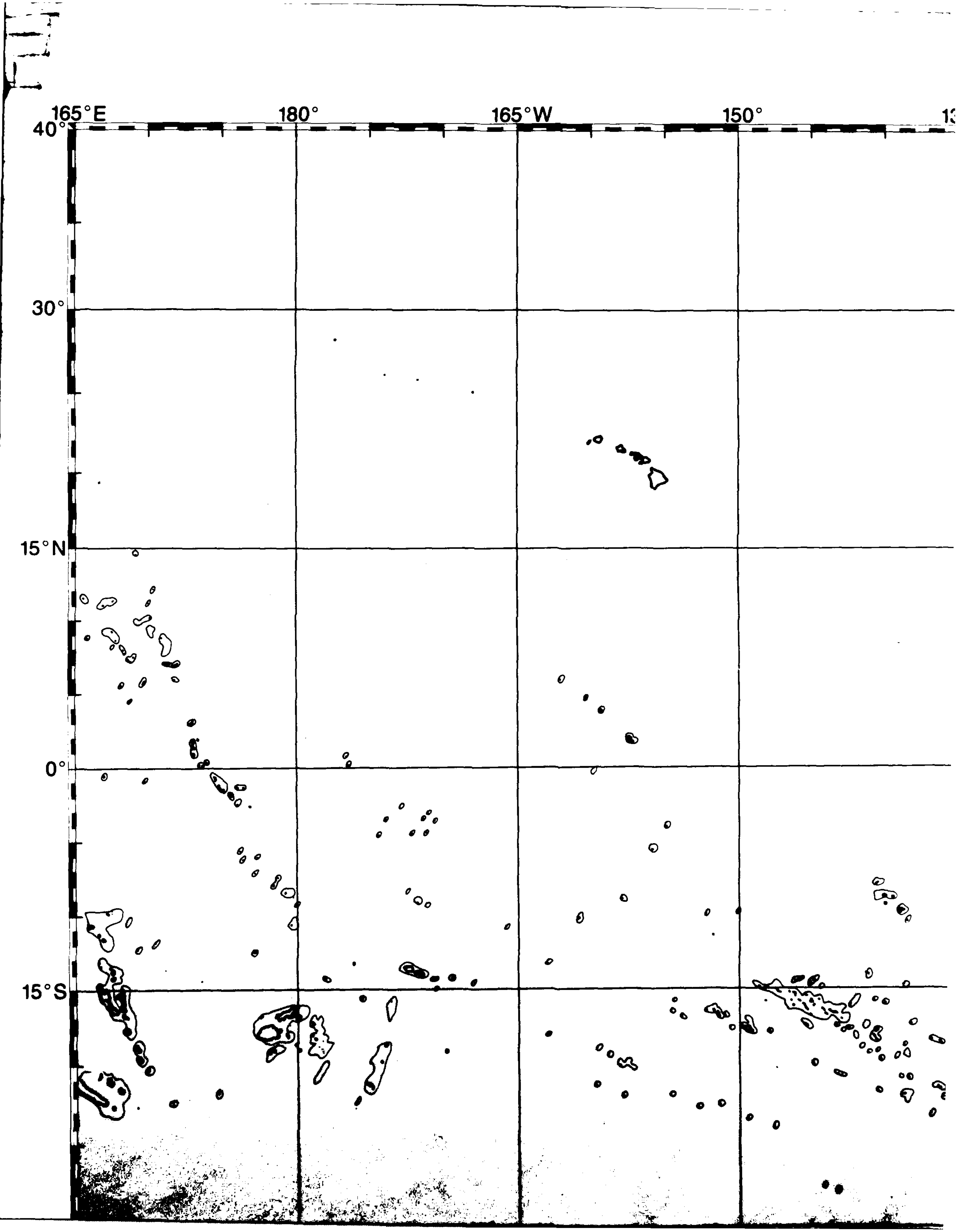

165°E
180°
165°W
150°
40°
30°
15°N
0°
15°S

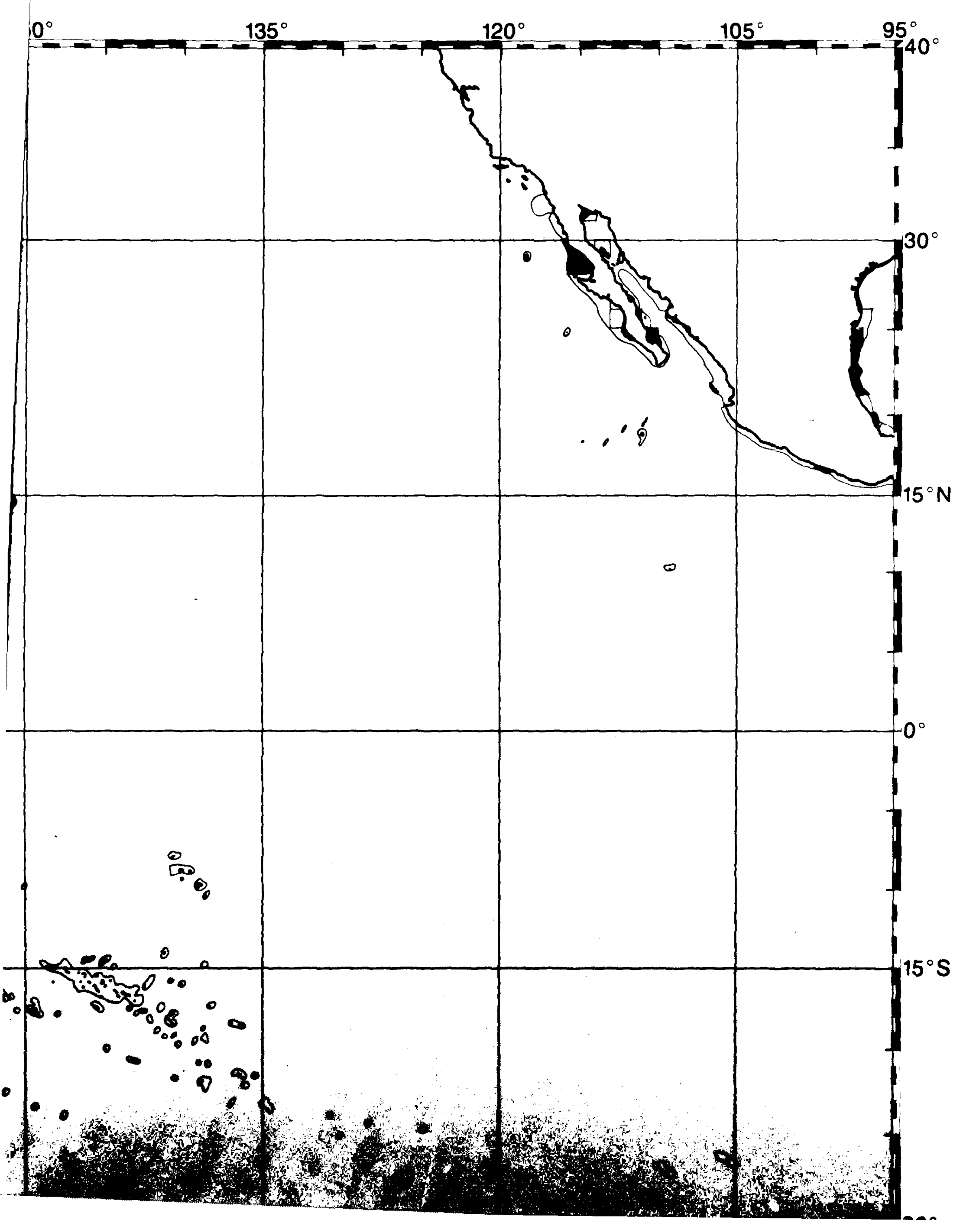

135°
120°
105°
95°
40°
30°
15°N
0°
15°S

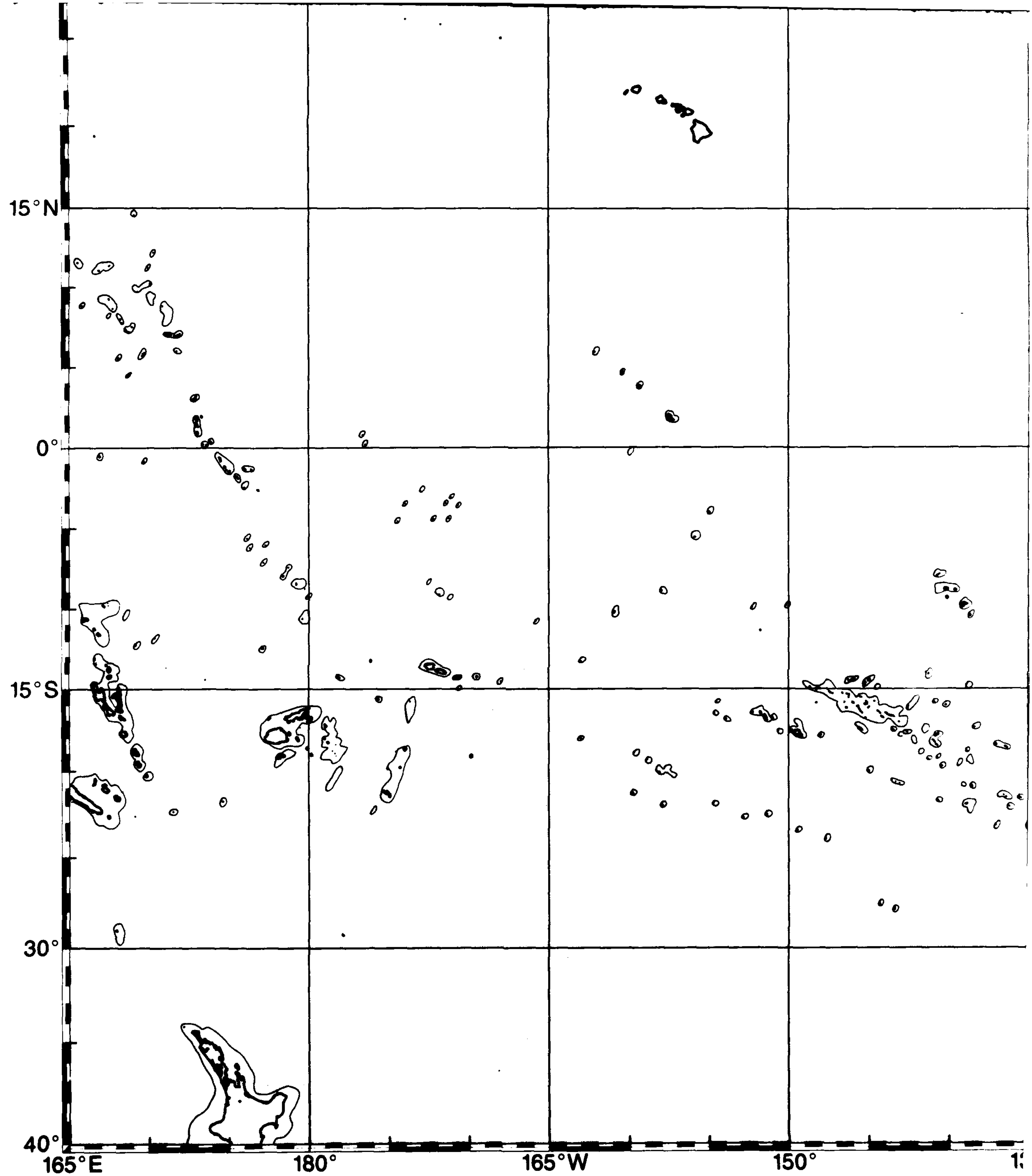

PLATE XX   ANNUAL MEAN

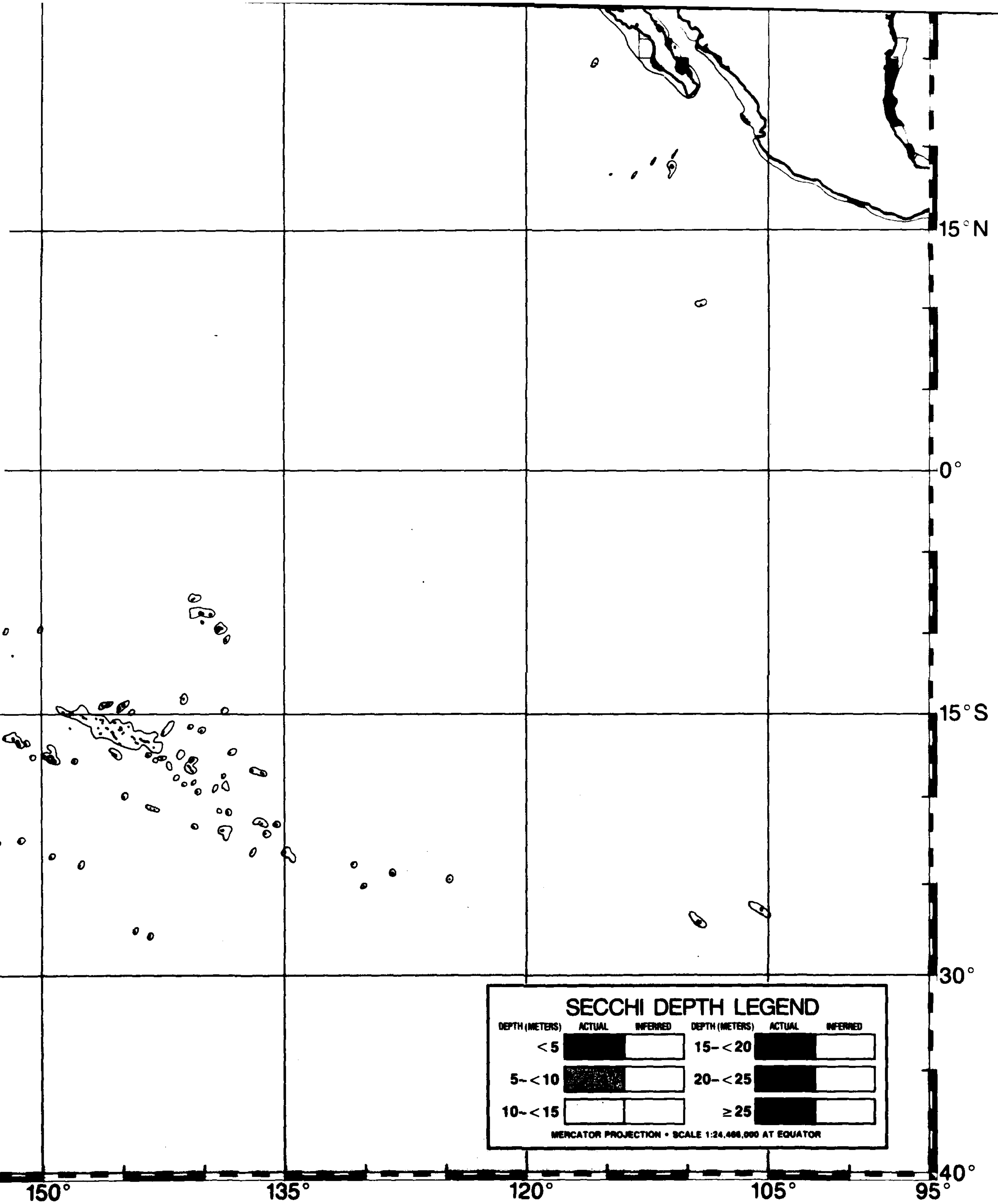

Compiled by: R.A. Arnone, F.A. Hilder, S.P. Tucker

Prepared for the Defense Mapping Agency by
the Naval Ocean Research and Development Activity
Remote Sensing Branch, NSTL, Mississippi